Universidade de Lisboa

Faculdade de Medicina de Lisboa

U LISBOA | UNIVERSIDADE DE LISBOA

Study the function of the newly discovered TrkB receptor fragment (TrkB-ICD) formed by calpain cleavage

João Filipe Fonseca Gomes

Orientadores:

Professora Doutora Maria José de Oliveira Diógenes Nogueira

Doutor André Jerónimo Santos

Dissertação especialmente elaborada para obtenção do grau de Mestre em Neurociências

2016

Universidade de Lisboa

Faculdade de Medicina de Lisboa

Study the function of the newly discovered TrkB receptor fragment (TrkB-ICD) formed by calpain cleavage

João Filipe Fonseca Gomes

Orientadores:

Professora Doutora Maria José de Oliveira Diógenes Nogueira

Doutor André Jerónimo Santos

Dissertação especialmente elaborada para obtenção do grau de Mestre em Neurociências

2016

Publications

In parallel with my Master project, I collaborated in other project whose results are now published (1). Moreover, I was invited to participate in the preparation of a review article already published (2):

1. Jerónimo-Santos A, **Fonseca-Gomes J,** Guimarães DA, Tanqueiro SR, Ramalho RM, Ribeiro A, Sebastião AM, Diógenes MJ (2015). Brain-Derived Neurotrophic Factor mediates neuroprotection against Aβ-induced toxicity through a mechanism independent on adenosine 2A receptor activation. *Growth Factors.* 33(4):298-308.

2. Ribeiro FF, Xapelli S, Miranda-Lourenço C, Tanqueiro SR, **Fonseca-Gomes J,** Diógenes MJ, Ribeiro JA, Sebastião AM (2015). Nucleosides in neuroregeneration and neuroprotection. *Neuropharmacology*. S0028-3908(15)30170-2.

Index

Figure Index

Tables Index

x

Abbreviations and symbol list

μg	Microgram
μL	Microliter
μM	Micromolar
aa	Amino Acid
Aβ	Amyloid-Beta
AD	Alzheimer's Disease
ADP	Adenosine Diphosphate
ANOVA	Analysis of Variation
APP	Amyloid Precursor Protein
ATP	Adenosine Triphosphate
BACE1	Beta-site amyloid precursor protein cleaving enzyme 1
BDNF	Brain-Derived Neurotrophic Factor
bp	Base Pairs
Ca^{2+}	Calcium (2+) Ion
CDK5	Cyclin-dependent Kinase 5
C&M	Fraction Enriched in Cytoplasmic and Membrane Proteins
CHX	Cyclohexamide
CMV	Cytomegalovirus
CNS	Central Nervous System
CTR	Control
Dapi	4',6-diamidino-2-phenylindole
DIV	Days *In Vitro*
DMSO	Dimethyl Sulfoxide
DNA	Deoxyribonucleic Acid
DTT	1,4-dithiothreitol
EDTA	Ethylenediaminetetraacetic Acid
EGFR	Epidermal Growth Factor Receptor
EGTA	Ethylene Glycol Tetraacetic Acid
ER	Endoplasmic Reticulum
EV	Empty Vector
iAβ	Intracellular Amyloid-Beta
IF	Immunofluorescence
FL	Full-Length
GAPDH	Glyceraldehyde 3-Phosphate Dehydrogenase
GC	Golgi Complex
H	Homogenate
H_2O	Water

HBSS	Hanks' Balanced Salt Solution
HEPES	N-2-Hydroxyethylpiperazine-N'-2-Ethanesulfonic Acid
ICD	Intracellular Domain
KCl	Potassium Chloride
Lipof.	Lipofectamine
MAPK	Mitogen-Activated Protein Kinase
MG132	Z-Leu-Leu-Leu-CHO
Mn^{2+}	Manganese (2+) Ion
mRNA	Messenger Ribonucleic Acid
MTT	3-(4,5-Dimethylthiazol-2-yl)- 2,5-Diphenyl Tetrazolium
N	Fraction Enriched in Nuclear Proteins
Na_3VO4	Sodium Orthovanadate
NaCl	Sodium Cloride
NaF	Sodium Floride
ng	Nanogram
NLS	Nuclear Localization Sequence
n.s.	Non Significant
NT	Neurotrophin
p75NTR	P75 Neurotrophin Receptor
PBS	Phosphate Buffered Saline
PC12	Pheochromocytoma Cell Line
PCN	Primary Cortical Neurons
PCR	Polymerase Chain Reaction
PD	Parkinson's Disease
PDL	Poly-D-Lysine
Pi	Phosphate Group
PI3K	Phosphatidylinositol 3-Kinase
PIP_2	Phosphatidylinositol-4,5-Bifosphate
PIP3	Phosphatidylinositol-3,4,5-Trisphosphate
PKA	Protein Kinase A
PKC	Protein Kinase C
PLC	Phospholipase C
ProBDNF	Precursor of BDNF
PVDF	Polyvinylidene Fluoride
RIPA	Radio-Immunoprecipitation Assay
ROS	Reactive Oxygen Species
rpm	Rotations *per* Minute
RT	Room Temperature
SDS-PAGE	Sodium Dodecyl Sulphate-Polyacrylamide Gel Electrophoresis
SEM	Standard Error Of The Mean
T1/2	Half-Life Time

Tc	Truncated
TBS	Tris-Buffered Saline
TBS-T	Tris-Buffered Saline-Tween
Trk	Tropomyosin-related Kinase
TrkB-ICD	TrkB-Intracellular Domain (calpain-generated)
TrkB-FL	TrkB Full-Length
TrkB-T'	TrkB Truncated (calpain-generated)
TrkB-T1	TrkB Truncated isoform 1
TrkB-T2	TrkB Truncated isoform 2
TrkB-Tc	TrkB Truncated (total pool)
UK	United Kingdom
USA	United States of America
WB	Western-Blot
wt:vol	Weight:volume

Acknowledgments

Gostava de dedicar esta tese a quem, desde sempre, esteve, está e estará comigo: os meus pais e o meu avô. Aos meus pais lhes agradeço todo o apoio, motivação, incondicional amizade e por serem sempre o meu porto de abrigo, quaisquer que sejam as situações e tenham mais ou menos razões para estarem do meu lado. Termino com um agradecimento especial ao meu avô que, esteja onde estiver, ficará feliz por me ver finalizar mais uma etapa. Embora não o tenha comigo, tenho a certeza que está orgulhoso de ver o seu neto conseguir mais uma conquista na vida.

Resumo

A Doença de Alzheimer (DA) é a forma mais prevalente de demência em todo o Mundo (totalizando entre 60 a 70% de todos os casos diagnosticados de demência). Esta é uma doença neurodegenerativa crónica caracterizada por diferentes estadios de progressão, culminando em atrofia cerebral globalizada e em perda neuronal substancial em áreas cerebrais particulares, com especial foco no hipocampo e no córtex entorrinal.

Com base nos inúmeros estudos desenvolvidos nas últimas décadas, actualmente, a comunidade científica considera a DA uma doença resultante da acumulação extraneuronal do péptido β-amilóide (Aβ) e acumulação intraneuronal da forma hiperfosforilada da proteína tau.

Para além da acumulação cerebral das proteínas anteriormente referidas, nesta doença, também se sabe estar presente uma desregulação da sinalização mediada pelo Factor Neurotrófico derivado do Cérebro (*Brain-derived neurotrophic factor*, BDNF). O BDNF, através da activaçao da isoforma completa do seu recetor (TrkB-FL), é responsável pela activação de vias moleculares essenciais à sobrevivência e diferenciação neuronais, bem como à transmissão e plasticidade sinápticas. Tanto em amostras de tecido cerebral *post-mortem* de pacientes com DA como em cérebros de modelos animais de DA foi possível detetar níveis diminuídos de BDNF e do receptor TrkB-FL bem como aumento significativo das isoformas truncadas do receptor TrkB (TrkB-Tc), consideradas inibidoras da sinalização do TrkB-FL. Este comprometimento da função do BDNF implica alterações profundas na homeostasia celular, uma vez que se assiste a uma perda significativa das funções celulares mediadas por esta neurotrofina. Desta maneira, actualmente considera-se que a perda de sinalização do BDNF poderá directamente contribuir para a morte neuronal associada à neurodegeneração.

Recentemente, foi descrito um novo mecanismo que está também subjacente à perda de sinalização do BDNF na DA: clivagem do recetor TrkB-FL. Na verdade, um dos efeitos neurotóxicos associados à acumulação do péptido Aβ está associado a um aumento significativo dos níveis de cálcio intracelulares, através de

inúmeros mecanismos, incluindo a interacção com receptores transmembranares (como os receptores NDMA), a disrupção membranar através da formação de poros e ainda a produção de espécies reactivas de oxigénios. Por sua vez, existe um grupo particular de enzimas dependentes dos níveis de cálcio que, neste contexto, são sobre-activados e conduzem à clivagem dos recetores TrkB-FL. Assim, como consequências desta clivagem, observa-se uma diminuição dos níveis do recetore TrkB-FL e a respectiva formação de dois fragmentos: 1) um novo receptor truncado (TrkB-T') e 2) um fragmento intracelular (TrkB-ICD) que é libertado para o citosol. Contudo, tendo em conta que este mecanismo associado à perda de sinalização do BDNF foi recentemente descrito, não existia, até ao momento, qualquer tipo de caracterização destes fragmentos e do seu possível papel na patofisiologia da DA. Desta maneira, este trabalho foi delineado por forma a caracterizar o fragmento intracelular TrkB-ICD e estudar o seu possível papel na DA.

Para responder aos objectivos propostos, foram usados dois tipos celulares distintos: linha celular de neuroglioma humano (células H4) e culturas primárias de neurónios corticais de rato. Inicialmente, procedeu-se à optimização de diversos parâmetros do protocolo de transfecção, de modo a garantir a expressão óptima da proteína de interesse (TrkB-ICD) em ambos os tipos celulares usados. De seguida, usando Ciclohexamida (CHX, 5 µM), composto inibidor da síntese proteica de células eucarióticas, foi avaliada a estabilidade do fragmento TrkB-ICD. Os resultados obtidos indicam que este fragmento é uma proteína estável e com um tempo de semi-vida próximo das oito horas, período suficientemente longo para ser possível colocar a hipótese de que o fragmento possa interferir com a homeostase da célula. Outro grupo de resultados obtidos através da técnica de imunofluorescência e de um protocolo de fraccionamento celular, indica claramente que o fragmento em estudo é gradualmente translocado para o núcleo, um processo que é dependente da actividade de cinase do próprio fragmento. É importante notar que a dinâmica de translocação é diferente nos tipos celulares usados. Nos neurónios primários, a translocação nuclear é observada após 24 horas de expressão do fragmento e na linha celular H4, após cerca de 48 horas. Este trabalho revelou ainda que, quando comparado com células não transfectadas, o fragmento TrkB-ICD induz uma fosforilação robusta em inúmeras proteínas, indicando que esta proteína apresenta

actividade de cinase. Para além disso, ensaios com CHX demonstram que esta actividade de cinase se mantém constante ao longo do tempo, enquanto que, ensaios com K252a (5 μM), fármaco inibidor da actividade de cinase dos recetores Trk, indicam que as proteínas fosforiladas pelo TrkB-ICD são rapidamente desfosforiladas, possivelmente através de fosfatases. Por fim, através do uso de um conjunto de seis fármacos inibidores das principais vias de sinalização descritas em células eucariotas, observámos que a fosforilação induzida pelo fragmento em estudo poderá ser positivamente modulada pela via que inclui a Proteína Cinase A, uma vez que se assiste a uma diminuição drástica do padrão de fosforilação induzido pelo fragmento TrkB-ICD quando as células transfectadas são incubadas com o inibidor desta via (H-89, 25 μM).

Assim sendo, as evidências acima enumeradas suportam a hipótese de que o fragmento TrkB-ICD poderá ter um papel importante na patofisiologia da DA, podendo actuar como regulador de vias de sinalização ou regulador da transcrição genética, uma vez que se acumula no domínio nuclear. Desta maneira, os resultados deste trabalho poderão vir a tornar-se a base de trabalho futuro que permita identificar novos alvos farmacológicos para o tratamento da DA.

Palavras-Chave:

Neurodegeneração, Doença de Alzheimer, Factor Neurotrófico derivado do Cérebro, receptor TrkB-FL, fragmento TrkB-ICD

xx

Abstract

Alzheimer's Disease (AD) is the most common form of dementia worldwide (60-70% of all cases) and the accumulation of amyloid-beta (Aβ) peptide in the brain is considered as one of the main hallmarks of this disease. Indeed, AD is a chronic neurodegenerative disease with different stages of progression, leading to general atrophy and neuronal loss of particular brain regions, such as hippocampus or entorhinal cortex, which promotes cognitive and functional impairment. Actually, accumulation of Aβ peptide contributes to neuronal death, since its accumulation on Aβ plaques induces neurotoxicity at different levels and through different mechanisms. Hence, AD is considered a protein misfolding disease and Aβ peptide is considered the main player of its etiology.

Simultaneously, Brain-derived neurotrophic factor (BDNF) signalling is seriously impaired in AD, which consequently compromises its physiological functions: neuronal survival, differentiation and plasticity. Actually, decreased levels of BDNF and its receptor (TrkB Full-Length, TrkB-FL), as well as increased levels of truncated TrkB receptors (TrkB-Tc), a dominant negative inhibitor of TrkB-FL, were already described in AD and led to the postulation that this loss of BDNF signalling could directly contribute to neurodegeneration.

Recently, it was discovered a new mechanism that also contributes to the impairment of BDNF signalling in AD: TrkB-FL cleavage. Indeed, accumulation of Aβ peptide promotes a sustained increase of intracellular Ca^{2+} levels, by distinct mechanisms, which in turn leads to calpains overactivation and subsequent TrkB-FL cleavage. As consequences, TrkB-FL levels decreases and two fragments are generated: a membrane-bound truncated receptor (TrkB-T') and an intracellular fragment (TrkB-ICD) that is released to cytosol. However, there was no further characterization about these new fragments. Thus, this work was designed to characterize TrkB-ICD fragment and to study its putative role in AD pathophysiology.

In this way, to reach the goal of this work, we used a human neuroglioma cell line (H4 cells) and primary rat cortical neurons. Initially, we optimized the transfection protocol in order to ensure the optimal TrkB-ICD expression on both cells type used. Then, we evaluated the stability of TrkB-ICD using cyclohexamide treatment (5 µM). The obtained data shows that this fragment is a stable protein with a half-life time of 8 hours, approximately, suggesting that TrkB-ICD is not immediately degraded. Immunofluorescence assays and subcellular fractionation protocols performed also indicate that TrkB-ICD accumulates within the cell nucleus over time, a translocation process dependent on its own

phosphorylation. Furthermore, we clearly show that TrkB-ICD induces a significant phosphorylation of several proteins at nucleus, soma and neuronal processes, showing that this fragment has constitutive tyrosine kinase activity. Finally, by using several inhibitors of the major signalling pathways in eukaryotic cells, we can conclude that protein phosphorylation induced by TrkB-ICD is probably modulated in a positive way by PKA pathway.

The results obtained support the hypothesis that the TrkB -ICD fragment may play a role in AD pathophysiology either by acting as regulator of signalling pathways or, since it accumulates in the nucleus, as regulator of gene transcription. Thus, data obtained in this work could underlie future work that might allow the identification of new pharmacological targets for the treatment of AD and further research on this fragment could also unveil if TrkB-ICD fragment can be considered a biomarker for AD.

1 Introduction

1.1 Neurotrophins

Neurotrophins (NTs) are a family of growth factors that belong to the broad group of neurotrophic factors and have a crucial importance in a healthy nervous system. NTs can have different functions depending on the cellular developmental stage or depending on the type of external insults [1–3]. In early developmental stage, these proteins control some aspects of growth, survival and differentiation of developing neurons, but, in mature neurons, they can also act as synaptic plasticity regulators. In addition to the role of neurotrophins on central neurons, they have also a crucial role on the peripheric nervous system, including sensory and sympathetic neurons [4,5]. Accordingly, NTs have crucial functions in both peripheral and central nervous systems homeostasis.

Nerve Growth Factor (NGF) was the first NT identified by an Italian biologist Rita Levi-Montalcini, who described its role on the morphological differentiation of neural-crest-derived nerve cells [6]. After this discovery, many other studies concerning NTs have started, resulting in the identification of new biological mediators involved in the promotion of cell growth, differentiation, function and survival of nerve cell populations. Thus, in addition to NGF, other three neurotrophins were found in mammals: Brain-derived neurotrophic factor (BDNF), Neurotrophin-3 (NT-3) and Neurotrophin-4/5 (NT-4/5) and another two NTs in fishes: Neurotrophin-6 (NT-6) and Neurotrophin-7 (NT-7) [7–12].

Each neurotrophin has different characteristics and properties, and they are recognized by specific receptors as shown in Figure 1.1. In general, there are two types of receptors for neurotrophins that mediate the activation of different signalling pathways with apparent opposite biological effects: the p75 neurotrophin receptor (p75NTR) and the tropomyosin-related kinase receptors (Trk) [2,13]. Currently there are three types of Trk receptors identified (TrkA, TrkB and TrkC) that are products of three different genes (*NTRK1, NTRK2* and *NTRK3,* respectively). Trk

receptors share some main characteristics, such as its structure and functioning [14–17]. Both Trk receptors and p75NTR are located at the cellular membrane, being activated by the binding of a ligand in their extracellular domain with consequences at intracellular level. This ligand-binding specificity is one of intrinsic characteristics of different Trk receptors that determine its classification, as mentioned above [2,3].

Briefly, the immature neurotrophins (pro-neurotrophins) are recognized by p75NTR, but after processing and maturation, the pro-neurotrophins are converted to neurotrophins that bind preferentially to Trk receptors, instead of p75NTR-binding (Figure 1.1) [4,18]. The activation of these two different subsets of receptors leads to distinct signalling cascades, which will be described in more detail below on *Section 1.1.1.B.*
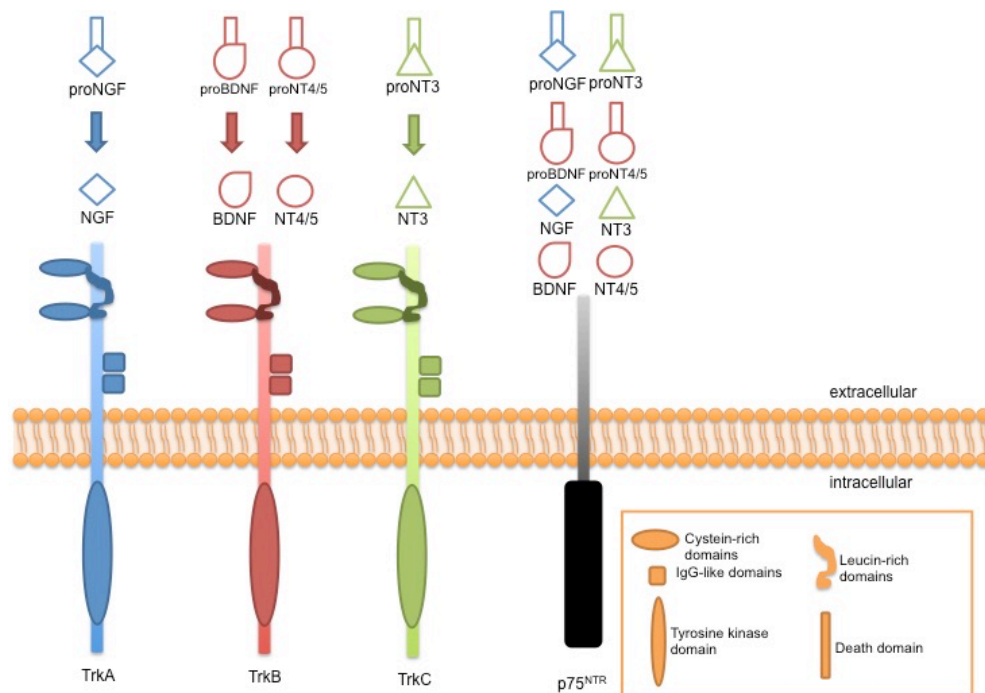
Figure 1.1 – Schematic representation of neurotrophins interactions with their receptors. The immature forms of neurotrophins (pro-neurotrophins) are recognized with high affinity by p75NTR, while each mature neurotrophin binds and activates specifically Trk receptors. In particular, TrkA recognizes NGF, TrkB recognizes BDNF and NT-4/5 and TrkC recognizes NT-3.

It should be noted that NTs have some common characteristics and properties, like processing or releasing processes. However, since BDNF is the NT directly associated with this work, hereinafter it will be given more emphasis to this molecule.

1.1.1 Brain-derived neurotrophic factor

BDNF was the first NT identified after the discovery of NGF and, nowadays, it is considered the NT with most widespread expression in mammalian brain. In 1982, Barde and collegues, using 1.5 kg of pig brain, were able to purify 1 µg of BDNF. This study identified the molecular weight of BDNF (12.3 kDa), its isoelectric point (pI = 10.1) and its biological activity (0.4 ng/mL/unit), which is similar to NGF using same approaches[7]. This similarity can be explained due to highly homology between protein sequence of BDNF and NGF [19]. It was also reported by Barde that this NT is important for survival and fibre outgrowth of cultured embryonic chick sensory neurons and for subpopulations not responsive to NGF, but the remaining characterization of its physiological function and structural properties was not much discussed on his initial research [1,7].

BDNF expression pattern changes during neurodevelopment, indeed, while BDNF is abundantly expressed in hippocampus, neocortex, amygdala and cerebellum during the first months of postnatal development, in adult stages, BDNF expression is homogeneous throughout the brain [20].

A) BDNF: processing and release

Similarly to other NTs, the initial pre-mRNA sequence of BDNF (pre-pro-BDNF) present in nucleus is converted to pro-BDNF (231 amino acids (aa)), after processing in endoplasmic reticulum (ER) and Golgi complex (GC). Then, this precursor form of BDNF can be processed to the mature protein (118-120 aa) by several cellular mechanisms. At intracellular level, pro-BDNF can be cleaved to homodimeric protein by two mechanisms: by furin or by proconvertase enzymes in regulated secretory vesicles. Thereby, BDNF can be released in a regulated-way dependent on neuronal activity or can be constitutively released, if occurs spontaneous fusion of vesicles with plasma membrane. On the other hand, when pro-BDNF is released as an unprocessed form, it can be directly processed by plasmin at extracellular level or can be recognized by p75NTR. Following this binding

to p75NTR, BDNF is endocytosed into the cell, being then cleave to mature BDNF within endosomes by proconvertase enzymes, what leads to its release to extracellular level [21–26]. In this way, mature BDNF present in extracellular side activates TrkB receptors and thereby promotes its effects, which includes neuronal survival and regulation of synaptic plasticity, as it will be described below. All these steps are schematically showed in Figure 1.2.
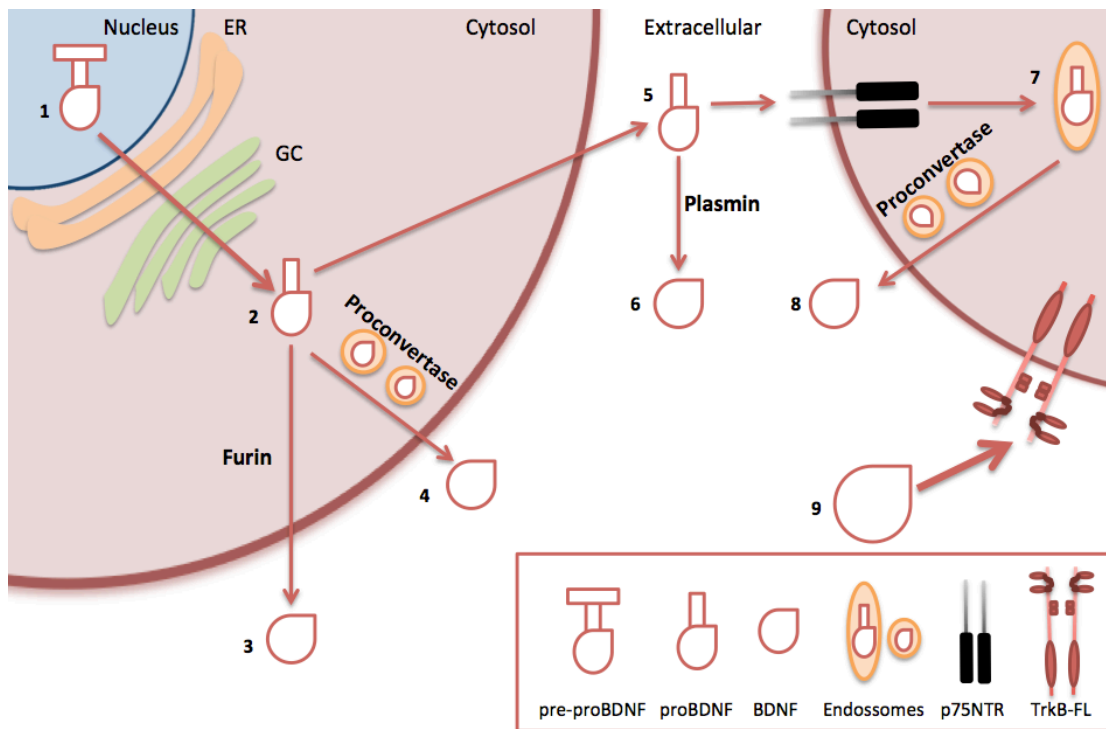
Figure 1.2 – Schematic representation of BDNF processing and release. Pre-mRNA sequence of BDNF present in nucleus (1) is converted to pro-BDNF, after processing in endoplasmic reticulum (ER) and Golgi complex (GC) (2). Then, this immature form can be cleaved by furin, releasing BDNF to extracellular side (3). However, BDNF can also reach extracellular side in regulated secretory vesicles, being pro-BDNF processed by proconvertase enzymes (4). When pro-BDNF is released directly to extracellular milieu (5), it can be processed by plasmin into its mature form (6) or can bind p75NTR (its selective receptor) that endocytosed it into endosomes (7), promoting its release as mature neurotrophin to extracellular side after proconvertase conversion (8). Then, all mature BDNF produced by diferent mechanisms here described can activate cell surface TrkB receptors (9).

B) BDNF receptors

As mentioned above, mature BDNF binds to TrkB receptor with high-affinity and with low-affinity to p75NTR. Interestingly and on the opposite, p75NTR recognizes pro-neurotrophins with high affinity [4,18]. As briefly mentioned above, the activation of each subset of receptors leads to distinct signalling cascades, which could lead to opposite effects on cell environment. p75NTR belongs to tumour necrosis factor (TNF) receptor superfamily and the signalling mediated by this receptor is not still fully understood. However, it is already described that its activation by pro-neurotrophins triggers mainly apoptotic pathways and impairs normal synaptic function, serving Sortilin as a co-receptor. On the other hand, TrkB activation is already well characterized and is involved in main physiologic functions of neurotrophin signalling pathways, including neuronal survival, synaptic plasticity and differentiation. However, it is important to mention that in some circumstances, p75NTR can act as a co-receptor of BDNF, acting synergistically on TrkB pathways [23,27].

Regarding the structure of TrkB, this receptor has several communalities with other receptors of its family. Briefly and as shown in Figure 1.3, at extracellular level, Full-Length (FL) form of TrkB receptor (TrkB-FL) are composed by two cysteine rich domains, one domain rich in leucines and, below these domains, it has two immunoglobulin-like (IgG-like) domains, which compose the binding site responsible for selective binding site. In turn, at intracellular level, TrkB-FL receptor is mainly constituted by tyrosine kinase domain between Shc protein binding site on the top (at juxtamembrane domain) and a C-terminal tail, which includes phospholipase C gamma (PLCγ) binding site [28]. Therefore, the intracellular domain of TrkB-FL is essential for signalling pathway activation (as will be detailed in Figure 1.4 and in *Section 1.1.1.C*).

Concerning TrkB receptors and in addition to TrkB-FL receptor, there are also truncated (Tc) isoforms (TrkB-Tc) of the receptor generated by alternative splicing of TrkB gene (*NTRK2*) [28–32]. The main truncated TrkB isoforms characterized are the TrkB-T1, TrkB-T2 or TrkB-T-Shc receptors. The truncated TrkB isoforms lack the tyrosine kinase domain and, thereby they are not able to trigger the canonical

signalling pathways. Moreover, these truncated receptors can act as negative modulators of TrkB-FL signalling since they can form non-functional heterodimers with TrkB-FL receptors inhibiting the downstream signalling, even in the presence of BDNF and functional TrkB-FL monomers [33]. In addition, truncated isoforms of TrkB receptor also bind BDNF that is internalized with its receptor, leading to a decrease of available extracellular levels of this neurotrophin [34].

As shown in Figure 1.3, all TrkB receptors isoforms share the same extracellular domain, being only distinguished by different length of C-terminal tail.
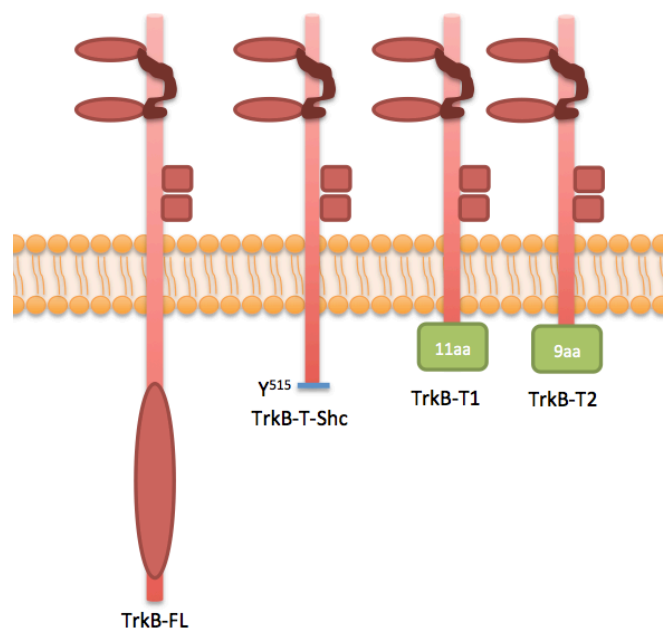
Figure 1.3 – Schematic representation of TrkB receptors isoforms: TrkB-FL and truncated forms (TrkB-T1, TrkB-T2 and TrkB-T-Shc). Alternative splicing of the TrkB mRNA (*NTRK2*) produces different isoforms of TrkB receptor: in addition to FL isoform, there are also another isoforms that have truncated cytoplasmic domains and, therefore do not have tyrosine kinase domain. TrkB-T-Shc has a cytoplasmic tail until Shc binding site, whereas TrkB-T1 and TrkB-T2 have a shorter cytoplasmic tail with 11 and 9 aa, respectively. In opposition to intracellular signalling cascades mediated by TrkB-FL receptor, truncated TrkB isoforms do not promote the activation of neurotrophic signalling.

C) BDNF/TrkB-FL system

As indicated above, the physiological consequences of BDNF signalling mediated by TrkB-FL are vital to the homeostasis maintenance of the mammalian nervous system, since it promotes neuronal growth, survival and differentiation or regulation of synaptic transmission and plasticity [2,3].

In vivo and in the presence of homodimeric BDNF, TrkB-FL receptors dimerize promoting the auto-phosphorylation of several tyrosine residues present in the catalytic domain, at intracellular level [35,36]. Hence, this phosphorylation triggers downstream signalling cascades. As represented in Figure 1.4, the TrkB-FL dimerization promotes fast phosphorylation of three tyrosine residues (Y) present on the tyrosine kinase domain (Y^{701}, Y^{705} and Y^{706}). In turn, this tyrosine kinase activity leads to the phosphorylation of another two tyrosine residues: Y^{515} (in juxta-membrane domain) and Y^{816} (at C-terminus), which will act as docking site for Shc adaptor protein (directly associated with Ras/MAPK/Erk and PI3K/Akt pathways) and PLCγ, respectively [35,37–40].

Thus, the major signalling pathways mediated by the activation of TrkB-FL receptors are:

- **Ras/MAPK/Erk pathway**

Phosphorylated Y^{515} of TrkB-FL promotes the formation of a complex involving Shc protein and another proteins, such as Grb2, Gab1/2 and SOS, which leads to a transient activation of small GTPases and, in particular, Ras protein. In turn, activated Ras sequentially stimulates Raf kinase, which will activate MAPK/ERK kinase (MEK), promoting an activated cascade of events that, at the end, contributes to the activation of several transcription factors. These transcription factors activated (as it is the case of c-Fos and NF-kB) are involved in the control of expression of many proteins directly involved in neuronal survival, growth and differentiation [40–44].

1 Introduction

- **PI3K/Akt pathway**

In addition to mentioned above, Ras protein is also involved in the activation of PI3K pathway, where there is a phosphorylation of PIP_2, resulting in production of PIP_3 that activates serine-theronine kinase Akt. In turn, this stimulated Akt will modulate the expression and function of a wide range of promoters directly associated with axonal growth and mainly neuronal survival, such as the inactivation of pro-apoptotic proteins. Some downstream effects of this pathway are shared with the first pathway described, since this via also promotes the activation of some transcription factors (like CREB or NF-kB) that control the expression of pro-apoptotic proteins [40,41,45].

- **PLCγ pathway**

Phosphorylation of Y^{816} promotes the binding of PLCγ1 that becomes activated via TrkB-FL kinase domain. So, activated PLCγ1 produces IP_3 and DAG from PIP_2 hydrolysis, stimulating DAG-regulated protein kinase C (PKC) and the release of Ca^{2+} from intracellular sources, respectively. This increase of intracellular Ca^{2+} levels will activate Ca^{2+}-regulated PKC and calmodulin-regulated kinase isoforms. Together, it contributes to the regulation of genes transcription (like CREB) with direct influence on neuronal connections, affecting synaptic plasticity and, consequently, memory and learning processes, which are dependent on long-term potentiation (LTP) [40,41,46].
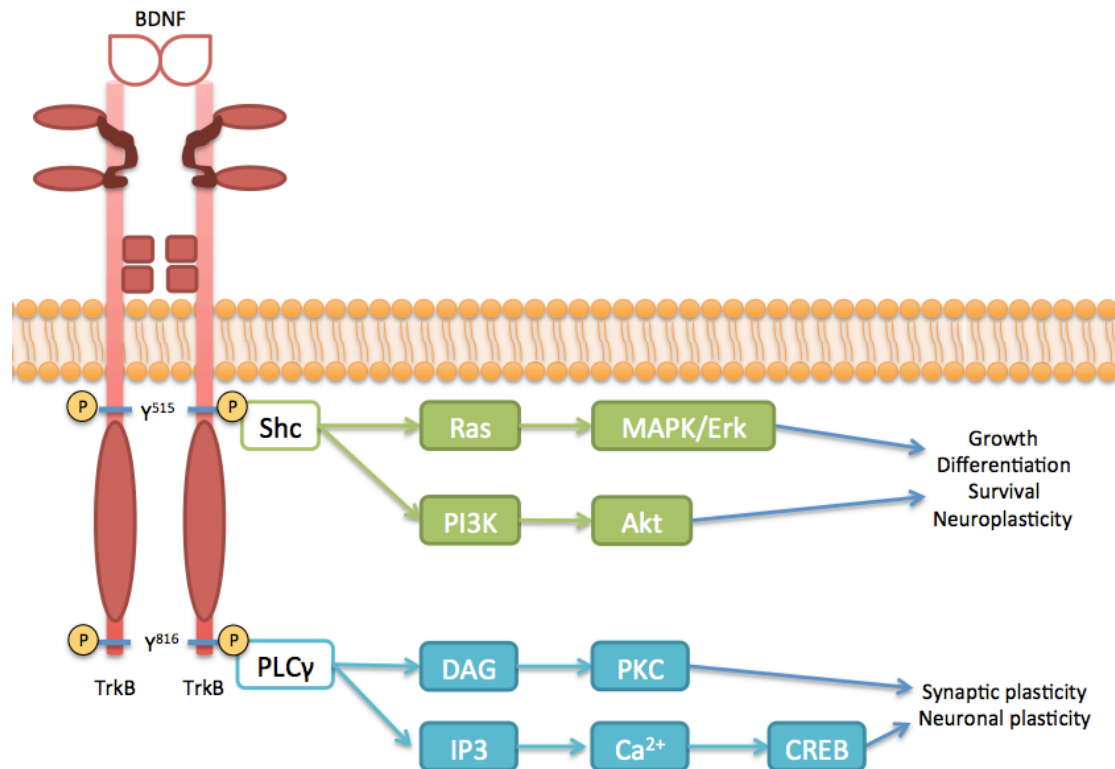
Figure 1.4 – Schematic representation of BDNF/TrkB-FL signalling. The binding of homodimeric BDNF promotes the dimerization of TrkB-FL receptors, activating the kinase domain present in intracellular side and trans-phosphorylating (P) this receptor in two tyrosine residues (Y^{515} and Y^{816}). Consequently, phosphorylated Y^{515} recruits the binding site of Shc adaptor protein, leading to the activation of Ras protein that in turn stimulates MAPK/Erk pathway. This phosphorylated tyrosine residue also activates and triggers PI3K/Akt pathway that promotes neuroplasticity and neuronal growth, differentiation and survival, as well as MAPK/Erk pathway. On the other hand, phosphorylated Y^{816} of TrkB-FL binds to PLCγ, activating its pathway, which leads to the promotion of transcriptional factors involved in synaptic and neuronal plasticity.

In summary, it is vital that the system composed by BDNF/TrkB-FL receptor and consequent downstream pathways are tightly regulated, in order to ensure homeostasis. Therefore, dysregulations on this system, such as decrease of TrkB-FL receptor or BDNF levels and increase of TrkB-Tc levels, could result in the impairment of neurotrophic support, which ultimately can lead to neuronal death contributing to neurodegeneration [47] (Figure 1.5).

Figure 1.5 – Schematic representation concerning the effects of dysregulations on BDNF/TrkB-FL system. Considering the importance of BDNF/TrkB-FL system on neuronal functioning, dysregulation on it leads to severe consequences on cell homeostasis. Since this system provides trophic support to neurons, when this signalling is impaired, there is a marked neuronal death that ultimately promotes neurodegeneration.

1.2   Neurodegeneration

Neurodegeneration is a common event present in many brain diseases and it is characterized by the progressive and irreversible loss of neuronal function and structure, which ultimately leads to neuronal death [48,49]. The absence of cell division is believed to be a core feature of neuronal identity and therefore a great loss of these cells may cause an irreversible impairment in brain functions.

Different neurodegenerative diseases, even with distinct clinical outcomes, share many characteristics, namely related to its pathogenesis. Neurodegenerative diseases can be caused by dysfunctions at molecular level, like protein misfolding, mitochondrial dysfunction, membrane damage, alterations on programmed cell death or even changes in protein degradation pathways [49,50]. In this way, these changes contribute to degeneration that supports brain and systemic dysfunction, such as movement disorders (ataxias) or dementia [49–51]. For instance, Parkinson's disease (PD) is characterized by the presence of misfolded proteins (α-synuclein) in substantia nigra and by the degeneration of dopaminergic neurons (which promotes the depletion of dopamine in basal ganglia), leading to ataxia (tremors, stiffness and also rigidity in the major muscles of the body) [50,52]. In the case of Alzheimer's Disease (AD), there is accumulation of β-amyloid (Aβ) peptide, hyperphosphorylation of tau protein and a marked cortical neurodegeneration contributing to dementia, which will be detailed below [53].

Interestingly, some neurodegenerative diseases, such as Huntington's disease (HD), PD or AD, have been associated with genetic mutations. However, concerning all neurodegenerative diseases, only a small part of them have genetic causes (about 5%). Therefore, intracellular dysregulations that could act simultaneously and synergistically underlying the genesis of neurodegenerative diseases have been intensively studied [48,54].

Despite all the research on this area, the current medication only alleviates the symptoms and it has no role on ethiopathology of these diseases. Hence, there is no cure for neurodegeneration. In addition, average life expectancy is being also increasing, allowing that the onset problems of this type of diseases have more time

to settle. Consequently, nowadays, these factors contribute for the higher levels of AD prevalence [49,55,56].

As mentioned above, there are several types of neurodegenerative diseases some of them related, in some stage, to dementia. It is estimated that there are, per year, 7.7 million new cases of dementia worldwide, implying one new case every 4 seconds, with AD representing approximately 60-70% of all cases, as demonstrated in Figure 1.6 [57,58]. In Portugal, the estimated number of patients with dementia represents 6% of total population with more than 60 years and there are approximately 100 000 Portuguese people with AD, which is also a consequence of the demographic aging [59].
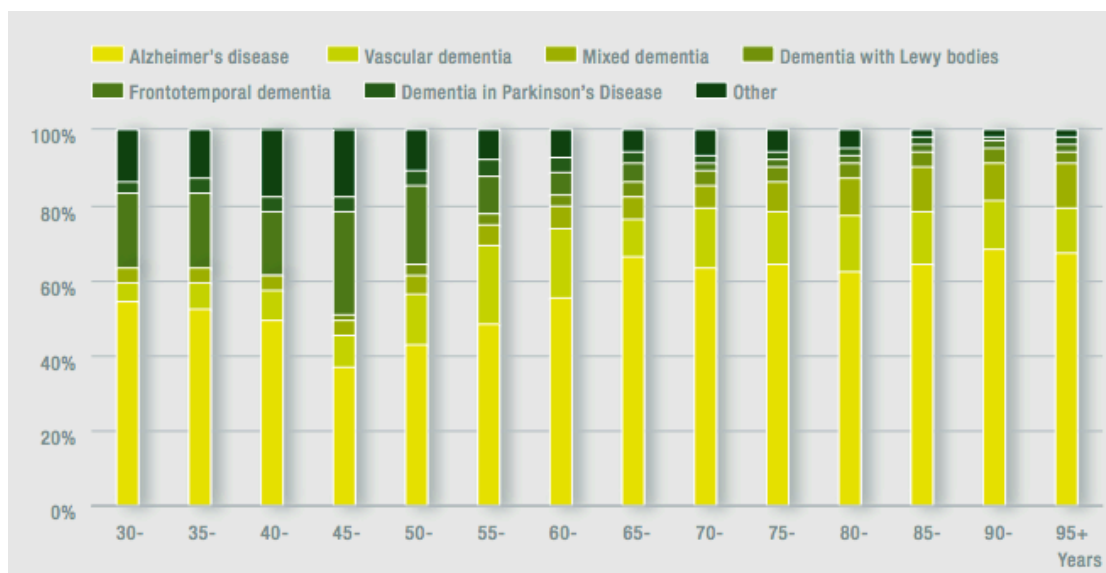
Figure 1.6 – Estimative of the proportion of all dementia cases subdivided by different dementia subtypes. These data (concerned women gender) show the higher proportion of AD cases (yellow), comparing to all dementia cases, where it is possible to observe that AD is clearly present in populations with > 65 years old [48].

1.2.1   Alzheimer's disease

AD is the most common form of dementia, affecting between 21 and 35 million people worldwide in accordance with an epidemiological study in 2010 [58,60]. This is a number that will grow exponentially, since age is the principal risk factor for AD. In other words, age *per se* does not lead to AD establishment and consequent diagnosis, but the incidence of this disease doubles every 5 years after 65 years of age and, therefore, aged populations have higher prevalence of AD. This is confirmed by the estimated incidence of AD on populations older than 85 years, which one in three persons has AD [48,60,61]. Besides age, in the last decades, other risk factors were also described, such as depression, female gender, rurality, head injuries, nutritional deficits and also low education or low social and professional differentiation [62–65] .

This pathology was identified in 1901 in a fifty-one old woman hospitalized on an asylum of Frankfurt, named Auguste Deter, by a German psychiatrist called Alois Alzheimer, which gave the name to this pathology. Doctor Alzheimer followed this case during five years until her death, and described other eleven cases in the following five years. In his original paper, Doctor Alzheimer refers that "clinical observation alone made the case appear so unusual that it could not be classified as one of the recognized illnesses". Furthermore, he also described that she had a progressive presenile dementia with general cortical atrophy, which strongly compromises her orientation and memory processes, saying that "she is completely disoriented in time and space (…) her memory is seriously impaired" [66–68]. These descriptions were just the start of a new era about neurodegenerative diseases and, in particular, about AD.

AD has been extensively studied for the last decades and constitutes one of the most financially costly diseases in developed countries [69,70]. Although many aspects of AD have been unraveled, still there are no therapies that halt or reverse its progression. Nevertheless, the research done so far allowed us to have important clues about its pathogenesis (where it has been proposed several hypothesis), diagnosis, biomarkers, prognosis or even some risk factors, such as sedentary

lifestyle, smoking or diet [71–74]. Nevertheless further research is needed to comprehend this complex disease and to give responses to all issues still unanswered.

As it is shown in Figure 1.7, AD is characterized by a significant reduction in the brain volume and weight, affecting differentially each brain region or neuronal population. Indeed, this decrease of brain size are directly associated with loss of neurons (mainly pyramidal cells of the entorhinal cortex and in the CA1 region of the hippocampus) and also the shrinkage and loss of neuronal processes, contributing to a dramatic reduction in neuronal branching (Figure 1.7) [75–77].

Besides general atrophy and neuronal loss, AD is also characterized by a progressive cognitive and functional impairment. Initially, the main symptoms of AD are memory impairments (directly associated with hippocampal dysfunction), but later on, this impairment converts into disorientation, judgement dysfunction, apraxia and also speech problems. The late stage of AD is characterized by a prolonged and tragic illness, where the patient loses its individuality, leading to death that normally involves pneumonia [61,65].
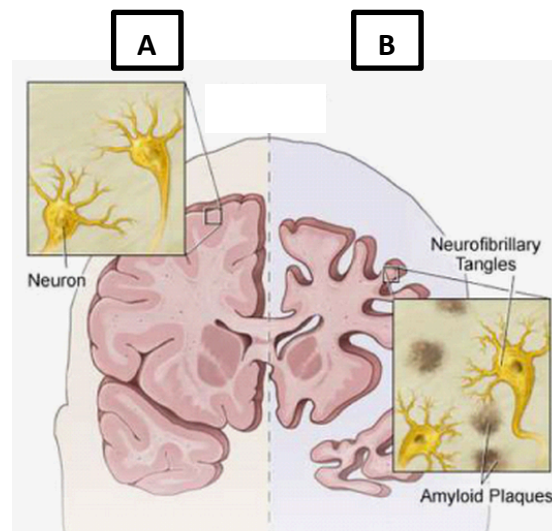
Figure 1.7 – Comparison between (A) a normal aged brain and (B) an AD brain. As pointed out, AD brain is characterized by the shrinkage of neuronal branching and decreased brain volume, comparing with a normal aged brain. At molecular level, it is described the presence of amyloid plaques between neurons and also neurofibrillary tangles (composed by tau protein) inside neurons, as will be further discussed below (adapted from Pescosolido, *et al.* [78]).

A) *Molecular features of AD*

In some families with early-onset familial AD, it was described an autosomal dominant mutation in the amyloid precursor protein (APP) gene and also mutations in *PSEN*1/2, which is a gene involved in γ-secretase complex. Both mutations are directly associated with increased Aβ production, facilitating its accumulation and the pathogenesis of AD [79–82]. However these mutations are present only in 5% of all AD cases. In the remaining cases (that constitutes sporadic AD) there are no known associated mutations that could explain its pathogenesis [83]. Thus, AD can be considered a major example of multifactorial diseases, since several molecular events contribute simultaneously to its pathology, including accumulation of misfolded proteins, oxidative and inflammatory agents, disruptions of Ca^{2+} homeostasis and its consequences on cell environment, as well as mitochondrial and synaptic dysfunction [58,61].

Currently, it is proposed that AD is predominantly a protein misfolding disease. This idea is supported by the presence of senile plaques in the AD brain, composed by aggregated Aβ peptides, and also by the accumulation of intraneuronal neurofibrillary tangles, composed by hyperphosphorylated tau protein (Figure 1.7) [84–86].

Concerning Aβ peptide, studies of genetic forms of AD, including Down's syndrome (where patients often develop AD) and familial AD, support the "amyloid theory" [79–81]. *In vivo*, Aβ peptides are derived from APP proteolytic cleavage by the sequential enzymatic actions of beta-site amyloid precursor protein–cleaving enzyme 1 (BACE-1), also known as β-secretase, and γ-secretase, constituting the amyloidogenic pathway. On the other hand, and as shown in Figure 1.8, there is a non-amyloidogenic pathway involving sequential APP cleavage by α-secretase and γ-secretase [87–90]. Therefore, an imbalance between those pathways, mitochondrial dysfunction or impairment on clearance of Aβ peptides, promote the release of several amyloid fragments (being $Aβ_{1-42}$ the most neurotoxic form) and consequent aggregation into senile plaques, which stay outside of the cells [53,91,92].
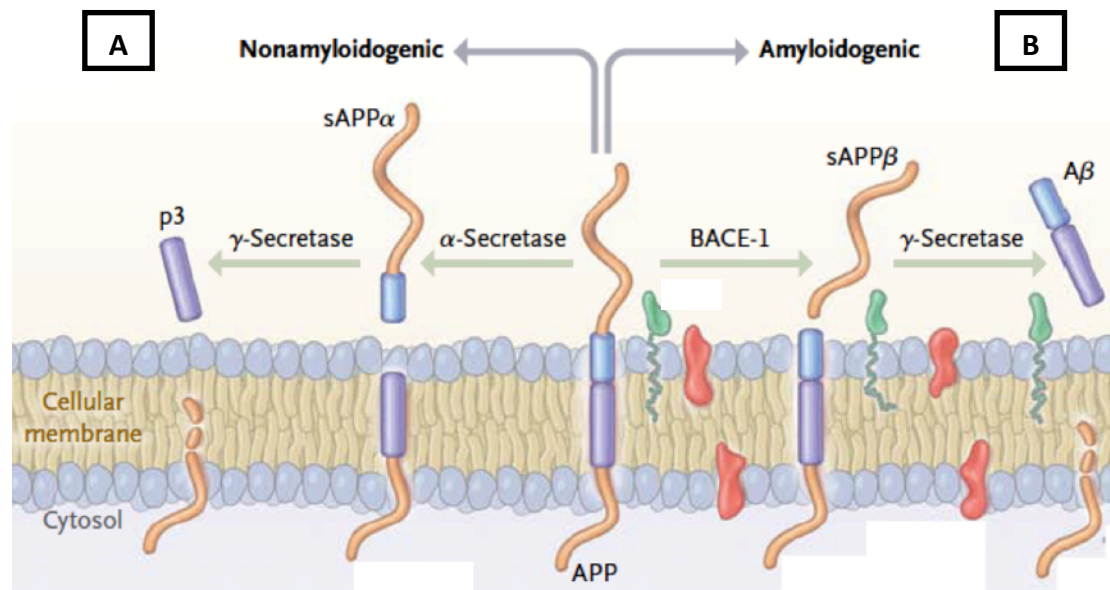
Figure 1.8 – Differential processing of APP: (A) non-amyloidogenic and (B) amyloidogenic pathways. APP can be processed by different sets of enzymes, leading to the establishment of two processing pathways: amyloidogenic pathway and non-amyloidogenic pathway. This last pathway mentioned (A) involves the action of α-secretase (cleaving the interior of Aβ peptide) and γ-secretase, releasing a soluble peptide (p3). However, when APP processing is initiated by β-secretase beta-site amyloid precursor protein–cleaving enzyme 1 (BACE-1) and then cleaved by γ-secretase, it is generated Aβ peptide that is released and can aggregated into amyloid plaques (B) (image adapted from LaFerla and Querfurth [58]).

B) Consequences of Aβ accumulation

Several works with distinctive approaches conclude that Aβ peptide has different neurotoxic effects, sustaining the hypothesis that it is the primary trigger of AD. These effects can act at different levels and through different mechanisms, but always contributing to neuronal death and other hallmarks of AD [61,93,94].

As mentioned above, besides accumulation of senile plaques, AD is also characterized by the accumulation of hyperphosphorylated form of tau protein, which is a neuronal protein mainly involved on stabilization of axonal microtubules assembly by interaction with tubulin. Indeed, Aβ peptide can promote the abnormal phosphorylation of tau protein, converting it into an atypical and insoluble form that can be released to the extracellular space, spreading to other cells, and leads to severe lesions on axonal transport culminating on neuronal death [53,76,80].

Currently, evidences have shown that Aβ induces neurotoxicity through several distinct mechanisms (Figure 1.9): oxidative stress, imbalance of Ca^{2+}

homeostasis, mitochondrial dysfunction or even interactions with different transmembranar receptors, such as NMDAR or RAGE [58,76,95].
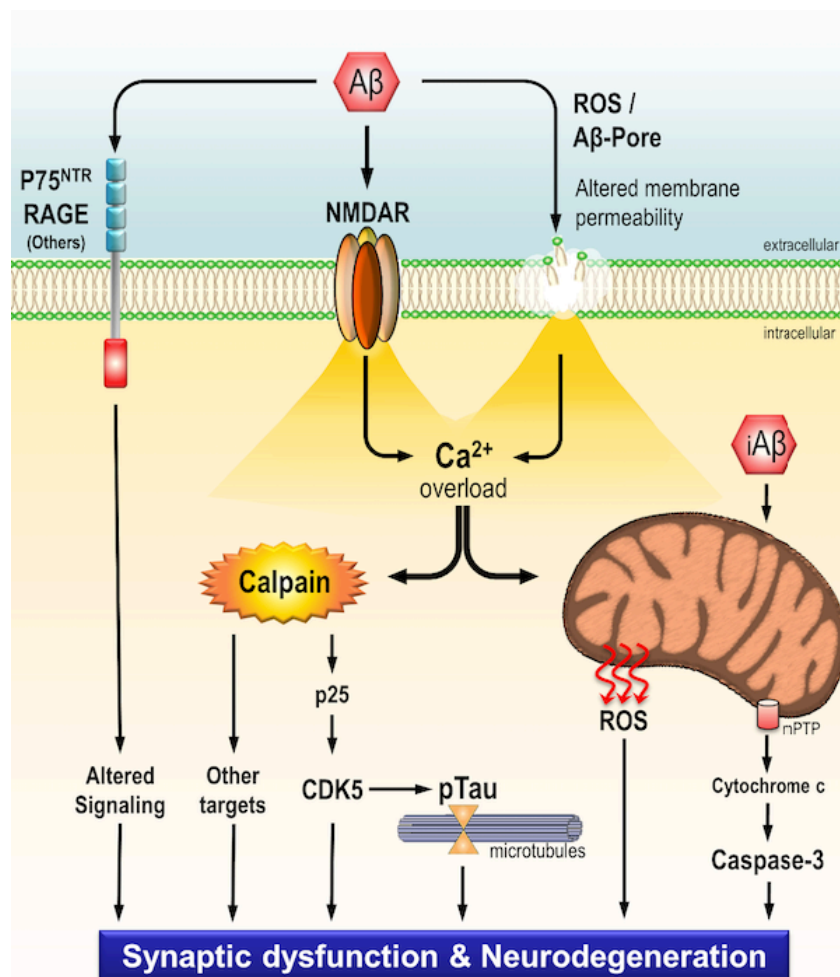
Figure 1.9 – Schematic representation of toxicity mechanisms induced by Aβ peptide. Deposition of extracellular Aβ peptides leads to neurodegeneration and synaptic dysfunction through several mechanisms. Aβ peptides can interact with multiple transmembranar receptors (such as: p75NTR, RAGE, NMDAR), leading to dysregulation of signalling pathways and also a sustained Ca^{2+} influx. Aβ peptide also promotes cell membrane leakage through a pore formation or reactive oxygen species (ROS) production, leading again to a sustained Ca^{2+} influx that induces calpains overactivation and also mitochondrial Ca^{2+} overload. Concerning overactivation of calpains, these enzymes cleave several substrates (such as p25 or mGluR1α), changing its function and leading, for instance, to tau hyperphosphorylation, an event mediated by CDK5 activity (as described below). On the other hand, mitochondrial dysfunction is also mediated by intracellular Aβ peptides, increasing ROS formation and caspase-3 activation. Taken together all these events, Aβ peptides strongly induces neurodegeneration and synaptic dysfunction (image from Jerónimo-Santos PhD thesis [96]).

1 Introduction

In the recent years, it has been shown that Aβ peptide disrupts Ca^{2+} homeostasis, promoting a sustained increase of intracellular Ca^{2+} levels. This increase is a result of: i) the interaction between Aβ peptide with neurotransmitters receptors and ion channels (including AMPA and NMDA glutamate receptors, nicotinic receptor α7-nAChr-Ca^{2+} dependent), ii) the formation of new Ca^{2+}-permeable membrane pores that allow the entry of Ca^{2+} into intracellular space and iii) the promotion of an uncontrolled release of Ca^{2+} from ER [97–102]. In turn, this increase of Ca^{2+} intracellular levels leads to excitotoxicity, oxidative stress, mitochondrial and synaptic dysfunction and also overactivation of calpains, resulting in several damages that compromise cell viability [103–105].

Interestingly, recent data demonstrate that calpains overactivation induces the cleavage of TrkB-FL receptors, impairing dramatically the BDNF function, which ultimately may contribute to neuronal dysfunction and death (as detailed in next *Section*) [106].

C) *BDNF/TrkB-FL system in AD*

As mentioned before, the signalling system composed by TrkB-FL receptor and its ligand, BDNF, has a crucial role on mammalian nervous system, especially because its downstream signalling cascades are directly involved in neuronal survival [36,41]. However, *in vitro* assays and even analysis of *post-mortem* human brain samples have been describing several dysregulations affecting this system on neurodegenerative diseases, with special attention to AD. Actually, existing data demonstrate that pro-BDNF, BDNF and TrkB-FL mRNA and protein levels are reduced in AD brain (specially in hippocampus and parietal cortex), whereas truncated TrkB isoforms levels are increased in frontal cortex and hippocampus of AD patients [47,107–110].

The evaluation of parietal cortex of pre-clinical stages of AD patients have correlated the decreased levels of pro-BDNF and BDNF with a progressive impairment of cognitive function [116–118]. Curiously, in single cholinergic basal forebrain neurons, the downregulation of TrkB receptors (FL and Tc isoforms) also

correlates in a positive way the cognitive decline of patients, as what was observed for BDNF expression [118]. Moreover, the increase of TrkB-FL and BDNF levels in AD mice models reduces cognitive impairment and ameliorates spatial memory deficits [93]. Thus, it is consensual that an impaired BDNF/TrkB-FL system plays a central role in the pathogenesis of AD [93,94,113–115]. There are still some aspects that are not fully understood, such as if the impairment on BDNF/TrkB-FL system is a cause or a consequence of neurodegeneration. It is proposed that there is a cycle, with positive feedback loop, involving the role of BDNF/TrkB-FL system and neurodegeneration, however it is hard to disclose where is the starting point or end point (Figure 1.10).
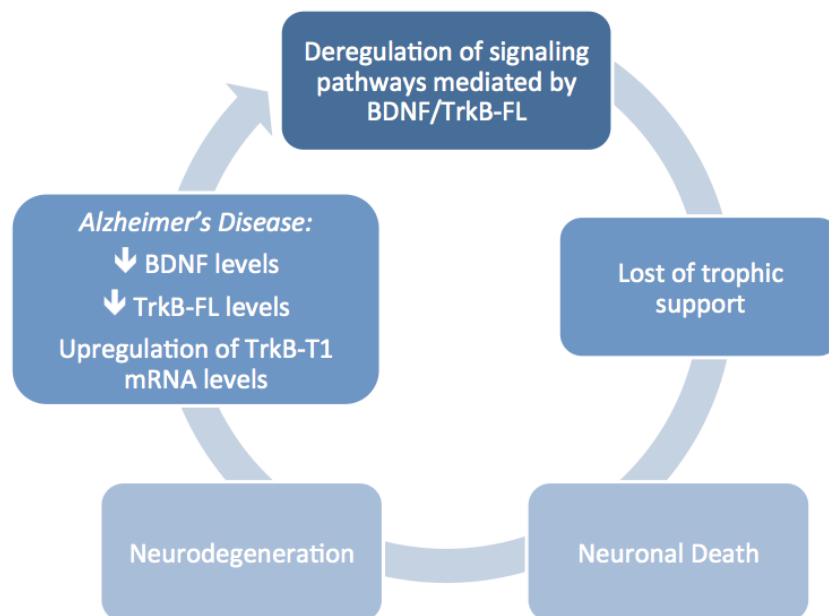
Figure 1.10 – Role of BDNF/TrkB-FL system on neurodegeneration: a putative cycle with positive feedback. As mentioned above, dysregulations on BDNF/TrkB-FL system leads to neurodegeneration, where it is described that there is a notorious decrease of BDNF and TrkB-FL levels and also upregulation of TrkB-T1 mRNA levels. Consequently, these indicated changes will then promote again dysregulations of signalling pathways mediated by BDNF/TrkB-FL, leading to the establishment of a closed cycle, where causes or consequences are not fully understood yet.

Concerning calpain-cleavage of TrkB-FL receptor, it is important to describe that are generated two new fragments: a new truncated TrkB receptor (TrkB-T') containing transmembranar domain and an intracellular fragment that is released to

cytosol composed by the intracellular kinase domain of TrkB-FL receptor (TrkB-ICD) [106]. So, we can hypothesize that these fragments can play a role on cell functioning. Indeed, being TrkB-T' a truncated receptor one could speculate whether it could act as negative regulator of TrkB-FL signalling, as other truncated isoforms. Moreover, being equided with tyrosine kinase domain, TrkB-ICD, could also have a role.
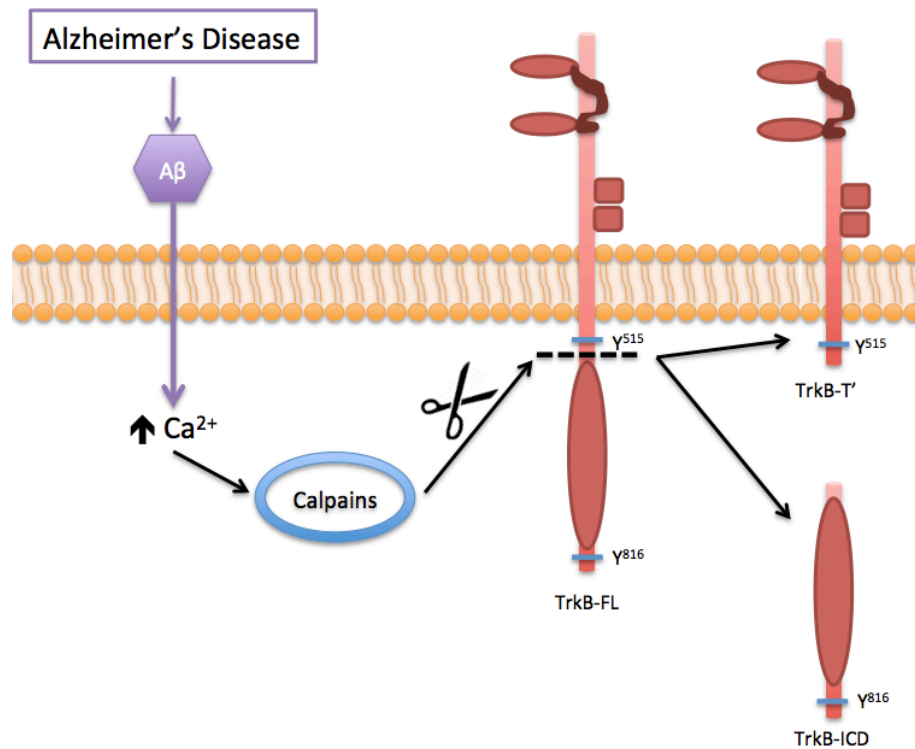
Figure 1.11 – Schematic representation of Aβ-induced overactivation of calpains and consequent cleavage of TrkB-FL receptor, generating TrkB-ICD and TrkB-T'. The accumulation of extracellular Aβ peptide has several consequences and different neurotoxic effects, being one of them associated with the dysregulation of Ca^{2+} homeostasis that will overactivate the calpains. In turn, this overactivation cleaves several substrates, including TrkB-FL receptor, promoting the release of TrkB-ICD to the cytosol and forms a truncated receptor TrkB-T'.

Although, the evidence that calpain overactivation can induce the cleavage of important proteins forming new fragments thought to be involved in AD pathophysiology, there was no information about the role of TrkB-ICD until the present thesis elaboration.

1.3   Calpains

Calpains are Ca^{2+}-activated proteases with biological and physiological importance, contributing to the regulation of cell homeostasis [116,117]. There are several isoforms of calpains, being the most expressed calpain-1 (μ-calpain) and calpain-2 (m-calpain). These isoforms have a key role on the regulation of many cellular processes, by cleavage of several substrates in interdomain regions [118,119]. In particular, these enzymes have a crucial role in several physiological processes, such as proliferation, motility, differentiation, apoptosis and memory [120]. Calpains are also involved in cytoskeletal turnover and remodelling, since these enzymes cleave some cytoskeletal proteins, including tau protein, microtubule-associated proteins (MAP), neurofilaments, spectrin and also actin [121–125].

Although calpains play an important role in physiology, they can also contribute to degeneration when persistently overactivated [118,126]. Multiple sclerosis, cancer or even allergic encephalomyelitis are examples of diseases where calpains may have a role [119,127,128]. And indeed, the sustained activation of calpains is considered as a pathogenic mechanism of AD. Actually, there are several reports showing calpains overactivation on AD *post-mortem* human brain samples. Moreover, *in vitro* studies demonstrated that calpain-1 overactivation promotes amyloid plaque formation and correlates calpains location with neurofibrillary tangles [118,129–133]. Importantly, studies with AD brains after short *post-mortem* intervals demonstrated that calpains overactivation really contributes to neuronal death, discarding the hypothesis that the activation of calpain-1 isoform could be a consequence of *post-mortem* autolytic processes [134,135]. In addition, it was also described that calpastatin, an endogenous calpain inhibitor, is markedly depleted from dendrites in AD brain, contributing also to calpains overactivation [136]. Concordantly, APP transgenic mice genetically deficient on calpastatin, show increased Aβ amyloidosis, tau phosphorylation, microgliosis and mortality when compared with the same mouse model of AD (APP) without genetic manipulation [143]. Remarkably, using also the APP mice, calpain inhibition rescues spatial-working memory and neuronal plasticity [137].

As a consequence of cleavages mediated by calpains, there is not only a loss of biological functions of original substrates, but also the generation of new stable fragments. Hence, fragments generated by calpains can acquire distinct functions and localizations when compared to the original substrate from which they were produced (Figure 1.12).
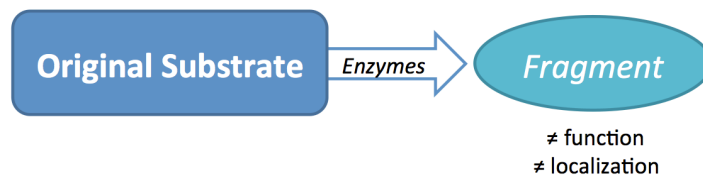
Figure 1.12 – Action of calpains on cell substrates. Cleavage mediated by calpains produces fragments with different function and localization than the original substrate, which may lead to disruption of cell homeostasis.

1.3.1   Fragments produced by calpain cleavage

In adition to TrkB-FL receptors, there are several other proteins known to be cleaved by calpains, such as Src, β-catenin, p35 and mGluR1α receptor.

A)   Src protein

Src protein is an enzyme involved in survival, growth and/or proliferation of neuronal cells, being also responsible for survival of glial cells, through cooperation with Ret receptor at the surface of these non-neuronal cells [138–140]. However, results obtained in cultured cortical neurons and in *in vivo* rat model of focal ischemic stroke (where there is a persistent increase of Ca^{2+} levels) demonstrated that this protein is cleaved by calpains. Consequently, its functions are lost and a new cytosolic fragment is formed which is known to mediate neuronal death, possibly through the inhibition of Akt pathway. In accordance with these findings, the administration of a fusion peptide that blocks the Src cleavage protects cells against excitotoxic neuronal death. This clearly shows that Src fragment has a crucial role on neuronal damage [141].

B) β-catenin protein

β-catenin is a protein that, in cooperation with the transcription factor Tcf/Lef, promotes signalling cascades involved in a wide variety of developmental process as well as in carcinogenesis [142–144]. Nevertheless, in hippocampal neurons, fragments originated by β-catenin calpain-cleavage are translocated to the nucleus, affecting gene transcription, by the activation of Tcf-dependent gene transcription [145]. Interestingly, there are several reports describing that dysregulations of β-catenin-Tcf-mediated gene regulation are a pathogenic process in innumerable neurological diseases, including bipolar disorder and AD [146–148].

C) p35 protein

The cleavage of p35 protein into p25 fragment is another example of calpains proteolytic processes, activated by increased levels of intracellular Ca^{2+}, which produces fragments with toxic effects on nervous system [149–151]. The evaluation of *post-mortem* brain tissues from AD patients and also *in vitro* assays demonstrated that there is a neuronal accumulation of p25 fragment, activating in a constitutive way the cyclin-dependent kinase 5 (CDK5), which acquires different cellular location and lost its substrate specificity [149]. These alterations of CDK5 properties impair its normal function (neurite growth), promoting, *in vivo*, hyperphosphorylation of tau protein. In addition, in cultured primary neurons, p25/CDK5 complex induces cytoskeletal disruption, morphological degeneration and also neuronal apoptosis, characteristic features of AD [149,152–154].

D) mGluR1α protein

The mGluR1α receptor plays a crucial role in the regulation of neurotransmission, as well as in the regulation of neuronal survival, through PI3K/Akt pathway [155,156]. Interestingly, it is described that an overactivation of NMDA receptors promotes a dramatic increase of Ca^{2+} intracellular levels that induces a

strong and sustained activation of calpains, which stimulates the cleavage of mGluR1α by calpains. This truncated form of mGluR1α contributes to excitotoxicity, since it is also capable of increase cytosolic Ca^{2+} levels and its capability of activating PI3K/Akt pro-survival signalling is lost [157].

E)   TrkB-FL receptor

As mentioned before, TrkB-ICD fragment were recently described, keeping this fragment in the shadows. Nevertheless, it is already described that Trk receptors can be cleaved with dramatic consequences on neuronal survival. In particular, caspase-3 is able to cleave TrkC receptor, impairing its signalling and, importantly, producing a fragment with pro-apoptotic activity, mediating cell death through a mechanism mediated by caspase-9 [158].

Interestingly, previous work on our lab already demonstrates the presence of TrkB-ICD in human brain samples, what indicates that this fragment can indeed play a role in AD pathophysiology [106]. Concordantly, unpublished data from our lab using *post-mortem* human brain samples (frontal cortex) from patient with AD and an age-matched control demonstrate that TrkB-FL receptors are decreased and TrkB-ICD levels are increased in the AD brain (Figure 1.13).
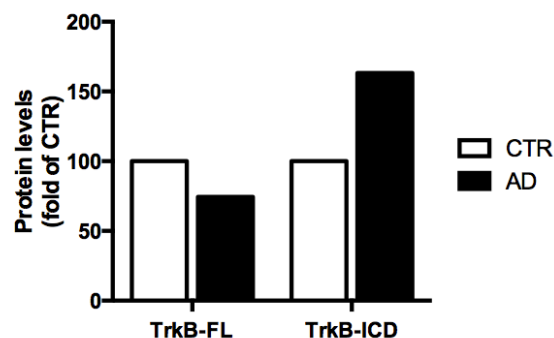
Figure 1.13 – Alterations of both TrkB-FL and TrkB-ICD levels in the brain of AD, when compared with an age-matched control (CTR). TrkB-FL receptor levels are decreased, while TrkB-ICD levels are increased on *post-mortem* human brain samples from an AD patient, when compared with an age-matched control (unpublished data).

Noteworthy that it was recently described that, under ischemia and excitotoxicity conditions, TrkB-FL is downregulated by calpains [159]. Although the authors did not identify TrkB-ICD fragment, it is expectable that, in that context, this fragment might be also formed given the calpain overactivation. Thus, one could anticipate that TrkB-ICD fragment can be produced in conditions where calpains are robustly activated.

1 Introduction

2 Aim

The main focus of this work was to characterize the intracellular TrkB receptor fragment (TrkB-ICD) originated from the TrkB-FL receptor cleavage by calpains overactivation induced by Aβ peptide.

Accordingly, this work had the following specific aims:

- To optimize transfection process and subcellular fractionation protocol (*Chapter 4*);
- To explore intrinsic characteristics of TrkB-ICD fragment:
  - Protein stability (*Chapter 5*);
  - Subcellular localization (*Chapter 6*);
  - Kinase activity (*Chapter 7*).

2 Aim

3 Methods

3.1 Cells cultures

3.1.1 H4 Cell line – Neuroglioma cells

H4 cells (Figure 3.1A) were purchased from ATCC (HTB-148 – Virginia, USA) and are a human neuroglioma cell line, obtained from a 37 year-old man. This cell line was chosen given its suitablility as a transfection host. H4 cells were cultured in Opti-MEM, containing 10% of FBS, 100 units/mL penicillin, 100 μg/mL streptomycin and 2 mM L-glutamine at 37°C under a humidified 5% CO_2 atmosphere. Cells were passaged every four days with a subcultivation ratio of 1:10 using a trypsin solution (0.025% (wt/vol)) after washed with Hanks' balanced salt solution (HBSS). Before each passage, cells never reached 100% of confluence to maintain its exponential growth and avoid the loss of its ability to resume exponential growing after passaging. Cells with more than 30 passages were discarded and renewed for new passages. For immunofluorescence cells were plated in glass coverslips previously coated with 10 μg/mL of poly-D-lysine (PDL).

3.1.2 Primary neuronal cultures

Primary cultures of cortical neurons (Figure 3.1B) were prepared from foetuses of 18-day pregnant females. The foetuses were collected in HBSS and rapidly decapitated to obtain the cortical brain, after the removal of meninges. The cerebral cortices were isolated and mechanically fragmented. Tissue digestion was performed with 0.025% (wt/vol) trypsin solution in HBSS without Ca^{2+} and Mg^{2+} (HBSS-2) for 15 min at 37°C. After trypsinization, cells were washed twice with a solution of HBSS containing serum, and resuspended in Neurobasal medium supplemented with 0.5 mM L-glutamine, 25 μM glutamic acid, 2% B-27 and 25 U/mL penicillin/streptomycin.

3 Methods

Cells were then plated on 10 µg/mL PDL-coated dishes at a density of 5x10^5 cells/cm^2 and maintained at 37°C in a humidified atmosphere of 5% CO_2.
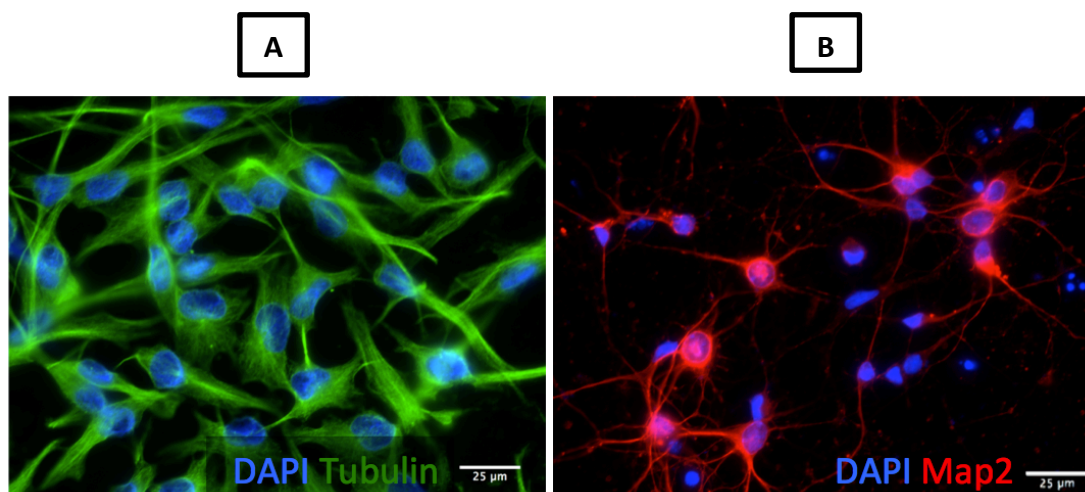
Figure 3.1 - Representative images of (A) H4 cells and (B) primary cortical neurons. (A) Representative immunofluorescence image of H4 cells. (B) Representative immunofluorescence image of 7 DIV primary cortical neurons. In both images, in blue it is represented the cell nuclei (DAPI staining), in green it is represented tubulin (cytosolic marker) (A) and in red it is represented Map2 (neuronal marker) (B). Widefield fluorescence images were acquired with a 63x objective in order to show a normal confluence of H4 cells and neurons with 7 days *in vitro* (DIV). Scale bar: 25 µm.

3.2 Cloning

Three types of DNA plasmids were used: TrkB-ICD-V5tag, TrkB-ICD and a control vector, Empty Vector (EV) (see Table 3.5).

Table 3.1 – Expression vectors used in this experimental work.

Vector	Molecular Weight (kDa)	Specific Antibody
Empty Vector (EV)	-	-
TrkB-ICD-V5 (ICD-V5)	37	Anti-V5 tag
TrkB-ICD (ICD)	32	Anti-Trk C-terminal (C-14)

Previously [96], TrkB-ICD fragment sequence had been already cloned into a mammalian expression vector fused with a V5-Tag (TrkB-ICD-V5, Figure 3.2A). Therefore, in this work, similar expression vector was constructed, but without the V5-Tag (TrkB-ICD, Figure 3.2B), to better represent the protein of interest when it is formed *in vivo*.
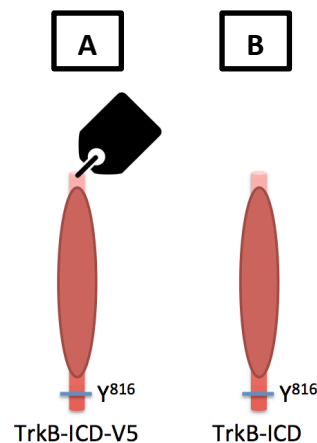
Figure 3.2 – Expression vectors used in this work: (A) TrkB-ICD-V5 and (B) TrkB-ICD. (A) represents the fragment with a V5 tag that is used to recognize specifically this protein (TrkB-ICD-V5); (B) represents the same fragment without tag, corresponding to a more physiologic form of the fragment studied (TrkB-ICD).

Initially, PCR primers were designed with the proper sequences to amplify TrkB-ICD sequence. Given that TrkB-ICD fragment sequence does not include an initiation code, and it is generated by calpain-cleavage of TrkB-FL receptor and not by *de novo* synthesis, primers' sequence contained the Kozak sequence with the initiation codon (ATG) to promote the initiation of translation. Furthermore, we also had to consider the presence of the required sequence to facilitate directional cloning (CACCA), the ratio of guanine and cytosine nucleotides (50<60%) and their melting temperature (54<60°C). In this way, the designed primers were: forward primer 5'-CACCATGAGCCAGCTCAAG-3' and reverse primer 3'-CTAGCCTAGGATGTCCAG-5'.

Then, the product was amplified by RT-PCR technique with the custom TrkB-ICD primers and a band with ~910bp corresponding to the expected TrkB-ICD length was obtained (Figure 3.3). Next, this band was isolated and purified using a DNA extraction kit (Wizard PCR Clean-Up system, Promega, Wisconsin, USA).

Primers: ICD Fw + ICD STOP = 913 bp
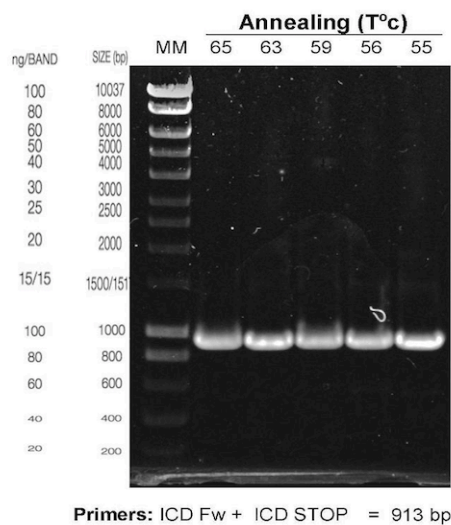
Figure 3.3 – Amplification of TrkB-ICD by PCR. Agarose-gel electrophoresis showing the amplification of TrkB-ICD fragment by PCR with different annealing temperatures. The expected size of TrkB-ICD product is 910bp, which corresponds to the bands obtained.

Following the purification process, the cloning step was performed, using the pcDNA3.2 Gateway Directional TOPO expression kit (Invitrogen, USA). The cloning reaction was constituted by 3 ng of purified TrkB-ICD product and 3 ng of linearized pcDNA 3.2 TOPO vector. Subsequently, the transformation of the chemically competent *E. coli* cells (TOP10, Invitrogen, USA) was performed and plated in selective media overnight at 37°C.

After the transformation process, *E. coli* colonies were selected and analysed by PCR technique with combination of different restriction enzymes in order to confirm the presence of the plasmid of interest with the TrkB-ICD inserted in the correct direction, being lastly chosen one of the plasmids to be sequenced by DNA sequencing.

Finally, neuroglioma cell line (H4 cells) was transfected with the expression vector. Throught western-blot assays (*Section 3.6*), it was possible to confirm the presence of a protein with the same expected molecular weight of TrkB-ICD fragment (~32kDa, Figure 3.4A). All the cloning process is summarized in Figure 3.4B.
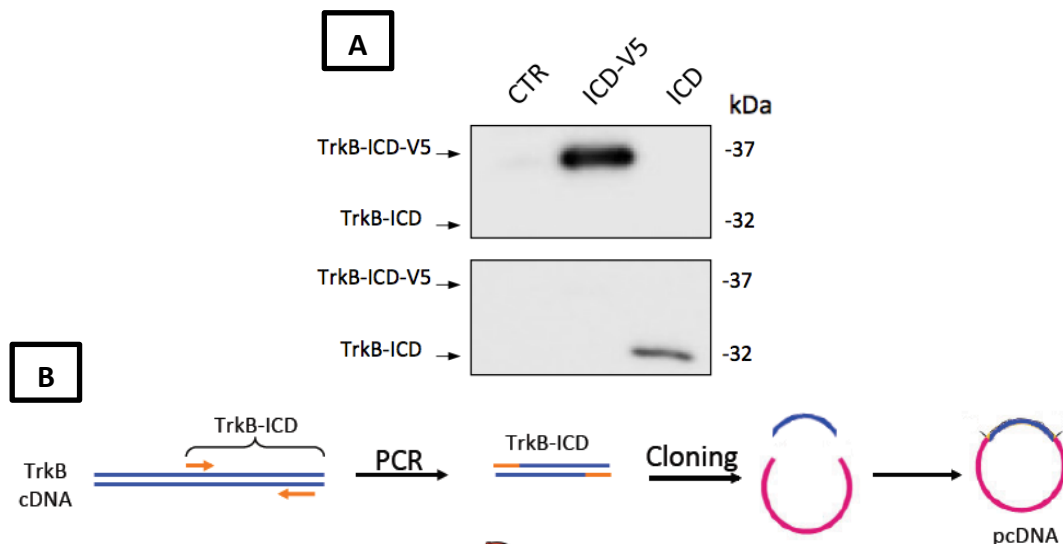
Figure 3.4 – (A) H4 cells transfected with TrkB-ICD-V5 and TrkB-ICD plasmids and (B) summary of plasmid cloning process. (A) Western-blot image of H4 cell line transfected with pcDNA-TrkB-ICD-V5 (second lane) and pcDNA-TrkB-ICD (third lane) after 24 hours of its expression. The first lane corresponds to non-transfected cells (CTR). Upper panel shows the probe with anti-V5tag antibody, which detects the expression of TrkB-ICD-V5 protein, whereas lower panel was probed with anti-Trk C-terminal tail (C-14) antibody, identifying TrkB-ICD fragment. (B) Schematic representation of all steps done performed to clone plasmids, as detailed above. Abbreviations: CTR, non-transfeted cells; ICD, TrkB-ICD; ICD-V5, TrkB-ICD-V5; PCR, Polymerase Chain Reaction.

3.3   Transfection

Cells were transfected using Lipofectamine 2000 reagent (Invitrogen, USA) according to the manufacturer's instructions, as schematically presented in Figure 3.5. Briefly, before transfection, cell medium was renewed and DNA plasmid and Lipofectamine reagent were diluted, separately, with equal volume of Opti-MEM medium for 5 minutes at room temperature (RT). Next, these two different solutions were gently mixed at RT, for 20 minutes, obtaining one final solution with diluted DNA and diluted Lipofectamine reagent. Following this incubation, we added this last solution to ~80% confluent cells. H4 cells were transfected with 2 DIV and primary neuronal cultures were submitted to transfection process at 7 DIV, since these DIV's correspond to the confluency needed. Initially, both DNA plasmid and Lipofectamine amounts were tested in order to optimize the transfection process and, after that, 1.5 µg of DNA and 1.5 µL of Lipofectamine reagent per mL of culture medium were used. It is important to mention that ratio optimized (1:1 (wt/vol)) is in accordance

with other studies that specially studied different parameters of transfection process [160,161]. Concerning duration of transfection, several times were tested (results shown in Figure 4.1), being the 16-24 hours of transfection the interval most used in all experiments.
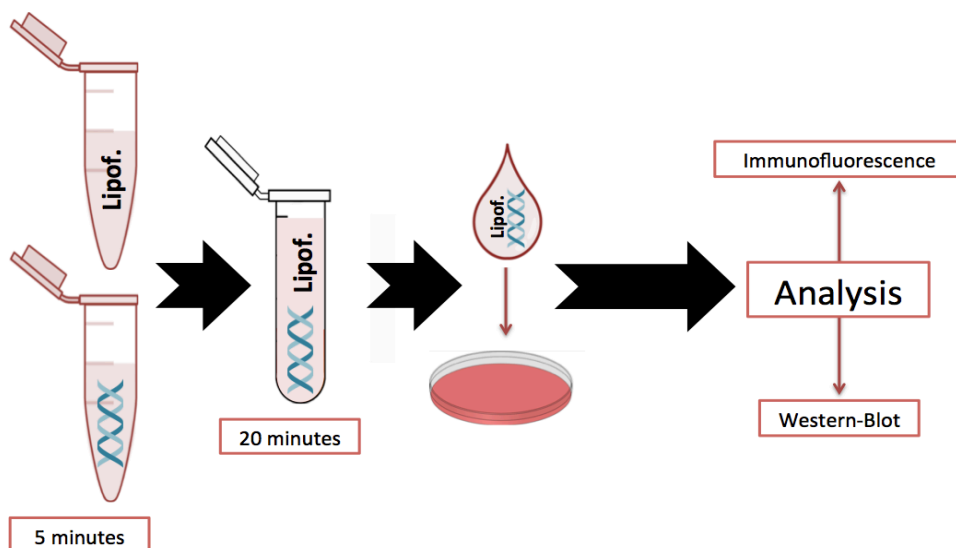
Figure 3.5 – Schematic representation of transfection process. This figure summarizes the steps of the transfection process. After incubation of the final mix, cells were fixed or lysed (generally after 24 hours), to analysis with immunofluorescence or western-blot assays, respectively. Abbreviations: Lipof. – Lipofectamine; – DNA plasmid.

3.4 Drug treatments

To evaluate protein stability and to estimate its half-life time ($T_{1/2}$), H4 cells with 2 DIV and primary neuronal cultures with 7 DIV were transfected with TrkB-ICD vectors for 16 hours, and incubated with an inhibitor of eukaryotic protein biosynthesis, cyclohexamide (CHX). CHX (5 µM) was incubated for 0, 4, 8 and 24 hours. After this treatment, protein levels were assessed by western-blotting, as described in *Section 3.6*. In order to determine mathematically $T_{1/2}$ of TrkB-ICD, we followed a strategy described by Belle *et al* [162]. Briefly, and assuming that protein degradation follows first-order decay kinetics, TrkB-ICD levels (*N* in the following equation) were initially log-transformed and then linear regression was used to determine the decay rate constant (*k*). Then, it is possible to calculate $T_{1/2}$, using the above equation.

$$\ln(N) - \ln(N_0) = -kt \Longrightarrow T_{1/2} = \frac{\ln(2)}{k}$$

In the experiments performed to evaluate the contribution of signalling pathways on protein phosphorylation (*Section 7.4*), a cocktail of drugs detailed in Table 3.2 (U 0126 (10 µM); H-89 (25 µM); K252a (200 nM); LY 294002 (10 µM); PP2 (10 µM); Staurosporin (100 µM) and U 73122 (4 µM)) were added 15 minutes before the administration of transfection mix to 7DIV primary neuronal cultures. 24 hours later, protein levels were assessed by western-blotting, as described in *Section 3.6*.

Each set of results has a timeline chronogram with the time points studied, in order to facilitate the understanding of associated methodology, as shown in Figures 4.3, 5.1 and 7.7.

3.5   Subcellular Fractionation

Cells were washed twice with ice-cold phosphate buffered saline (PBS) (137 mM NaCl, 2.7 mM KCl, 8 mM $Na_2HPO_4.2H_2O$ and 1.5 mM KH_2PO_4, pH 7.4) and placed on ice. After that, cells were detached from the plate surface with PBS-EGTA solution (1.0 mL per plate) and collected into a microcentrifuge tube. Cells were centrifuged at 800g for 5 minutes at 4°C to collect the cells and discard the remaining supernatant. Then, cell pellets were resuspended in an ice-cold harvest buffer (0.3 mL per plate) containing 10 mM HEPES (pH 7.9), 50 mM NaCl, 0.5 M sucrose, 0.1 mM EDTA, Triton X-100 (0.5%), 1 mM DTT and protein inhibitors: 10mM NaF, 5 mM Na_3VO_4 and protease inhibitors cocktail (Roche, Penzberg, Germany). The homogenate was incubated on ice for 5 minutes (50 µL of this solution was stored at -20°C corresponding to homogenate), and then centrifuged at 1200g for 10 minutes at 4°C to collect the nuclear fraction (pellet) and the cytoplasmic and membrane proteins fraction (supernatant). The fraction enriched in cytoplasmic and membrane proteins was cleaned up through a re-centrifugation at 16000g, for 15 minutes.

The fraction enriched in nuclear proteins was resuspended in 1mL of Buffer A, composed by 10mM HEPES (pH7.9), 10mM KCl, 0.1 mM EDTA, 0.1 mM EGTA, 1 mM DTT and protein inhibitors: 10 mM NaF, 5 mM Na_3VO_4 and protease inhibitors

cocktail and centrifuged at 1200g for 10 minutes at 4°C. The pellet obtained was resuspended in 25 µL of Buffer C (10 mM HEPES (pH 7.9), 500 mM NaCl, 0.1 mM EDTA, 0.1 mM EGTA, 0.1% NP-40, 1 mM DTT and protease and phosphatase inhibitors) and mixed vigorously for 15 minutes at 4°C. After a new centrifugation at 16000g for 10 minutes at 4°C, the supernatant (nuclear fraction) was collected.

The three fractions obtained in this protocol (homogenate (H), fraction enriched in cytoplasmic and membrane proteins (C&M) and fraction enriched in nuclear proteins (N)) were stored at -20°C until analysis by western-blotting (Figure 3.6).
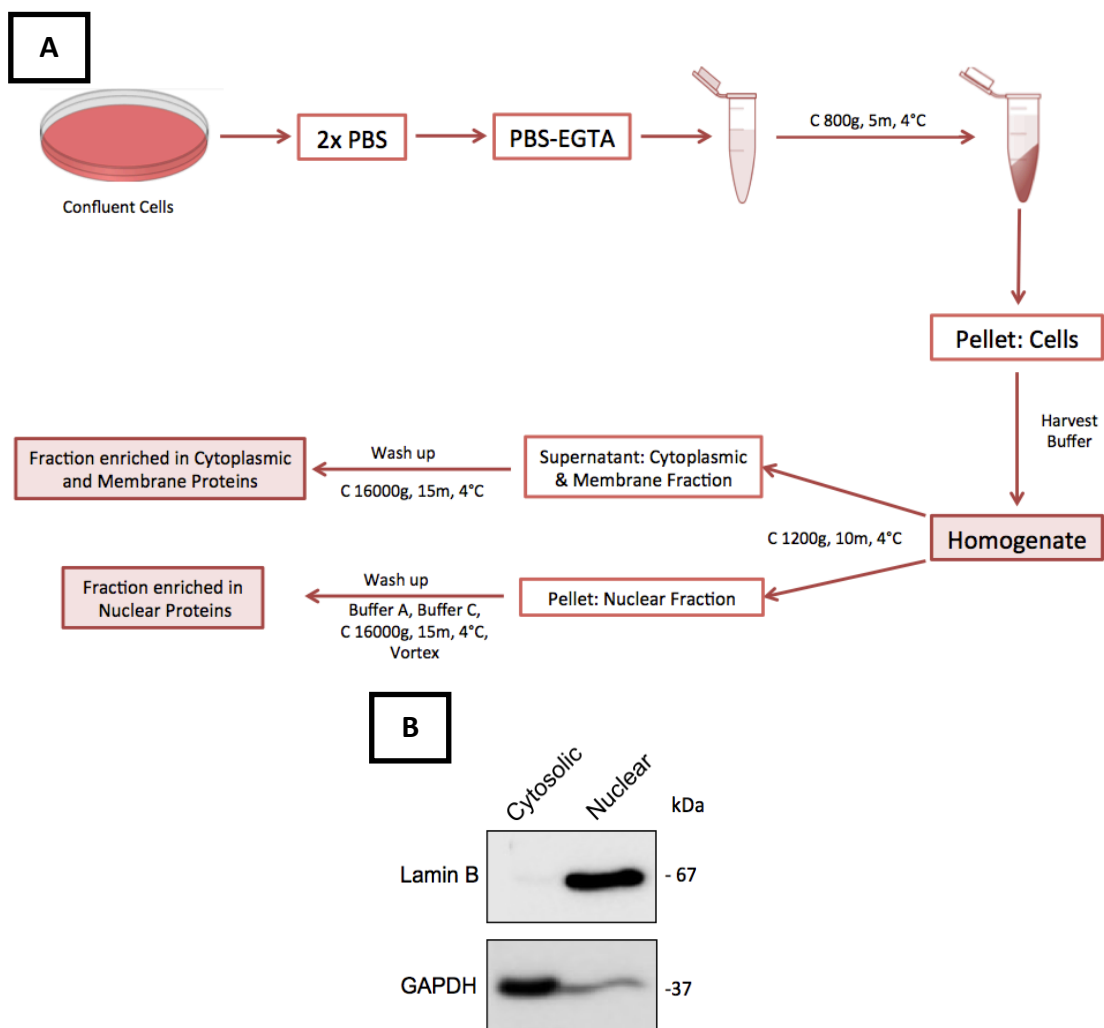
Figure 3.6 – Subcellular fractionation protocol: (A) summary of all steps and (B) preliminary results. (A) Protocol for subcellular fractionation including solutions, buffers and conditions of centrifugations (identified with a "C" over the arrows). (B) Western-blot image of H4 cells validating the subcellular fractionation protocol in order to distinguish cytosolic and membrane fraction from nuclear fraction. Lamin B is a nuclear protein, whereas GAPDH is a cytosolic protein and therefore these proteins can be considered as nuclear and cytosolic markers, respectively.

3.6   Western-blot

Both H4 and neuronal cultures, were washed with ice-cold PBS and lysed with a Radio-Immunoprecipitation Assay (RIPA) buffer containing: 50mM Tris-HCl (pH 7.5), 150mM NaCl, 5mM EDTA, 0.1% SDS, 1% Triton X-100 and protein inhibitors: 10mM NaF, 5 mM Na_3VO_4 and protease inhibitors cocktail previously mentioned. After resuspension and sonication, cell lysates were clarified by centrifugation (16000g, 10 minutes at 4°C) and the amount of protein in the supernatant was determined by Bio-Rad DC reagent. All samples were applied with same amount of total protein, separated on 10% sodium dodecyl sulphate-polyacrylamide gel electrophoresis (SDS-PAGE) and transferred onto PVDF membranes (GE Healthcare, Buckinghamshire, UK). Membranes were stained with Ponceau S solution to confirm the transference efficacy. After blocking with 5% non-fat dry milk solution in TBS-T (20 mM Tris base, 137 mM NaCl and 0.1% Tween-20), membranes were washed three times with TBS-T, before incubation with the primary (overnight at 4°C) and with the secondary antibodies (1 hour at RT). Finally, immunorreactivity was visualized using ECL chemiluminescence detection system (Amersham-ECL Western Blotting Detection Reagents from GE Healthcare, Buckinghamshire, UK) on Chemidoc XRS+ system (Bio-Rad, California, USA) and bands intensities were quantified by digital densitometry (*ImageJ 1.45* software, Maryland, USA). The intensities of GAPDH bands were used as loading control.

3.7   Immunofluorescence

For immunofluorescence assays, cultured cells were fixed and permeabilized in methanol for 15 min at RT. After this process, cells were incubated with primary antibodies, overnight at 4°C, washed in PBS and subsequently incubated with the fluorescent-labeled secondary antibodies for 1 hour at RT. After the incubation with the specific antibodies, a solution of DAPI (1:7500) was added for 10 minutes to stain the cell nuclei. Afterwards and before mounting the preparations in Mowiol, the cells were washed with PBS. Fluorescence images were recorded using an Axiovert microscope (Carl Zeiss Inc., Göttingen, Germany).

3.8   Statistical analysis

The data are expressed as mean ± SEM of the *n* number of independent experiments. The significance of differences between the means of two conditions was evaluated by Student's *t*-Test. To perform multiple comparisons between the means of more than two conditions a one-way ANOVA followed by a Bonferroni *post-test* was performed. Values of $p<0.05$ were considered to represent statistically significant differences. *Prism GraphPad* software (La Jolla, California, USA) was used for statistical analysis.

3.9 Reagents, drugs and antibodies

3.9.1 Culture reagents

Table 3.2 – Drugs/Mediums used in cell cultures.

Reagents	Description/Purpose
B-27 Supplement	Serum-free supplement to increase viability and growth of neuronal cell culture.
Fetal Bovine Serum (FBS)	Promotes trophic support to cell cultures since it contains growth factors. It is also used to inhibit trypsin due to the presence of the protein α1-antitrypsin, allowing the adherence of cells to plate's surface.
Glutamine (Q)	Unstable essential amino acid required in culture media, due to its instability in liquid state and physiological pH.
Lipofectamine 2000	This drug is able to consistently transfect many cell types, such as H4 neuroglioma cells and primary neuronal cultures.
Neurobasal Medium	Medium specially formulated to grow embryonic neuronal cells, such as primary neuronal cultures.
Opti-MEM Medium	Reduced-serum medium recommended to dilute lipofectamine reagent and nucleic acids before complexing. Medium also used to grow H4 cells.
Pen-Strep solution	Solution composed by two antibiotics (penicillin and streptomycin) used to avoid contaminations of cell cultures with microbiological organisms.
Trypsin	Proteolytic enzyme used to dissociate cells.

3 Methods

3.9.2 Drugs

Table 3.3 – Drugs used for cells treatment.

Drugs	Description/Purpose	Final concentration used	Supplier
Cyclohexamide (CHX)	Inhibitor of protein biosynthesis in eukaryotic organisms through the blockage of translational elongation.	5 µM	Sigma
U 0126	Selective inhibitor of ERK 1/2.	10 µM	Tocris Bioscience
H-89	Inhibitor of Protein kinase A.	25 µM	Sigma
K252a	Non-selective tyrosine kinase inhibitor. Inhibits Trk kinase activity.	200 nM	Tocris Bioscience
LY 294002	Selective inhibitor of PI3K.	10 µM	Tocris Bioscience
PP2	Selective inhibitor of Src-family tyrosine kinases.	10 µM	Tocris Bioscience
Staurosporin	Potent protein kinase C inhibitor. Analogue compounf of K252a.	100 µM	Sigma
U 73122	Selective inhibitor of PLCγ.	4 µM	Tocris Bioscience

3.9.3 Antibodies

Table 3.4 – Primary antibodies used in Western-blot and Immunofluorescence assays.

Primary Antibodies	Technique and Dilution	Supplier
Rabbit polyclonal anti-Trk C-terminal tail (C-14)	WB – 1:1250 IF – 1:150	Santa Cruz Biotechnology (sc-11)
Rabbit polyclonal anti-V5 probe (G-14)	WB – 1:1250	Santa Cruz Biotechnology (sc-83849)
Mouse monoclonal anti-pTyr (anti-PY99)	WB – 1:1000 IF – 1:150	Santa Cruz Biotechnology (sc-7020)
Rabbit polyclonal anti-α-tubulin	IF – 1:150	Abcam (ab4074)
Mouse monoclonal anti-GAPDH	WB – 1:5000 IF – 1:150	Life Technologies (AM4300)
Goat polyclonal anti-Lamin B (C-20)	WB – 1:500	Santa Cruz Biotechnology (sc-6216)
Mouse monoclonal anti-GFAP	IF – 1:100	Abcam (ab10062)
Mouse monoclonal anti-MAP2 (clone AP20)	IF – 1:150	Millipore (MAB-3418)
Rabbit polyclonal anti-Tau	IF – 1:150	Synaptic Systems (314 002)

Table 3.5 – Secondary antibodies used in Western-blot and Immunofluorescence assays.

Secondary Antibodies	Technique and Dilution	Supplier
Goat anti-mouse IgG-HRP	WB – 1:10000	Santa Cruz Biotechnology (sc-2005)
Goat anti-rabbit IgG-HRP	WB – 1:10000	Santa Cruz Biotechnology (sc-2004)
Donkey anti-goat IgG-HRP	WB – 1:10000	Santa Cruz Biotechnology (sc-2020)
Goat anti-mouse Alexa F488	IF – 1:400	Invitrogen (ab150113)
Goat anti-mouse Alexa F568	IF – 1:400	Invitrogen (ab175473)
Goat anti-rabbit Alexa F488	IF – 1:400	Invitrogen (ab150077)
Goat anti-rabbit Alexa F568	IF – 1:400	Invitrogen (ab175471)

3 Methods

4 Optimization and characterization of the transfection process

4.1 Rational

In order to characterize TrkB-ICD fragment, the cells used in this work were transfected with respective DNA plasmid and several conditions were tested to obtain the highest efficiency of transfection, since each cell culture type responds differentially to the transfection process and TrkB-ICD expression profile had never been characterized before.

Therefore, this chapter presents the work developed in order to optimize the transfection process, including the determination of optimal time of transfection and moment of medium renewal. Moreover the transgene expression (TrkB-ICD fragment) over time was evaluated and as well as the type of cells transfected in primary rat neuronal cultures (since cultures are constituted by 80% of neurons and 20% glial cells) [163].

4.2 Determination of optimal time transfection and moment of medium renewal

The expression levels of TrkB-ICD fragment were evaluated throughout time, after transfection. As shown in Figure 4.1, the TrkB-ICD fragment levels increase until 24 hours of transfection and, after that, TrkB-ICD levels progressively decrease for longer times of transfection (data not shown).

Figure 4.1 – TrkB-ICD expression on H4 cells transfected with pcDNA-TrkB-ICD-V5 plasmid. (A) Upper part shows a timeline chronogram that summarizes the protocol used to this characterization, including the moment of transfection and later cells collection. (B1) Representative western-blot probed with anti-V5tag antibody for H4 cells after different times of transfection: 4h, 8h, 16h and 24 hours. Note that TrkB-ICD evaluation was performed at 0h, 2h, 4h, 8h, 16h and 24h, however in the presented western-blot the evaluation at 2h was not studied. (B2) Analysis of bands intensities represented from densitometry quantification of TrkB-ICD-V5 immunoreactivity of 3-5 independent cultures. Data is normalized for 24 hours of TrkB-ICD expression. GAPDH was used as loading control. Data represented are mean ± SEM of n independent experiments (*p<0.5; **p<0.01; ***p<0.005; ****p<0.001; compared to "ICD 24h"; ANOVA followed by Bonferroni *post-test*). Abbreviations: ICD, TrkB-ICD; ICD-V5, TrkB-ICD-V5.

Afterwards, other transfection parameters, such as the moment of medium renewal were optimized. This optimization is of great importance since the moment of medium renewal could be determinant to understand if the presence of Lipofectamine/DNA complexes that did not transfect the cells and stayed in suspension could contribute to lower transfection efficiency. Thus, two different timepoints of medium renewal were evaluated: i) medium renewal before transfection and ii) 6 hours after transfection. The data obtained (Figure 4.2) show that the moment of medium renewal does not affect TrkB-ICD expression, at least in

the two tested conditions. Thus, in the following experiments, cell medium was changed before the transfection to simplify the experimental design.
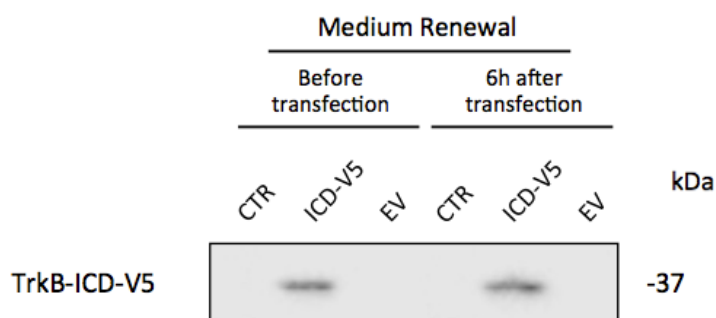
Figure 4.2 – Transfection optimization of H4 cells transfected with pcDNA-TrkB-ICD-V5: moment of medium renewal. Western-blot probed with anti-V5tag antibody for H4 cells, 24 hours after its transfection. On the left side of this panel, medium was renewed before incubation of the transfection mix, whereas on the right side of this panel, the medium was changed to a new and fresh medium 6 hours after the start of the transfection process. Abbreviations: CTR, control; EV, empty vector; ICD-V5, TrkB-ICD-V5.

The data obtained in this first step of the thesis were crucial to establish the optimal conditions of transfection, allowing proceeding to the following planned studies.

4.3   TrkB-ICD expression on primary neuronal cultures

In addition to H4 cells, primary neuronal cultures were also successfully transfected with pcDNA-TrkB-ICD using similar conditions optimized for H4 cells. However, primary neuronal cultures are constituted by 80% of neurons and 20% glial cells (mainly astrocytes) [163]. Therefore, in order to determine which type of cells were being transfected, at 24 hours of transfection, cells were labeled with specific glial and neuronal immunofluorescence markers.

We observed that the great majority of cells transfected with TrkB-ICD were also stained for Map2 (a neuronal marker) (Figure 4.3B). On the other hand, we did not detect TrkB-ICD expression in cells stained with GFAP, an astroglial marker (Figure 4.3A). These data strongly suggest that expression of TrkB-ICD fragment mainly occurs in neurons. Given the complexity related on the assessment of all cultured cells, we cannot ensure that transfection is closely restricted to neurons.
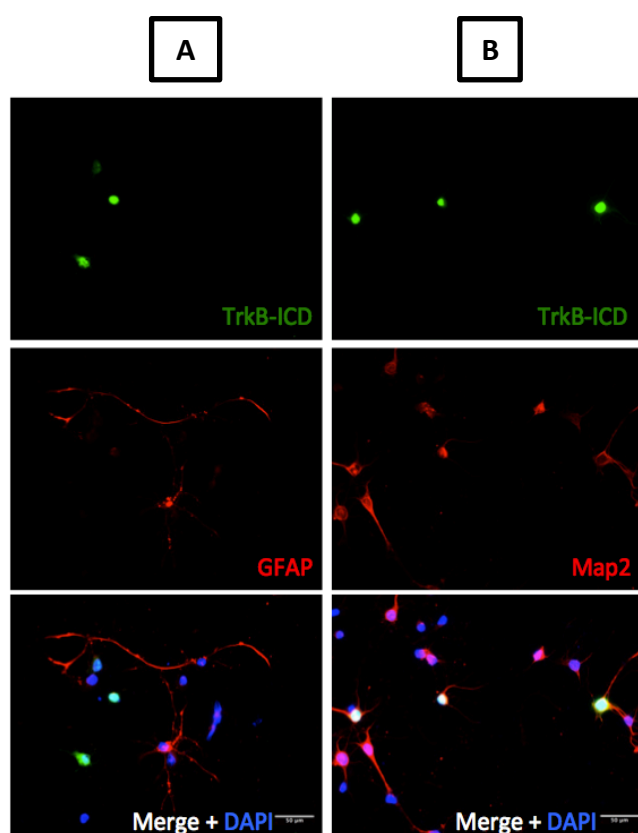
Figure 4.3 – TrkB-ICD fragment is mainly expressed in neurons. Representative immunofluorescence images of 7 DIV primary cortical neurons transfected with pcDNA-TrkB-ICD plasmid for 24 hours. In green, it is represented TrkB-ICD (stained with anti-Trk C-terminal antibody (C-14)). In the left column (A), red staining identified glial cells (stained with anti-GFAP antibody) and in the right column (B) red colour recognized neurons (stained with anti-Map2 antibody). The merge images with DAPI staining in blue (that identifies cell nuclei) are shown in the last row of panels. Widefield fluorescence images were acquired with a 40x objective in order to show that transfection is mainly a neuronal process. Scale bar: 50 μm.

Finally, and to further characterize the transfection process, the percentage of transfected cells were calculated. The relative percentage of transfected cells was approximately 15% of total cultured cells (Figure 4.4 is a representative image of a neuronal transfection). This efficiency of transfection was similar on H4 cells and on primary neuronal cultures.
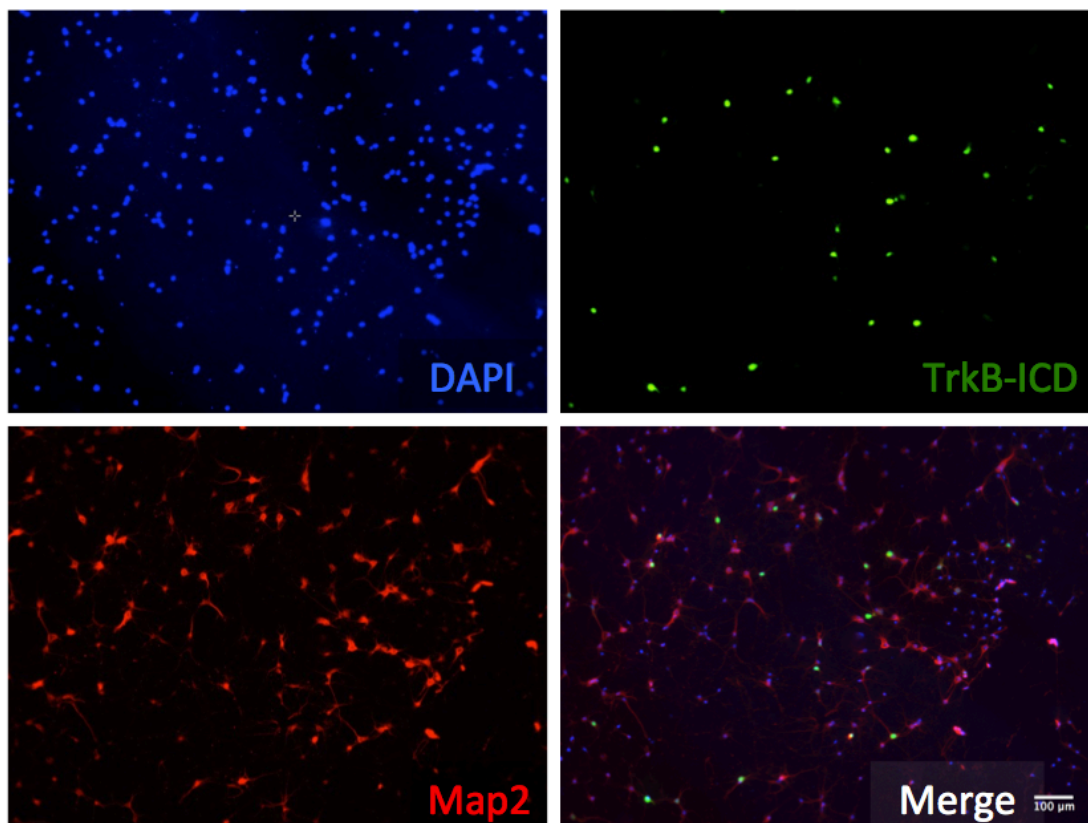
Figure 4.4 – Percentage of transfected cells is approximately 15% of total cells. Immunofluorescence image of 7 DIV primary cortical neurons transfected with pcDNA-TrkB-ICD plasmid for 24 hours. In blue it is represented the cell nuclei (DAPI staining), in red neuronal marker (stained with anti-Map2 antibody) and in green TrkB-ICD (stained with anti-Trk C-terminal antibody (C-14)). Last image represents all channels merged. Widefield fluorescence images were acquired with a 10x objective in order to quantify neurons transfected with success (36 cells expressing TrkB-ICD fragment in a total of 247 cells). Scale bar: 100 µm.

4.4 Discussion

Lipofectamine 2000 reagent is a cationic liposome formulation that acts by formation of complexes with DNA plasmids. These complexes are taken up by the cell, since it overcomes the electrostatic repulsion of the cell membrane and are actively transported across the cell membrane by an endocytotic mechanism [164,165]. This transfection reagent is used in a wide range of mammalian cell types, but it has lower transfection efficiency on primary cells, when compared with immortalized cell lines. This decrease of transfection efficiency can be explained by susceptibility of primary cells to toxic agents and the possibility of exogenous DNA plasmids be easily degraded in the cytoplasm of the cells, which will decrease the DNA available to transfect the cells [166]. Another factor that could compromise the transfection efficiency on primary cells concerns the penetration of exogenous DNA into the nucleus. Indeed, in actively dividing cells (such as H4 cell line), exogenous DNA enters in the nucleus after the reassembly of the nuclear envelope at the end of the mitosis [167]. However, post-mitotic cells (such as primary neuronal cultures) do not have mitotic processes, as its designation suggests, and exogenous DNA penetrates in the nucleus through intact nuclear envelopes, a mechanism supported by Lipofectamine reagent [165]. Compared with other methods (such as electroporation or microinjection), Lipofectamine reagent is mainly used, because provides significantly higher transfection efficiency of post-mitotic cells [165,168].

Given that TrkB-ICD expression profile had never been characterized before. This chapter was focused on the optimization of transfection protocol to allow the characterization of this fragment.

Regarding transfection time, we observed an increase on TrkB-ICD expression until 24 hours. After 24 hours of transfection, a decrease of TrkB-ICD expression levels was observed. Interestingly, these results do not completely match with the ideal transfection time mentioned by the others for other proteins [165,166,168], who indicated 48 hours as the optimal time of transfection to obtain a higher protein expression. This difference might be explained through several hypotheses, including

different accumulation pattern or half-life time of each protein studied and also possible adverse role of TrkB-ICD fragment on living cells. Moreover we should also consider other assumptions associated with specific characteristics of cells used. Regarding H4 cells, the cells confluence may be a problem, since we transfected these cells with ~80% of confluence (as advised by manufacturer) and, after transfection, its confluence reaches to 100%, leading to competition of confluent cells for the nutrients, which triggers apoptosis process on weakest cells. So, after 24 hours of transfection, when total confluence was already achieved, cell viability can be compromised and, consequently, we may assist to the decrease of heterologous proteins expression. On the other hand, it is possible that H4 cells that were not transfected have more capacity to divide, which may lead to a possible overlap of transfected cells and may contribute to decreased expression of TrkB-ICD fragment.

To transfect post-mitotic cells, Lipofectamine reagent is widely used, since it demonstrates higher efficiency, comparing with other transfection methods (transfection efficiency in primary neuronal cultures: Lipofectamine – 20-25%, other methods – <3%) [168,169]. However, after optimization steps, our transfection efficiency was around 15%. This difference (20-25% vs. 10-15%) can be associated with few protocol differences (as the preparation of primary neuronal cultures or cell density) or could suggest that the TrkB-ICD fragment has toxic properties, committing cell viability. It is important to mention that transfection efficiencies around 20-25% were obtained using a traditional gene reporter that does not affect cell viability (β-galactosidase, in the case of Ohki *et al.* [168]). Unexpectedly, the transfection efficiency of H4 cells was approximately the same obtained for cultured neurons, which could be explained by the above discussed points.

As an alternative to transfection with Lipofectamine 2000 reagent, other approaches, to express a particular protein, could be used such as the use of a different transfection reagents (NeuroMag, for instance) or viral transduction methods. Regarding viral transduction, the use of modified viruses that are more efficient, might allow the long-term expression of the protein of interest (and not

transient expression) [168,170]. Thus, to bypass some limitations of Lipofectamine reagent, we are currently optimizing viral transduction for future experiments.

Lipofectamine-DNA complexes are stable for 6 hours at RT and therefore we evaluated if its presence in suspension could affect the transfection efficiency [165]. The results obtained do not indicate differences on TrkB-ICD levels when we remove these complexes (as described by Dalby *et al* [165]), suggesting that toxicity associated to transfection is due to the process itself and it is independent on the presence of remaining complexes in suspension.

Although primary neuronal cultures have approximately 20% of glial cells (mainly astrocytes)[163], we observed that the majority of cells transfected with TrkB-ICD are positive for MAP2 staining and negative for GFAP, indicating that cells transfected were neurons.

In vivo, TrkB-FL receptor cleavage occurs in neurons, since astrocytes and other glial cells mainly express truncated isoforms of TrkB receptor. Curiously, with the transfection process used, we observed that TrkB-ICD expression is mainly present in neurons, matching to what happens *in vivo*. Indeed, this preferential cell transfection can be explained by the presence of cytomegalovirus (CMV) promoter on the pcDNA vector used. Indeed, other studies also described that CMV promoter is specifically expressed in neurons, whereas other promoters (such as SFFV promoter) are selectively expressed by glial cells [171].

Taken together, all steps optimized contributed to a successfully transfection process, allowing us to study cells expressing the fragment of interest without the exposure to Aβ.

5   Study of TrkB-ICD stability

5.1   Rational

The protein half-life time ($T_{1/2}$) corresponds to the time required for the levels of a particular protein fall to half its initial value. The $T_1/_2$ of a particular protein could range from minutes to hours or, in some particular cases, days. The determination of this parameter could be of great importance as a predictor of the protein stability and therefore about the possible impact of the specific protein on cell homeostasis. Accordingly, to determine TrkB-ICD stability, the $T_{1/2}$ was calculated. For that propose, cells were treated with cyclohexamide (CHX) (5 µM), an inhibitor of protein biosynthesis in eukaryotic cells as described in methods section.

5.2   Determination of TrkB-ICD half-life time

The experiments were conducted using H4 cells and primary neuronal cultures transfected for 16 hours and then incubated with CHX (5 µM) for different time periods: 0, 4, 8 and 24 hours as schematically represented in Figure 5.1A.

The results on H4 cells show a gradual decrease of TrkB-ICD expression levels with the increasing periods of CHX incubation. In particular, the presence of CHX for 8 hours induced a significant decrease of TrkB-ICD expression levels compared to the cells non-treated with CHX (CHX 0h) (100.0% vs. 52.2±2.3%; n=3-5; p<0.001; Figure 5.1B1/B2), whereas incubation of the same drug for 24 hours induced a dramatic decrease of TrkB-ICD expression levels, leading to the detection of residual levels of the protein (100.0% vs. 12.1±2.3%; n=3-5; p<0.001; Figure 5.1B1/B2).

In accordance with H4 cells, data obtained using primary neuronal cultures also suggest that there is a significant decrease on TrkB-ICD expression levels for longer incubations with CHX in a similar way of what detected for H4 cells (Figure 5.1C1/C2). Throught the direct interpretation of the data graphically presented in

Figure 5.1, it is possible to estimate a similar $T_{1/2}$ of TrkB-ICD, expressed in H4 cells and primary neuronal cultures, of approximately 8 hours.

To more accurately determine the $T_{1/2}$ of TrkB-ICD, the data obtained for H4 cells were used. A mathematical approach was applied as described in Methods section (*Section 3.5*) [162]. Figure 5.2 shows the first-order decay function of TrkB-ICD levels, which allow us to estimate the degradation rate constant (k=0.09128) and, using the equation present in *Section 3.5*, to estimate the $T_{1/2}$ of TrkB-ICD (7 hours and 36 minutes).
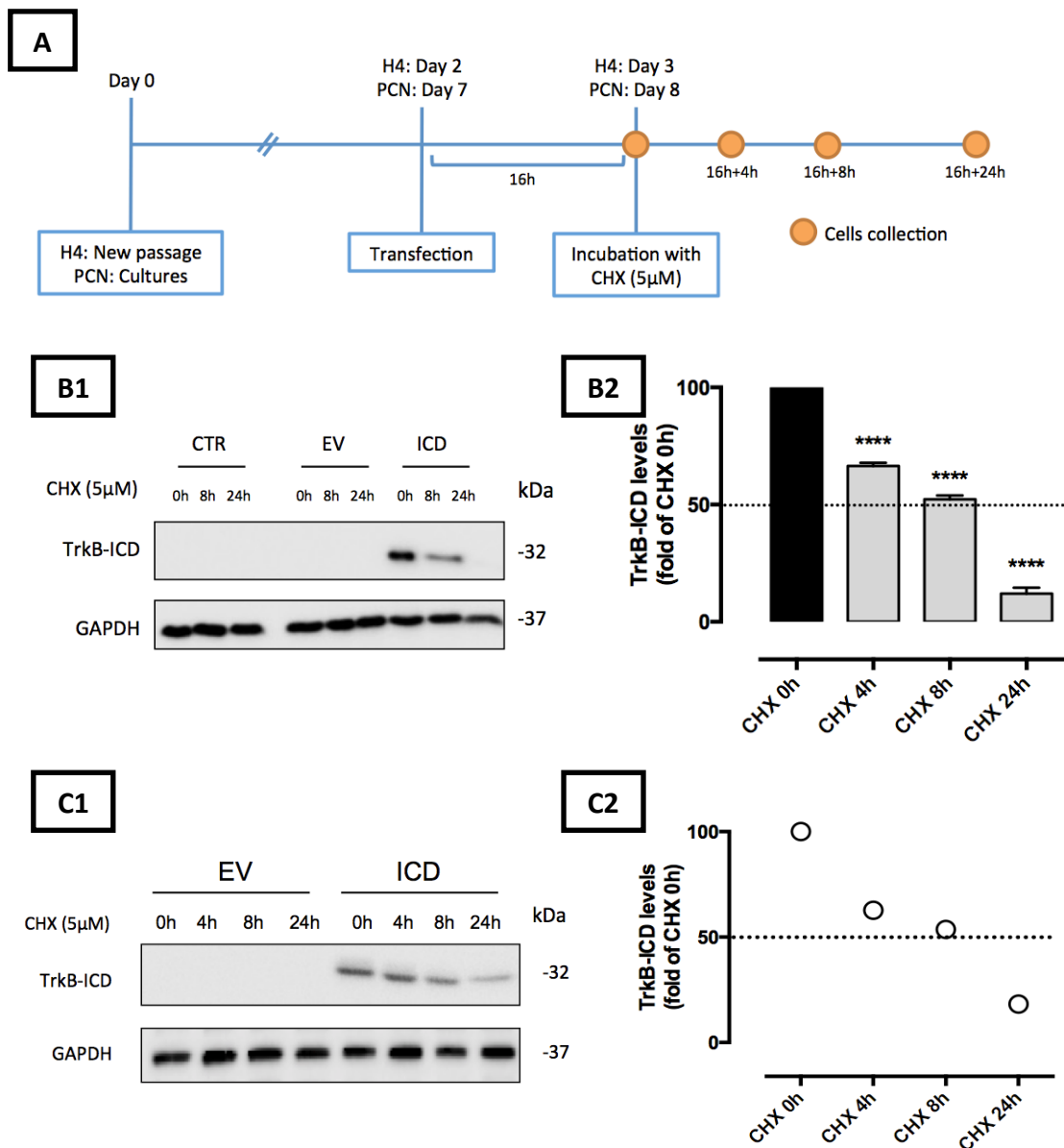
Figure 5.1 – Time course analysis of TrkB-ICD stability after CHX (5 µM) treatment on (B1, B2) H4 cells and (C1, C2) primary neuronal cultures. Upper panel (A) shows a timeline chronogram that summarizes the protocol used to CHX experiments, including the moment of transfection, incubation with CHX and later cells collection. (B1) Representative western-blot probed with anti-Trk C-terminal antibody (C-14) for H4 cells transfected with pcDNA-TrkB-ICD plasmid incubated with CHX for different times: 8 and 24 hours. (B2) Analysis of bands intensities represented in (B1) from densitometry quantification of TrkB-ICD immunoreactivity of 4-5 independent cultures. Data is normalized for amount of TrkB-ICD fragment detected on cells non-treated with CHX (CHX 0h). GAPDH was used as loading control. Data represented are mean ± SEM of *n* independent experiments. (****$p<0.001$; compared to "CHX 0h"; ANOVA followed by Bonferroni *post-test*) (C1) Representative western-blot probed with anti-Trk C-terminal antibody (C-14) for 7 DIV primary cortical neurons transfected with pcDNA-TrkB-ICD plasmid incubated with CHX for different times: 4, 8 and 24 hours. (C2) Analysis of bands intensities represented in (C1) from densitometry quantification of TrkB-ICD immunoreactivity of 1 independent culture. Data is normalized for amount of TrkB-ICD fragment detected on cells non-treated with CHX (CHX 0h). GAPDH was used as loading control. Abbreviations: CHX, cyclohexamide; CTR, control; EV, empty vector; ICD, TrkB-ICD; PCN, Primary Cortical Neurons.
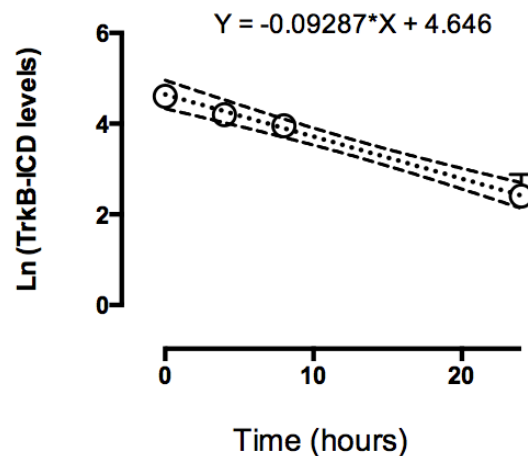
Figure 5.2 – First order decay function: an intermediate step to determine TrkB-ICD half-life time. After CHX treatment, TrkB-ICD levels were log-transformed ant then a linear least-squares fit was used to determine the decay rate constant, which corresponds to the slope of the linear regression.

5.3   Discussion

Given that CHX successfully halts protein biosynthesis, we used it to determine the stability of TrkB-ICD fragment. So, we observed that this fragment is stable for long periods of time and its half-life time calculated was higher than 7 hours, which is a quite different, comparing with other known intracellular fragments.

Cyclohexamide treatment is a useful strategy to determine the turnover rate of a specific protein, since it inhibits the protein synthesis, blocking the translocation step in elongation [172].

Actually, using the same pharmacological approach (CHX treatment), extensive analyses of proteins half-life were performed in many different contexts, such as described for the p25 fragment or the Yeast proteome. Concerning p25 fragment, which is a protein also formed on AD context, through the cleavage of p35 protein by calpains (mentioned in *Section 1.3.1*), it is transiently detectable only for 3 hours. Nevertheless, it has an impact on cell homeostasis, since it overactivates CDK5 protein and induces hyperphosphorylation of tau protein and cytoskeletal disruption [149]. Regarding the Yeast proteome, it was measured the half-life time of 3,751 proteins and the mean of half-life time measured was approximately 45 minutes, which is very different than TrkB-ICD stability [162].

Concerning TrkB-ICD degradation that contributes to the decrease of its levels, we can consider two different proteolytic pathways: ubiquitin-proteasome pathway or lysosomal pathway. However, this topic was not evaluated in the present work. In future, it is our goal, using inhibitors for each pathway such as MG132 (a proteosome inhibitor) and leupeptin (a blocker of lysosomal degradation), to evaluate this aspect.

TrkB-ICD half-life time of approximately 8 hours could mean that, given its stability, this fragment can possibly have a biological role. Therefore, on following chapters we studied the subcellular dynamic of TrkB-ICD fragment in order to unveil if this fragment accumulates in some part of the cell and then we also evaluated its impact on cells phosphorylation pattern, since TrkB-ICD is constituted by the tyrosine kinase domain of TrkB-FL receptor.

—

6 Subcellular expression of TrkB-ICD fragment

6.1 Rational

In the first chapter it was possible to demonstrate that the expression levels of TrkB-ICD fragment after transfection, on H4 cells and primary neuronal cultures, were transient with an half life time of approximately 8 hours. This observation leads to hypothesis that this fragment could play a role on cell homeostasis. Therefore, in the present chapter its subcellular dynamic was evaluated.

To test this hypothesis, we designed two types of approach. First, we performed a subcellular fractionation protocol in order to obtain two different cellular fractions: one enriched in nuclear proteins and another enriched in cytoplasmic and membrane proteins, as previously described in Methods (*Section 3.5*). Moreover, to complement this technical approach, immunofluorescence assays were also performed for different time points on order to follow TrkB-ICD expression within the cell.

6.2 Distribution of TrkB-ICD fragment on H4 cells

H4 cells were transfected, as previously described, with TrkB-ICD or an empty vector (EV). The results obtained for 24 hours of transfection on H4 cells showed that TrkB-ICD is only present in the fraction enriched in cytoplasmic and membrane proteins, identified through GAPDH staining (cytosolic marker). This fragment was not visually detected in the fraction expressing Lamin B, which corresponds to the fraction enriched in nuclear proteins (Figure 6.1).

To check possible contaminations between the studied fractions, we analysed GAPDH and Lamin B levels and we confirmed that the chosen subcellular fractionation protocol did not indicate possible contaminations. Accordingly, the fraction enriched in nuclear proteins has no detectable levels of GAPDH (cytosolic protein) and the fraction enriched in cytoplasmic and membrane proteins has no levels of Lamin B, considered as a nuclear protein.
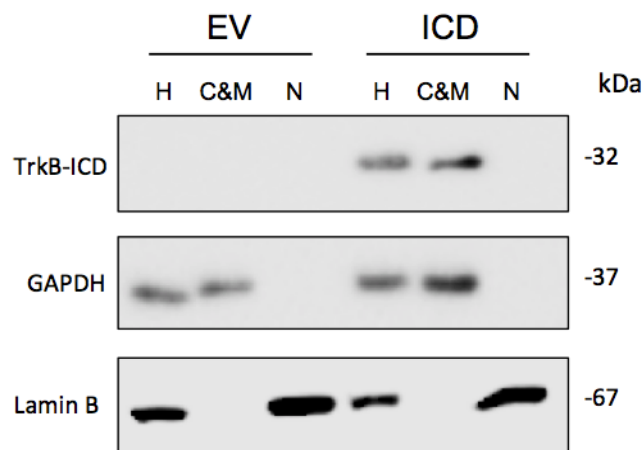
Figure 6.1 – Distribution of TrkB-ICD fragment on H4 cells transfected with pcDNA-TrkB-ICD: subcellular fractionation. Western-blot image of homogenate (H), cytosolic and membrane (C&M) and nuclear (N) fractions of H4 cells transfected for 24 hours with pcDNA-TrkB-ICD plasmid, showing the levels of GAPDH (cytosolic protein), Lamin B (nuclear protein) and TrkB-ICD. Abbreviations: C&M, fraction enriched in cytoplasmic and membrane; EV, empty vector; H, Homogenate; ICD, TrkB-ICD; N, fraction enriched in nuclear proteins.

The transfected H4 cells with pcDNA-TrkB-ICD for 24 hours only present TrkB-ICD staining in cytoplasm, as shown in Figure 6.2. Therefore, these data is in accordance with data obtained by western-blotting, suggesting that TrkB-ICD fragment is mainly present in cytoplasmic and membrane domains of H4 cells after 24 of transfection.
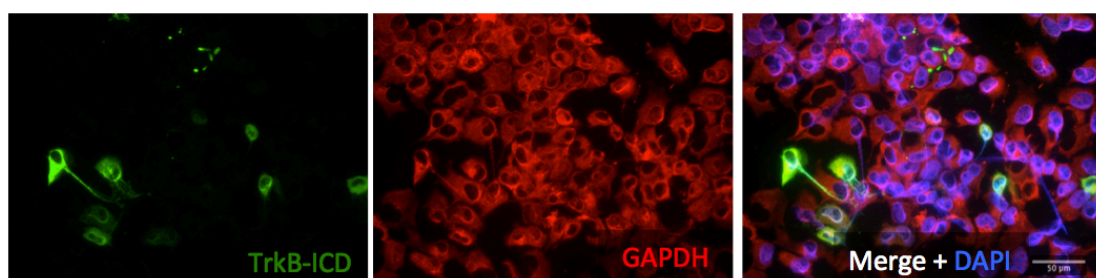
Figure 6.2 – Distribution of TrkB-ICD fragment on H4 cells transfected with pcDNA-TrkB-ICD (24h): immunofluorescence assay. Immunofluorescence image of H4 cells transfected with pcDNA-TrkB-ICD plasmid for 24 hours. In green, it is represented TrkB-ICD (stained with anti-Trk C-terminal antibody (C-14)), in red cytosolic marker (stained with anti-GAPDH antibody). Last image represents all channels merged with cell nuclei staining in blue (DAPI staining). Widefield fluorescence images were acquired with a 40x objective. Scale bar: 50 µm.

Interestingly, 48 hours after transfection with the pcDNA-TrkB-ICD-V5 plasmid, immunoflourescence experiments show that TrkB-ICD-V5 expression is mainly present at nucleus of H4 cells (Figure 6.3).
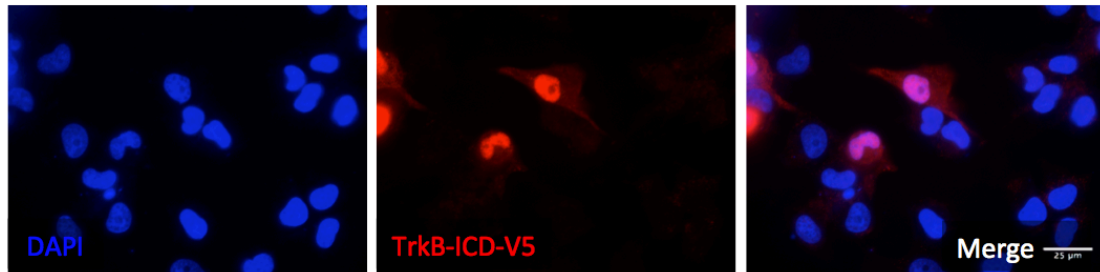
Figure 6.3 – Distribution of TrkB-ICD-V5 fragment on H4 cells transfected with pcDNA-TrkB-ICD-V5 (48h): immunofluorescence assay. Immunofluorescence image of H4 cells transfected with pcDNA-TrkB-ICD-V5 plasmid for 48 hours. In blue it is represented the cell nuclei (DAPI staining) and in red TrkB-ICD-V5 (stained with anti-V5). Last image represents both channels merged. Widefield fluorescence images were acquired with a 63x objective. Scale bar: 25 μm.

Although the results presented in Figures 6.2 and 6.3 had been obtained using different DNA plasmids, the expressed protein of interest is the same differing only in the presence of a fused V5-tag. Theoretically, this tag does not have any biological function and it is not involved in nuclear translocation of proteins, but we cannot exclude the possibility of V5-tag as the responsible for the observed differences. Therefore, using the same DNA plasmids, primary neuronal cultures were transfected and TrkB-ICD expression evaluated (*Section 6.3*).

Taken together, the results on transfected H4 cells suggest that TrkB-ICD fragment has different localization over time, being initially detected at cytosol and then, at nucleus.

6.3 Distribution of TrkB-ICD fragment on primary neuronal cultures

Similarly of what had been previously described for H4 cells, equivalent experimental procedures were performed for primary neuronal cultures to evaluate the subcellular localization of TrkB-ICD fragment on these cells.

In opposition to the results obtained from H4 cells transfected for 24 hours (Figure 6.1 and Figure 6.2), western-blotting analysis revealed that, in primary neuronal cultures, TrkB-ICD fragment is present in both fractions studied (Figure 6.4). Unexpectedly, a different isoform of GAPDH (~35 kDa) was observed in nuclear fraction in addition to the normal GAPDH isoform (37 kDa). This observation points towards neuronal death, since GAPDH nuclear isoform is a characteristic of apoptotic and oxidative conditions [173,174], as it will be detailed below on Discussion (*Section 6.4*).
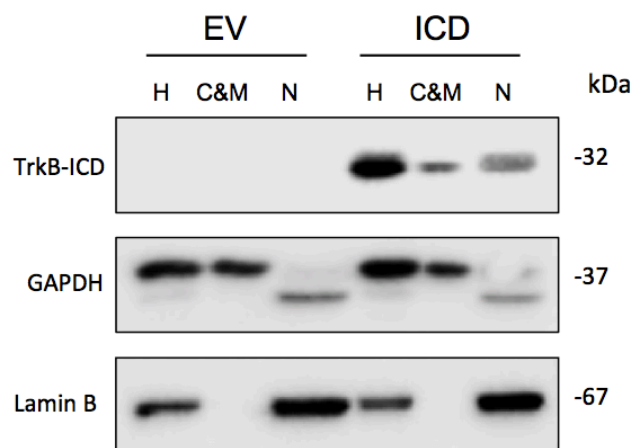
Figure 6.4 – Nuclear translocation of TrkB-ICD fragment in 7 DIV neurons transfected with pcDNA-TrkB-ICD: subcellular fractionation. Western-blot image of homogenate (H), cytosolic and membrane (C&M) and nuclear (N) fractions of 7 DIV primary neuronal cultures transfected for 24 hours with pcDNA-TrkB-ICD plasmid, showing the levels of GAPDH (cytosolic protein), Lamin B (nuclear protein) and TrkB-ICD. Abbreviations: C&M, fraction enriched in cytoplasmic and membrane; EV, empty vector; H, Homogenate; ICD, TrkB-ICD; N, fraction enriched in nuclear proteins.

As confirmed by immunofluorescence assays using MAP2 antibody (neuronal protein) and DAPI (nuclear marker), expression of TrkB-ICD fragment for 24h on primary neuronal cultures is mainly detected in nucleus of neurons (right column of Figure 6.5 – 6.5B). Interestingly, the same assay was performed only after 4 hours of transfection and the obtained results were different. Accordingly, TrkB-ICD expression after 4 hours of transfection was, not only detected in nucleus, but also in cytoplasm (left column of Figure 6.5 – 6.5A).
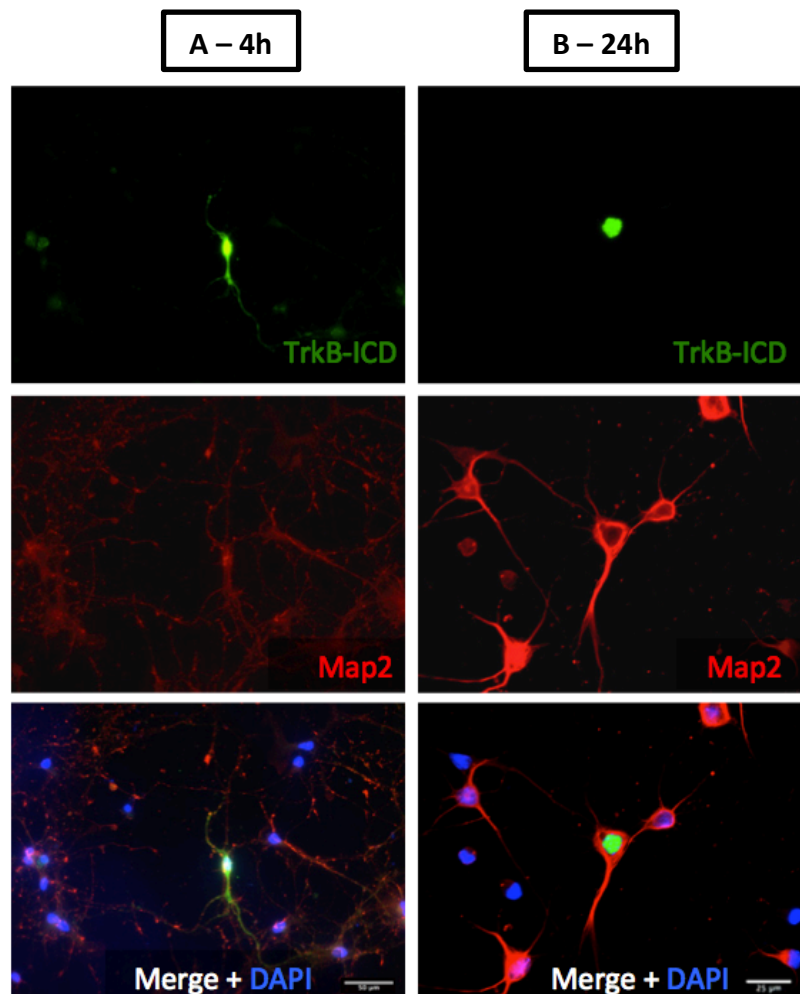
Figure 6.5 – Nuclear translocation of TrkB-ICD fragments in 7 DIV neurons transfected with pcDNA-TrkB-ICD: immunofluorescence assay. Immunofluorescence image of 7 DIV primary neuronal cultures transfected with pcDNA-TrkB-ICD plasmid for 4 hours (column A) and 24 hours (column B). In green, it is represented TrkB-ICD (stained with anti-Trk C-terminal antibody (C-14)) and in red neuronal marker (stained with anti-Map2 antibody). Last image represents all channels merged with DAPI staining (cell nuclei). Widefield fluorescence images were acquired with a 40X objective (column A) and 63x objective (column B). Scale bar: 50 µm (A) and 25 µm (B).

Together these data, obtained on H4 cells and primary neuronal cultures, suggest that TrkB-ICD fragment is translocated from cytosol to cell nuclei.

6.4   Discussion

The experimental procedure performed in this chapter was designed to evaluate the subcellular localization of TrkB-ICD fragment, on H4 cells and on primary neuronal cultures that transiently express this protein. TrkB-ICD localization could give some hints about its function and, possibly, about it consequences at cellular and molecular level.

As briefly mentioned above, exogenous DNA must reach the cell nuclei to become available to the transcriptional machinery, which produces the respective mRNA. Then, this mRNA enters the cytoplasm and its sequence is read by the ribosome, producing the protein of interest that is released in the cell cytosol, as schematically presented in Figure 6.6 [165,168]. In this way, similarly to other proteins, TrkB-ICD is initially produced at the cytosol.
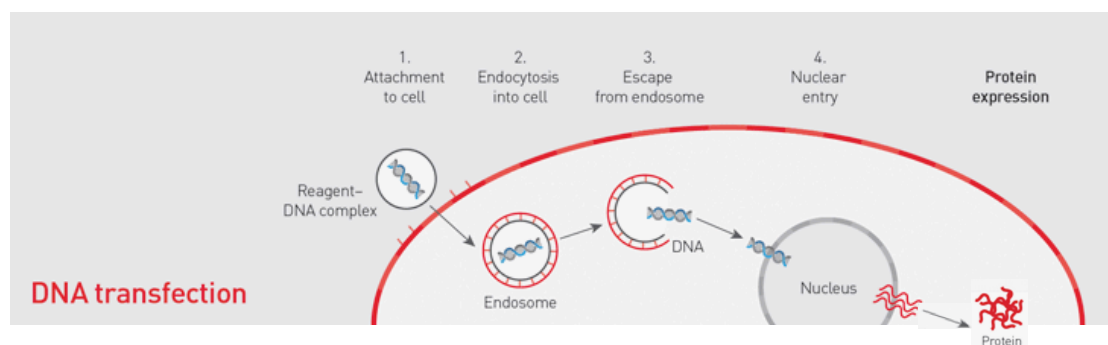
Figure 6.6 – Schematic representation of transfection steps until protein release in cell cytoplasm. Illustration of DNA transfection using Lipofectamine reagent: initially Lipofectamine/DNA complex is attached to the cell (1), being then endocytosed (2) and, after escape from the endosome (3), reach the cell nuclei (4), where mRNA is produced. This mRNA is then read by the ribosome and protein of interest is expressed (adapted from *Lipofectamine Messenger Max Website*).

Concerning H4 cells transfected, both technical approaches, subcellular fractionation protocol followed by western-blotting and immunofluorescence assays, indicate that, at 24 hours of transfection, TrkB-ICD is mainly detected at cytosol (Figures 6.1 and 6.2). Although the inability to detect TrkB-ICD at nucleus, one cannot exclude the possibility of the presence of residual levels at this cellular compartment. After 48 hours of transfection, we observed that TrkB-ICD

accumulates within the cell nucleus (Figure 6.3), suggesting that TrkB-ICD is translocated into nucleus over time.

Regarding primary neuronal cultures, the obtained data show that TrkB-ICD accumulates within the cell nucleus, at 24 hours of transfection. Moreover, this nuclear translocation might be gradual, since for shorter period of transfection (4h), the fragment is detected dispersed at cytosol.

So, taken together, results obtained with H4 cells and primary neuronal cultures provide evidence that TrkB-ICD is translocated to the cell nuclei with a different temporal pattern, where it accumulates and, possibly, exerts its function (Figure 6.7). This different temporal pattern of nuclear translocation might be associated with possible intracellular mechanisms that are distinct in both cells type studied.
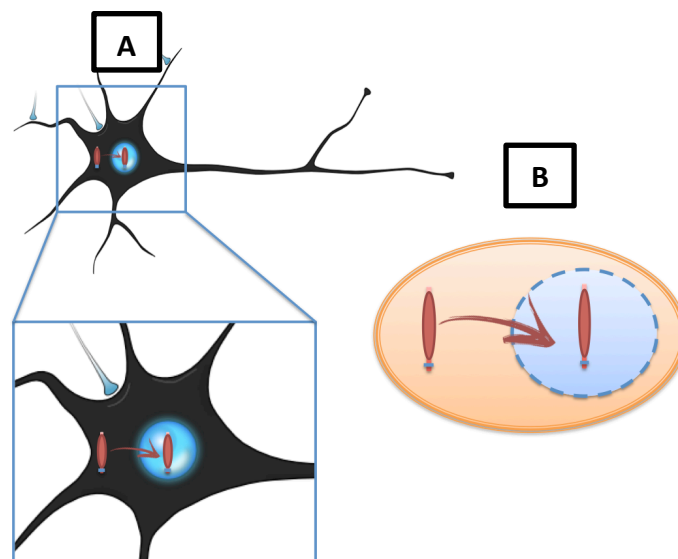
Figure 6.7 – Schematic representation of TrkB-ICD translocation to the nucleus on (A) primary neuronal cultures and (B) H4 cells. Both images illustrate the nuclear translocation of TrkB-ICD fragment detected using (A) primary neuronal cultures and (B) H4 cells.

It is not known the mechanism that mediates the nuclear translocation of TrkB-ICD. Nevertheless, it is widely described in the literature that several proteins can be selectively imported to nucleus from the cytosol, such as histones, DNA and RNA polymerases, gene regulatory proteins and also RNA-processing proteins [175]. In particular, the selectivity of this nuclear import can be due to the presence of Nuclear Localization Sequence (NLS), which is rich in basic residues, mainly: lysine

and arginine. After interaction with proteins located on the nuclear envelope or at the nuclear pore complex (such as RAN-GTP and importins), proteins containing NLS are translocated into the nucleus, through a mechanism dependent on ATP [175–178]. Regarding NLS, it can be classified into monopartite or bipartite NLS, depending on its putative consensus sequence. Whereas monopartite NLS has a single cluster of basic residues that could signal nuclear import, bipartite NLS contains two clusters of basic residues separated by a linker with 10-12 aa [179–181]. Considering that TrkB-ICD is originally formed from TrkB-FL receptor that is a transmembranar domain and NLS are mainly present in nuclear proteins [175], we anticipated that this fragment might not contain a nuclear import signal. Nevertheless, to test this hypothesis, we analysed TrkB-ICD sequence under NLS prediction algorithms, and we observed that monopartite NLS is not present in the TrkB-ICD fragment. However there was one prediction tool (*cNLS Mapper* software) that predicted a bipartite NLS in TrkB-ICD sequence. Actually, *cNLS Mapper* software suggests that TrkB-ICD contains two predicted bipartite NLS that respect its consensus sequence. Thus, Figure 6.8 presents the output obtained using *cNLS Mapper* software, where red represents two different predicted bipartite NLS and its respective scores. In summary, stronger NLS activity are indicated by higher scores, which 9/10 indicates exclusively nuclear proteins and scores of 1/2 represent only cytoplasmic proteins. So, in our particular case, scores of 5.5 and 6.5 indicate proteins that could be localized to both nucleus and cytoplasm [181], which could suggest that TrkB-ICD is translocated over time to nucleus through classical mechanisms of NLS signalling. However, it is of interest to mention that some predicted NLS that match the consensus sequence could not be functional and therefore, we cannot ensure what is the exact mechanism of nuclear translocation of TrkB-ICD fragment.

```
     SQLKPDTFVQHIKRHNIVLKRELGEGAFGKVFLAECYNLCPEQDKILVAV  50
     KTLKDASDNARKDFHREAELLTNLQHEHIVKFYGVCVEGDPLIMVFEYMK  100
[A]  HGDLNKFLRAHGPDAVLMAEGNPPTELTQSQMLHIAQQIAAGMVYLASQH  150
     FVHRDLATRNCLVGENLLVKIGDFGMSRDVYSTDYYRVGGHTMLPIRWMP  200
     PESIMYRKFTTESDWSLGVVLWEIFTYGKQPWYQLSNNEVIECITQGRV  250
     LQRPRTCPQEVYELMLGCWQREPHMRKNIKGIHTLLQNLAKASPVYLDIL  300
     G                                                  301
```

Predicted bipartite NLS		
Pos.	Sequence	Score
25	EGAFGKVFLAECYNLCPEQDKILVAVKTLKD	5.5
249	RVLQRPRTCPQEVYELMLGCWQREPHMRKNIKGI	6.5

Figure 6.8 – Results obtained from *cNLS Mapper* software about prediction of NLS on TrkB-ICD sequence. After reading TrkB-ICD sequence, this tool provides predicted monopartite and bipatrtite NLS and the localization of each one on total sequence analysed (A), as well as other characteristics, such as the initial amino acid position or respective score associated (B).

On the other hand, another hypothesis that could explain this translocation could involve Sec61 translocon. Actually, there are already several reports with toxins, SV40 virus and Epidermal growth factor receptor (EGFR) that describe this mechanism [182–185]. In particular, after activation of EGFR tyrosine kinase, this receptor is internalized into endosomes and then, via Golgi complex or not, endosomal EGFR are translocated to ER. Subsequently, there is a new retranslocation from ER to the cytosol via Sec61 translocon followed by association with HSP70 protein that, in turn, interacts with β-importin and leads finally to nuclear translocation [186]. However, this hypothesis was not tested yet and, so far, we do not know the exact mechanism underlying TrkB-ICD nuclear translocation. In the future, we aim to better evaluate the dynamics of TrkB-ICD translocation by using live cell imaging with an expression vector containing eGFP protein fused to TrkB-ICD.

Regarding possible molecular consequences of TrkB-ICD nuclear accumulation, there are already some studies describing that the overactivation of calpains induces the cleavage of several proteins, contributing to neurodegeneration and decreased synaptic plasticity [187,188]. Some fragments originated by calpain action are translocated to nucleus, affecting normal gene transcription, as happens with β-catenin fragment (*Section 1.3.1*) or even with a fragment derived from APP

proteolytic cleavage [145,189–191]. In addition to these fragments, calpains are also involved in the cleavage of Huntingtin (Htt) protein, releasing intracellular fragments that accumulate in nucleus, and play a critical role on cell homeostasis that, ultimately, leads to the progression of Huntington's disease [192]. Considering these examples, we can hypothesize that TrkB-ICD translocation to nucleus can have biological consequences. Therefore, it would be very interesting to study possible changes in gene expression profile, caused by our protein, performing microarray analysis of cells transfected with TrkB-ICD fragment and respective controls. Additionally, other molecular techniques (including two hybrid screening) could be performed to confirm specific interactions between TrkB-ICD and other proteins, which will allow us to infer for the possible functions of TrkB-ICD on nuclear compartment.

Surprisingly, we detected a special isoform of GAPDH protein with lower molecular weight at nuclear fraction of primary neuronal cultures (Figure 6.4). Interestingly, the induction of apoptosis and oxidative conditions enhance the nuclear translocation of GAPDH, where can act as a nuclear carrier for pro-apoptotic molecules (proapoptotic function) or as a DNA repair enzyme (protective function) [173,174]. Thus, since we observe a similar expression of this isoform in both conditions studied (transfected with TrkB-ICD and transfected with an empty vector), these data could suggest two facts: 1) transfection process could have toxicity consequences and 2) 24 hours of TrkB-ICD expression do not promote additional cell death, since nuclear GAPDH levels are similar in both conditions.

7 Impact of TrkB-ICD fragment on cells phosphorylation pattern

7.1 Rational

Since TrkB-ICD fragment is originated from the cleavage of TrkB-FL receptor and contains the tyrosine kinase domain, we evaluated whether this fragment *per se* could have kinase activity.

Thus, we studied the phosphorylation dynamics from different perspectives. Moreover, we also evaluated the contribution of the canonical signalling pathways on phosphorylation dynamics. Since TrkB-FL has a tyrosine kinase domain, we used an antibody (PY99) that specifically detects phosphotyrosine-containing proteins (instead detection of phosphoserine or phosphothreonine).

7.2 Evaluation of tyrosine kinase activity of TrkB-ICD fragment on H4 cells and primary neuronal cultures

Cells were transfected with pcDNA-TrkB-ICD-V5 and pcDNA-TrkB-ICD plasmids for 24 hours, as described before, and phosphotyrosine immunoreactivity was evaluated by western-blotting. Expression of TrkB-ICD fragment, on H4 cells (Figure 7.1A) and primary neuronal cultures (Figure 7.1B), induced a remarkable phosphorylation pattern when compared to non-transfected cells (CTR) or cells transfected with an empty vector (EV). Thus, these data suggest that TrkB-ICD fragment has a constitutive tyrosine kinase activity, promoting the phosphorylation of a wide range of proteins. Interestingly, some phosphorylated proteins show strong intensity, with special relevance for proteins with a relative molecular weight of approximately 40, 70, 90 and 120-130 kDa.
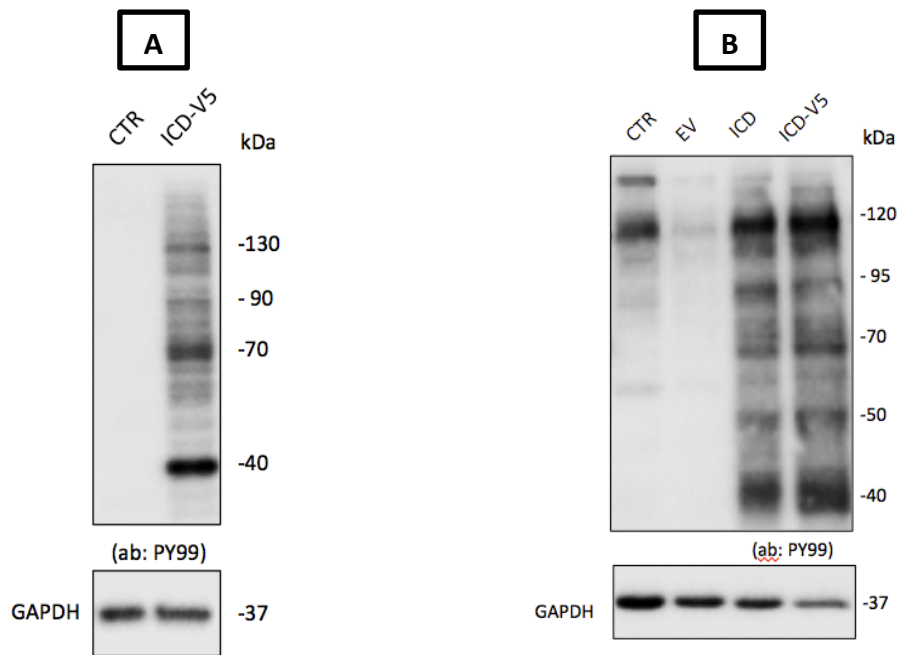
Figure 7.1 – Levels of tyrosine phosphorylated proteins on (A) H4 cells and (B) primary neuronal cultures. Representative western-blot images of tyrosine phosphorylated proteins (stained with PY99 antibody) on (A) H4 cells and (B) 7 DIV primary neuronal cultures transfected for 24 hours. Abbreviations: CTR, non-transfeted cells; EV, empty vector; ICD, TrkB-ICD; ICD-V5, TrkB-ICD-V5.

Through immunofluorescence assays, and using the same experimental design, we also observed that TrkB-ICD fragment has kinase activity. H4 cells transfected with pcDNA-TrkB-ICD plasmid for 24 hours showed a strong staining with PY99 antibody (Figure 7.2), suggesting that these cells have proteins phosphorylated, in accordance with western-blot results described in Figure 7.1A. It is important to mention that only cell nucleus shows staining for phosphotyrosine residues, being this staining co-localized with DAPI. Interestingly, all cells stained for phosphorylated tyrosines, express TrkB-ICD fragment, which demonstrates the kinase activity of this fragment. However, at this time (24 hours), there are some cells expressing TrkB-ICD fragment that do not present staining for phosphotyrosine residues, suggesting that this phosphorylation pattern could be transient (hypothesis studied in *Section 7.3*).
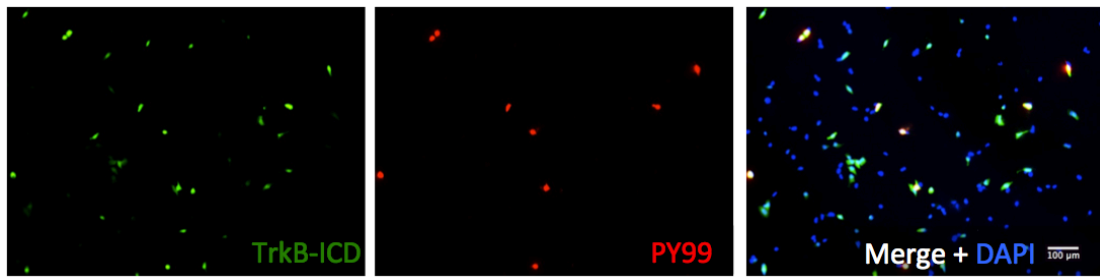
Figure 7.2 – Localization of tyrosine phosphorylated proteins on H4 cells transfected with pcDNA-TrkB-ICD plasmid. Immunofluorescence image of H4 cells transfected with pcDNA-TrkB-ICD plasmid for 24 hours. In green it is represented TrkB-ICD (stained with anti-Trk C-terminal tail antibody (C-14)) and in red phosphorylated proteins (stained with anti-PY99 antibody). Last image represents all channels merged, including cell nuclei staining with DAPI (in blue). Widefield fluorescence images were acquired with a 10x objective. Scale bar: 100 μm.

Concerning primary neuronal cultures, the results obtained in immunofluorescence assays match the results obtained by western-blotting (Figure 7.1B). Cells expressing TrkB-ICD fragment show staining for phosphorylated proteins at tyrosine residues. However, comparing with H4 cells (Figure 7.2), in primary neuronal cultures, a different phosphorylation pattern is observed. In this case, the staining for PY99 is not restricted to the cell nuclei. Actually, data using primary neuronal cultures indicate that, in addition to phosphorylation on soma and nucleus, this phosphorylation pattern are also present in axons, as Figure 7.3 clearly demonstrates, using different antibodies.
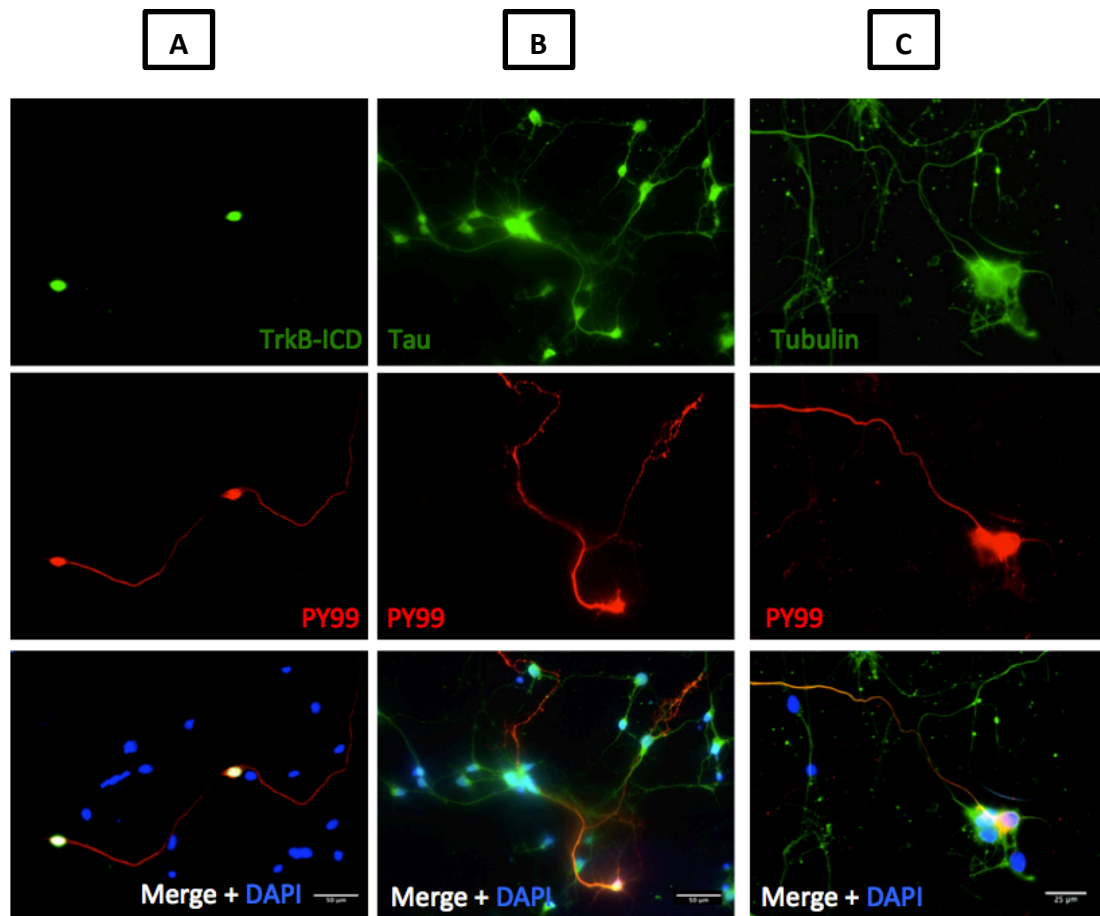
Figure 7.3 – Localization of tyrosine phosphorylated proteins on 7 DIV primary neuronal cultures transfected with pcDNA-TrkB-ICD. Immunofluorescence image of 7 DIV primary neuronal cultures transfected with pcDNA-TrkB-ICD plasmid for 24 hours. Each column shows different images with different staining in green channel: left (A) – TrkB-ICD (stained with anti-Trk C-terminal tail antibody (C-14)); mid (B) – Tau (stained with anti-Tau); right (C) – Tubulin (stained with anti-Tubulin). In red it is represented phosphorylated proteins (stained with anti-PY99 antibody). Last image represents all channels merged, including cell nuclei staining with DAPI (in blue). Widefield fluorescence images were acquired with a 40x (left and mid columns, A and B) and 63x (right column, C) objectives. Scale bar: 50 µm (A and B) and 25 µm (C).

7.3　Kinetics of phosphorylation induced by TrkB-ICD fragment

In order to evaluate over time the phosphorylation pattern induced by TrkB-ICD fragment, we used the same experimental approach described in *Section 4.2*. Therefore, the levels of phosphotyrosine residues were evaluated throughtout time, starting at 2 hours of TrkB-ICD expression until 24 hours of its expression.

Data obtained from H4 cells suggest that phosphorylation induced by TrkB-ICD fragment is transient, reaching a maximum at 16 hours of its expression (Figure 7.4A). At 40 hours of expression the phosphotyrosine residues are present at very low levels (data not shown). Moreover, it is important to note that, at that time, TrkB-ICD fragment levels are also decreased compared to 24 hours of its expression, due to its transient expression, (*Section 4.2*) and therefore our results suggest that the phosphorylation follows the total amount of TrkB-ICD fragment.

Accordingly, the same pattern of phosphorylation was detected in primary neuronal cultures (Figure 7.4B).

Figure 7.4 – Transient phosphorylation pattern on (A1, A2) H4 cells and (B) 7 DIV primary neuronal cultures transfected with pcDNA-TrkB-ICD-V5. (A1) Representative western-blot probed with anti-V5tag antibody and anti-PY99 antibody (identifying TrkB-ICD-V5 and phosphorylated proteins, respectively) for H4 cells after different times of transfection: 4, 8, 16 and 24 hours. (A2) Analysis of bands intensities represented in (A1) from densitometry quantification of phosphorylated proteins immunoreactivity of 3-5 independent cultures. Data is normalized for 24 hours of TrkB-ICD transfection. GAPDH was used as loading control. Data represented are mean ± SEM of *n* independent experiments (**p<0.01; compared to "ICD 24h"; ANOVA followed by Bonferroni *post-test*). (B) Representative western-blot probed with anti-Trk C-terminal tail (C-14) and anti-PY99 antibodies (identifying TrkB-ICD and phosphorylated proteins, respectively) for 7 DIV primary neuronal cultures after different times of transfection: 8, 16, 24 and 40 hours. Abbreviations: CTR, non-transfeted cells; EV, empty vector; ICD, TrkB-ICD; ICD-V5, TrkB-ICD-V5.

In order to evaluate if kinase activity of TrkB-ICD fragment is constant over time or depends on its *de novo* synthesis, experiments were performed on cells transfected with pcDNA-TrkB-ICD for 16 hours and then treated with CHX for different times (methodology present in Figure 5.1A).

The obtained results suggest that TrkB-ICD induces a transient phosphorylation pattern on H4 cells and primary neuronal cultures that follows TrkB-ICD levels. In particular, H4 cells transfected present different levels of tyrosine phosphorylated proteins. The results show that phosphorylation levels follow TrkB-ICD expression levels (Figure 7.5A1/A2). Accordingly, results obtained from primary neuronal cultures (Figure 7.5B) also suggest that phosphorylation induced by TrkB-ICD fragment decreases with lower levels of the TrkB-ICD fragment.

Concerning our hypothesis, it is premature to extract final conclusions from these data. However, given that it was possible to detect phosphorylated proteins after 8 hours of CHX incubation, this suggests that TrkB-ICD kinase remains active at that time, which could indicate that TrkB-ICD activity is constant over time and does not depend on its constitutive synthesis.
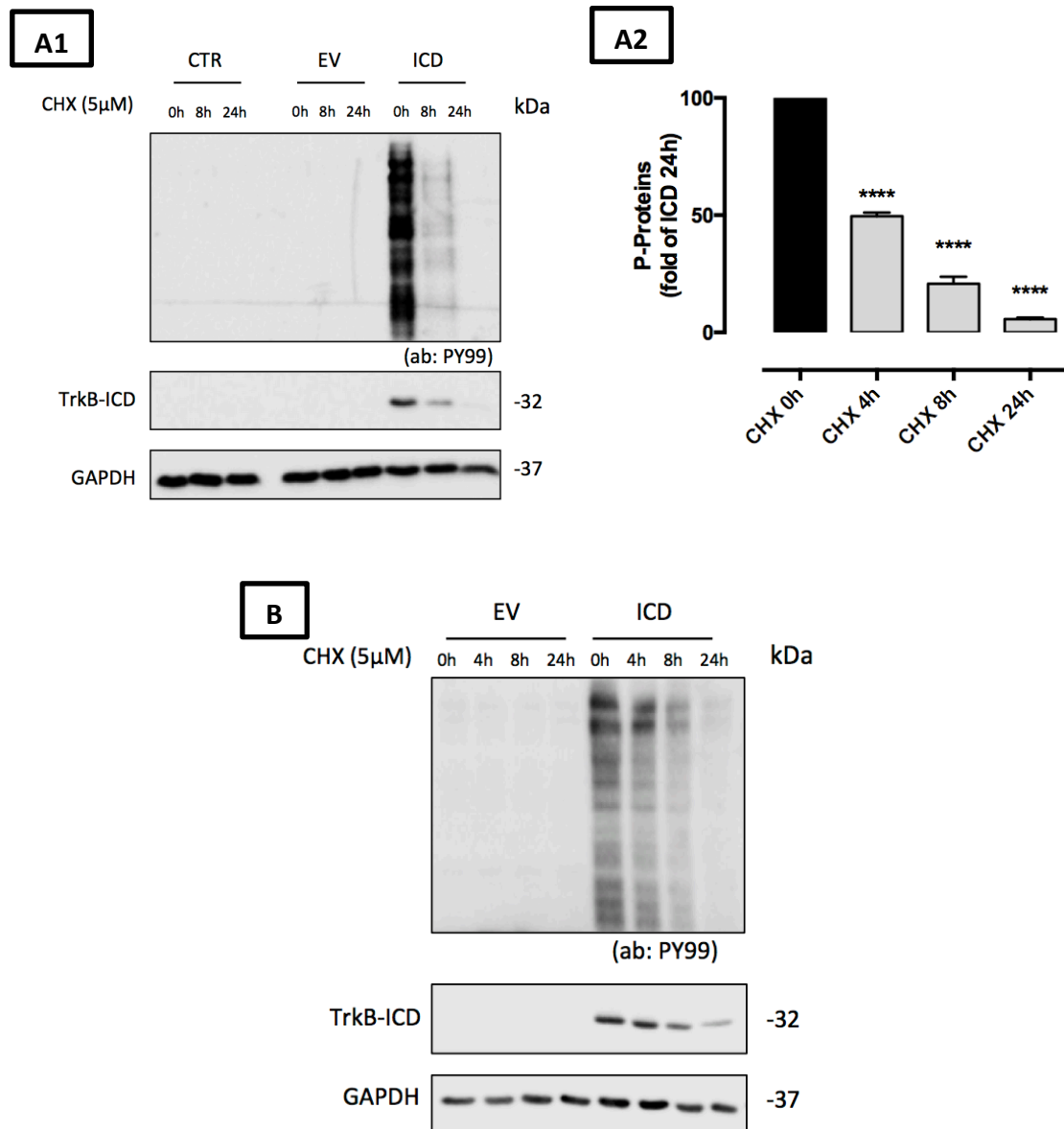
Figure 7.5 – CHX (5 µM) treatment effects on levels of tyrosine phosphorylated proteins on (A1, A2) H4 cells and (B) 7 DIV primary neuronal cultures transfected with pcDNA-TrkB-ICD. (A1) Representative western-blot probed with anti-Trk C-terminal tail antibody (C-14) and anti-PY99 antibody for H4 cells transfected with pcDNA-TrkB-ICD plasmid for 16 hours that were then incubated with CHX for different times: 8 and 24 hours. (A2) Analysis of bands intensities represented in (A1) from densitometry quantification of phosphorylated proteins immunoreactivity of 4 independent cultures. Data is normalized for initial amount of TrkB-ICD fragment (CHX 0h). GAPDH was used as loading control. Data represented are mean ± SEM of *n* independent experiments (****p<0.001; compared to "CHX 0h"; ANOVA followed by Bonferroni *post-test*). (B) Representative western-blot probed with anti-Trk C-terminal tail antibody (C-14) and anti-PY99 antibody for 7 DIV primary neuronal cultures transfected with pcDNA-TrkB-ICD plasmid for 16 hours that were then incubated with CHX for different times: 4, 8 and 24 hours. Abbreviations: CHX, cyclohexamide; CTR, non-transfeted cells; EV, empty vector; ICD, TrkB-ICD.

In order to assess if the phosphorylated proteins, by TrkB-ICD fragment, continue phosphorylated over time, an experimental approach was designed involving the use of K252a (5 µM) compound. This drug acts on the intracellular domain of Trk-FL receptors, inhibiting selectively the ATP binding site, leading to the inhibition of its kinase activity.

Incubation of H4 cells (Figure 7.6A) and primary neuronal cultures (Figure 7.6B) with K252a clearly eliminates the phosphorylation pattern induced by TrkB-ICD without affecting its levels, compared to non-treated cells (ICD + K252a (0h)). Thus, these results demonstrate that 1) K252a inhibits TrkB-ICD fragment activity, and that 2) proteins phosphorylated by TrkB-ICD are quickly de-phosphorylated in the absence of TrkB-ICD activity.
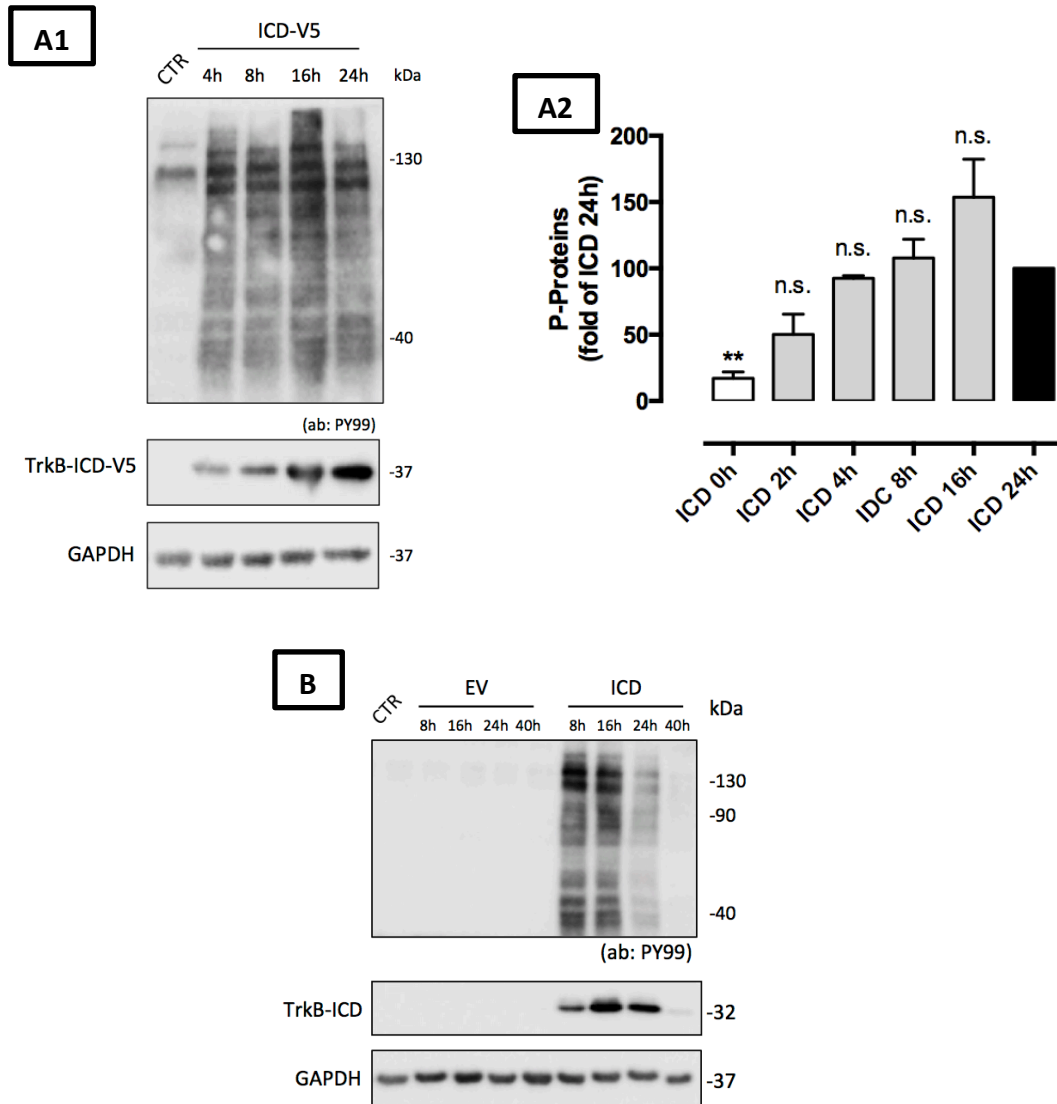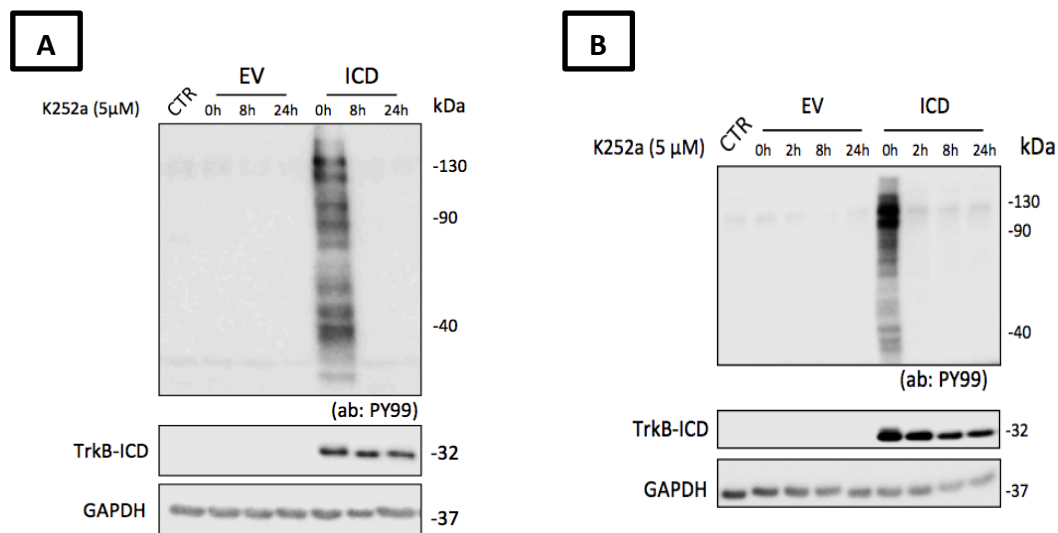

Figure 7.6 – K252a (5 µM) treatment effects on levels of tyrosine phosphorylated proteins on (A) H4 cells and (B) 7 DIV primary neuronal cultures transfected with pcDNA-TrkB-ICD. (A) Representative western-blot probed with anti-Trk C-terminal tail antibody (C-14) and anti-PY99 antibody for H4 cells transfected with pcDNA-TrkB-ICD plasmid incubated with K252a for different times: 8 and 24 hours. (B) Representative western-blot probed with anti-Trk C-terminal tail antibody (C-14) and anti-PY99 antibody for 7 DIV primary neuronal cultures transfected with pcDNA-TrkB-ICD plasmid incubated with K252a for different times: 2, 8 and 24 hours.

In this set of results, we demonstrated that phosphorylation pattern induced by TrkB-ICD fragment is transient, follows the levels of TrK-ICD expression and its kinase activity is constant over time, while proteins phosphorylated by TrkB-ICD are quickly de-phosphorylated.

7.4 Signalling pathways contribution for protein phosphorylation induced by TrkB-ICD

As previously described, TrkB-ICD fragment induces a remarkable protein phosphorylation on H4 cells and primary neuronal cultures. Therefore, we next evaluated the putative involvement of the known signalling pathways in the phosphorylation process. Accordingly, transfected cells were incubated for 24 hours with the inhibitors of the major signalling pathways (see Table 7.1) involved, directly or indirectly, on TrkB-FL signalling (Figure 7.7A). It is important to note that, in this set of data, only primary neuronal cultures were used.

Table 7.1 – Drugs used and respective signalling pathway inhibited.

Drug	Signalling pathway
PP2 (10 µM)	Src
LY 294002 (10 µM)	Akt/PI3K
U 73122 (4 µM)	PLCγ
U 0126 (10 µM)	Erk
H-89 (25 µM)	PKA
Staurosporin (100 µM)	PKC

The results show that, the inhibition of Src and Akt pathways by PP2 (10 µM) and LY294022 (10 µM), respectively, induced an increase of phosphorylated proteins levels on TrkB-ICD transfected neurons when compared to TrkB-ICD transfected neurons without any treatment, represented in Figure 7.7B/C as "ICD − ". On the other hand, incubation with inhibitors of Erk, PKA and PKC pathways (U0126 (10 µM), H-89 (25 µM) and Staurosporin (100 µM), respectively) dramatically decreases phosphorylated proteins levels (n=8, $p<0.005$ and $p<0.001$) when compared to "ICD − "). Curiously, inhibition of PKA and PKC pathways has similar effects of those obtained by the incubation with K252a (a tyrosine kinase inhibitor), suggesting that these pathways might be involved in the the phosphorylation mediated by TrkB-ICD fragment. Moreover, the inhibitor of PLCγ pathway, U73122 (4 µM), did not affect significantly the phosphorylation levels (Figure 7.7B1/B2).

Interestingly, data shown in Figure 7.7B1/B2 also indicate that drug incubations affect TrkB-ICD levels, which, in turn, could explain different levels of phosphorylated proteins. Hence, we then evaluated TrkB-ICD levels present in all conditions studied to understand if inhibitors used could interpose in its synthesis or degradation leading consequently to changes on TrkB-ICD expression and ultimately differences on phosphorylation levels (Figure 7.7C).

Next, by perfoming the ratio between total levels of phosphorylated proteins and TrkB-ICD, it is possible to conclude that inhibition of PKA and PKC pathways significantly decreases this ratio, suggesting that these inhibitors could directly influence the phosphorylation induced by TrkB-ICD fragment. Interestingly, both inhibitors promote an effect with a magnitude similar to K252a (Figure 7.7D).
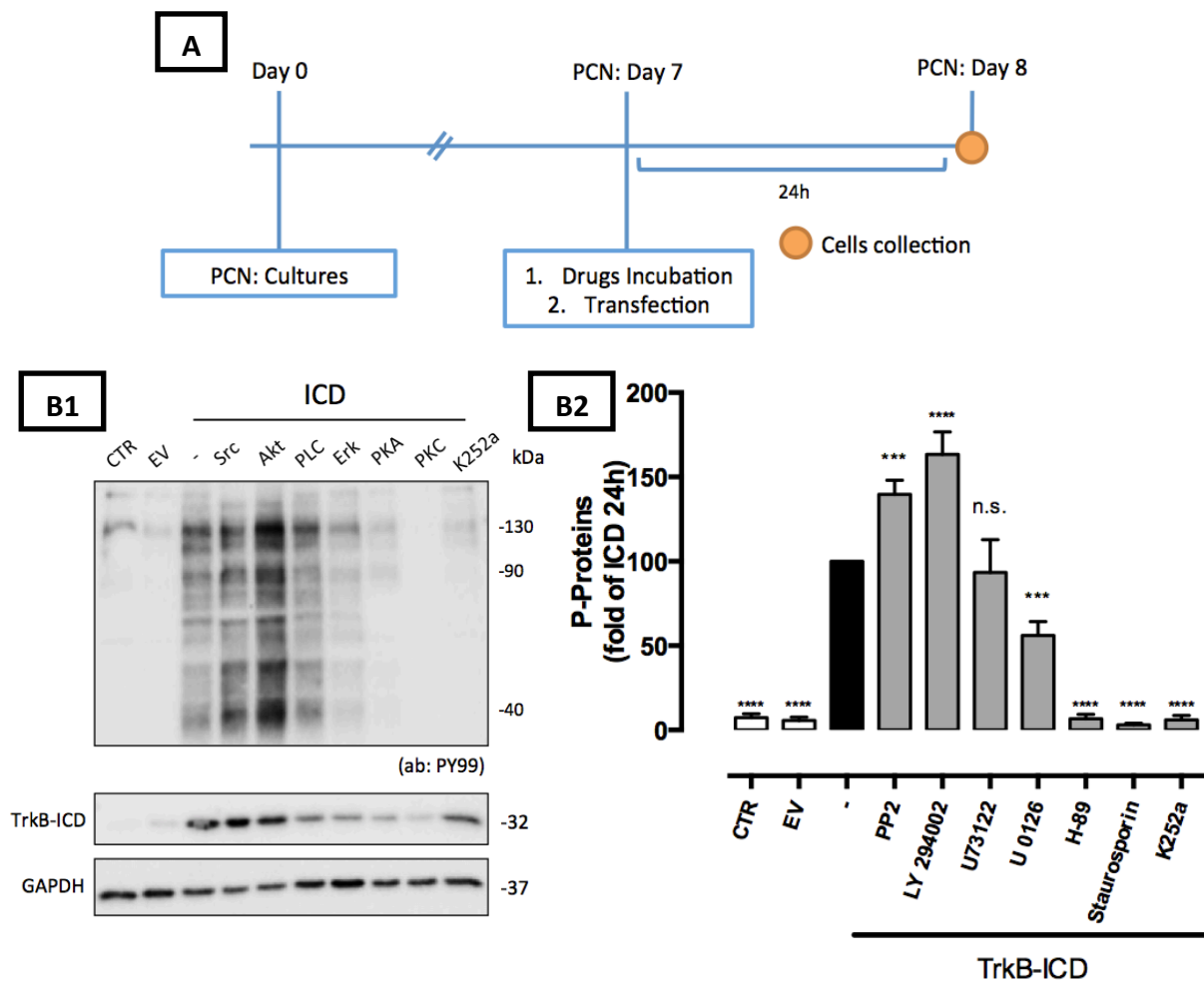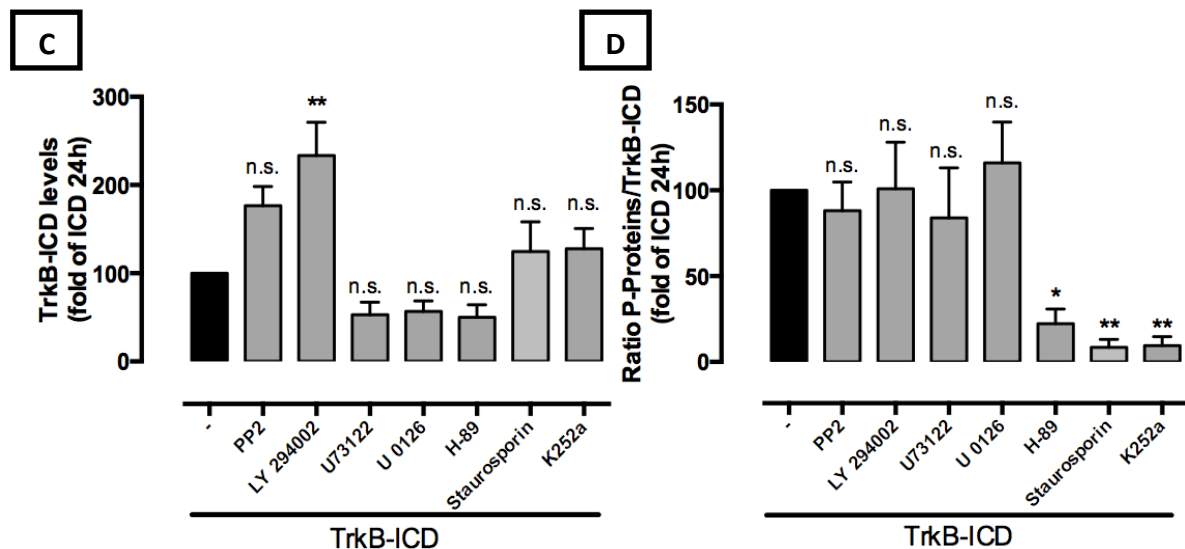
Figure 7.7 – Contribution of signalling pathways on TrkB-ICD levels and ratio between phosphorylation levels and TrkB-ICD fragment amount (7 DIV primary neuronal cultures). (A) Timeline chronogram that summarizes the protocol used to this characterization, including the moment of transfection and incubation of pathways' inhibitors and cells collection. (B1) Representative western-blot probed with anti-Trk C-terminal tail antibody (C-14) and anti-PY99 antibody for 7 DIV primary neuronal cultures transfected with pcDNA-TrkB-ICD plasmid incubated with inhibitors for 24 hours. (B2) Analysis of bands intensities represented in (B1) from densitometry quantification of phosphorylated proteins immunoreactivity of 8 independent cultures. Data is normalized for levels of phosphorylated proteins with TrkB-ICD transfection ("ICD −"). GAPDH was used as loading control. Data represented are mean ± SEM of *n* independent experiments (***p<0.005; ****p<0.001; compared to "ICD −"; ANOVA followed by Bonferroni *post-test*). (C) Analysis of bands intensities represented in Figure 7.7B from densitometry quantification of TrkB-ICD immunoreactivity of 8 independent cultures. Data is normalized for levels of TrkB-ICD fragmet without any treatment ("TrkB-ICD −"). GAPDH was used as loading control. Data represented are mean ± SEM of *n* independent experiments. (**p<0.01; compared to "ICD −"; ANOVA followed by Bonferroni *post-test*) (D) Ratio of quantification of phosphorylated proteins immunoreactivity (Figure 7.7C) and quantification of TrkB-ICD immunoreactivity (Figure 7.8A) (*p<0.5; **p<0.01; compared to "TrkB-ICD −"; ANOVA followed by Bonferroni *post-test*). Abbreviations: CTR, non-transfeted cells; EV, empty vector; ICD, TrkB-ICD; PCN, primary cortical neurons.

Taken together, data presented in these experiments suggest that PKA and PKC inhibitors could directly and positively modulate the phosphorylation induced by TrkB-ICD fragment. However, it is known that PKC inhibitor is an analogue compound of K252a [193–195] and could be directly inhibiting the kinase activity of TrkB-ICD and, therefore, it is possible that only PKA pathway could indeed modulate in a positive way the phosphorylation pattern induced by TrkB-ICD, as it will be detailed in Discussion (*Section 7.7*).

7.5   Phopshorylation   pattern   induced   by   TrkB-ICD fragment: evaluation on subcellular fractions

Using the same experimental design described in *Section 6*, including a subcellular fractionation protocol and immunofluorescence assays, phosphotyrosine proteins immunoreactivity were evaluated in order to study the phosphorylation pattern on the different subcellular fractions.

TrkB-ICD expression levels on H4 cells obtained for 24 hours of transfection is mainly detected at cytoplasm and at membranes (Figure 6.1). Curiously, data presented in Figure 7.9A identify phosphorylation mainly at nuclear fraction, being the cytosolic and membrane proteins phosphorylation almost absent. This suggets that phosphorylated proteins do not necessarily co-localize with TrkB-ICD fragment, which indicates that TrkB-ICD fragment has kinase activity, leading to the phosphorylation of several proteins that, in turn, are translocated to the nucleus, or that nuclear TrkB-ICD induces phosphorylation on nucleus, as will be discussed in *Section 7.7*.

In primary neuronal cultures transfected with pcDNA-TrkB-ICD for 24 hours, the results, show a pronounced phosphorylation pattern at nuclear fraction, where there is a higher expression levels of TrkB-ICD fragment (Figure 7.9B).

Taken together this set of results shows that proteic phosphorylation is mainly detected at nuclear fraction, even if TrkB-ICD fragment has residual expression levels in this fraction.
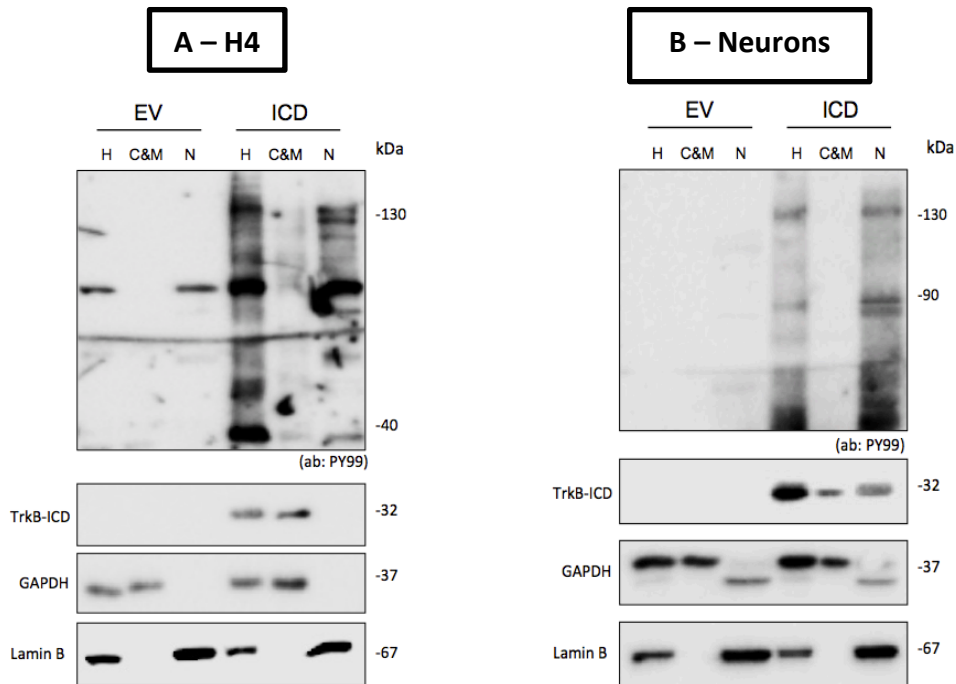
Figure 7.8 – Levels of tyrosine phosphorylated proteins on different fractions of (A) H4 cells and (B) 7 DIV primary neuronal cultures transfected with pcDNA-TrkB-ICD. (A) Western-blot image of homogenate (H), cytosolic and membrane (C&M) and nuclear (N) fractions of H4 cells transfected for 24 hours with empty vector (EV) or pcDNA-TrkB-ICD plasmid (ICD), showing the levels of phosphotyrosine proteins (anti-PY99), GAPDH (cytosolic protein), Lamin B (nuclear protein) and TrkB-ICD (probed with anti-Trk C-terminal tail antibody (C-14)). (B) Western-blot image of homogenate (H), cytosolic and membrane (C&M) and nuclear (N) fractions of 7 DIV primary neuronal cultures transfected for 24 hours with empty vector (EV) or pcDNA-TrkB-ICD plasmid (ICD), showing the levels of phosphotyrosine proteins (anti-PY99), GAPDH (cytosolic protein), Lamin B (nuclear protein) and TrkB-ICD (probed with anti-Trk C-terminal tail antibody (C-14)). Abbreviations: C&M, fraction enriched in cytoplasmic and membrane; EV, empty vector; H, Homogenate; ICD, TrkB-ICD; N, fraction enriched in nuclear proteins.

7.6 Relationship between phosphorylation pattern and TrkB-ICD nuclear translocation

Considering that TrkB-ICD is translocated into nucleus over time and that it induces a dramatic phosphorylation pattern, the next set of experiments was designed to assess if nuclear translocation of TrkB-ICD fragment was dependent on its kinase activity. Thus, to evaluate this possibility, immunofluorescence assays were performed using transfected primary neuronal cultures incubated with K252a (5 µM) compound for 24 hours, to inhibit phosphorylation mediated by TrkB-ICD fragment.

Data presented in Figure 7.10 indicate that TrkB-ICD nuclear translocation is dependent on its kinase activity. In fact, we can observe that K252a incubation influence TrkB-ICD localization, since this fragment is highly dispersed throughout all cell body and axons (Figure 7.10B). On the other hand, on cells non-treated with K252a compound, it is clear that TrkB-ICD is only located on nucleus, as already described on *Section 6.3* (Figure 7.10A).
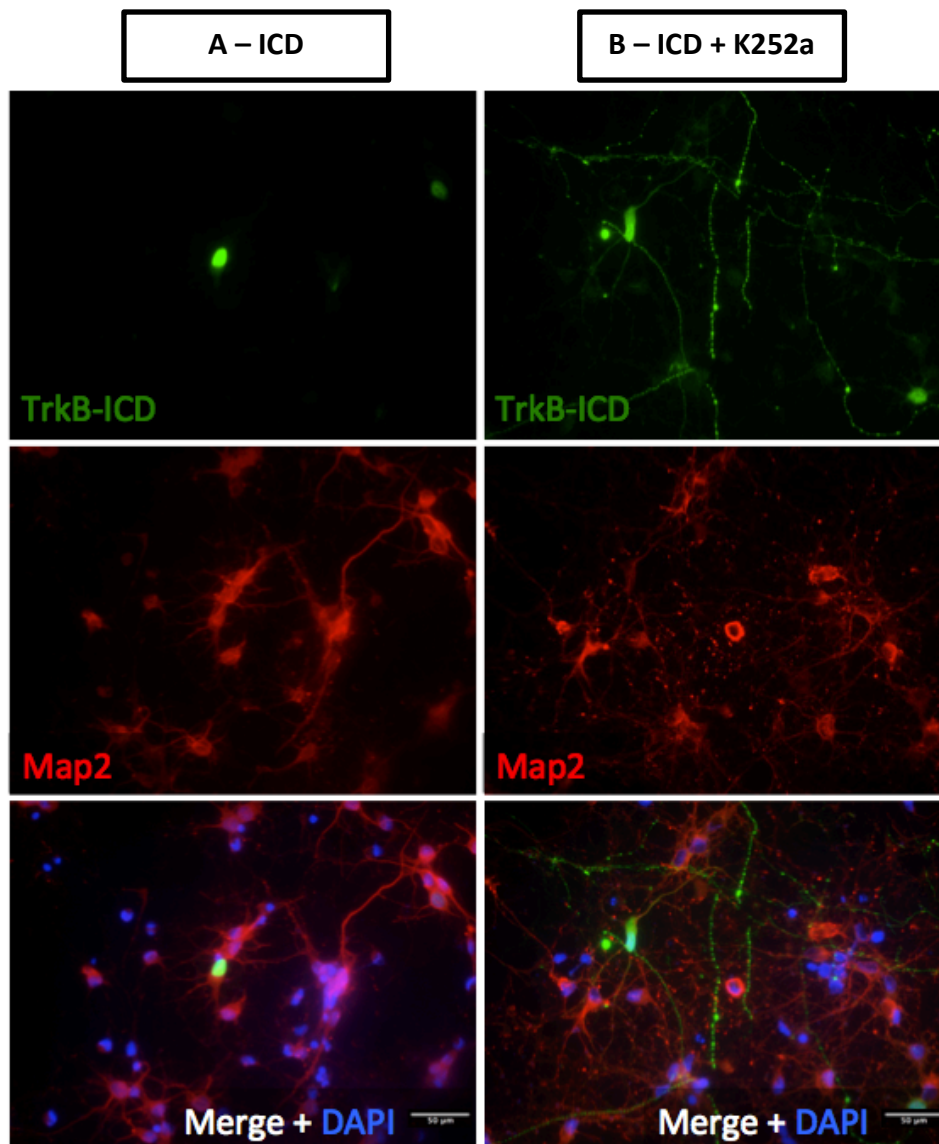
Figure 7.9 – Localization of TrkB-ICD fragment on 7 DIV primary neuronal cultures (A) transfected with pcDNA-TrkB-ICD and (B) simultaneously treated with K252a compound. Immunofluorescence image of 7 DIV primary neuronal cultures transfected with pcDNA-TrkB-ICD plasmid for 24 hours: non-treated with K252a (A) and treated simultaneously with K252a for 24 hours (B). In both conditions, green represents TrkB-ICD (stained with anti-Trk C-terminal tail antibody (C-14)) and in red phosphorylated proteins (stained with anti-PY99 antibody). Last image represents all channels merged, including cell nuclei staining with DAPI (in blue). Widefield fluorescence images were acquired with a 40x objective. Scale bar: 50 μm.

7.7   Discussion

In summary, this chapter shows evidences that TrkB-ICD fragment has spontaneous tyrosine kinase activity, leading to the phosphorylation of a wide range of proteins at nucleus, soma and neuronal processes (Figures 7.1-7.3 and 7.8). Furthermore, we observed that total amount of phosphorylated proteins correlate with TrkB-ICD levels and the inhibition of TrkB-ICD activity leads to a fast and global fading of phosphorylation, suggesting that the phosphorylated proteins by TrkB-ICD are rapidly dephosphorylated in absence of TrkB-ICD activity (Figures 7.4-7.6). Results also suggest that PKA pathway could positively modulate the phosphorylation pattern induced by TrkB-ICD (Figure 7.7). Finally, data also demonstrate that TrkB-ICD translocation to the cell nuclei is dependent on its kinase activity (Figure 7.9).

Activation of receptor tyrosine kinases, including TrkB-FL receptor, triggers the activation of signalling pathways, which are a crucial mechanism for intra- and inter- cellular communication. Thus, these receptors play a critical role on cell homeostasis from initial stages of development to adult organisms. However, dysregulations on cell signalling mediated by kinase activity (mainly constitutive phosphorylations) are directly involved in the pathophysiology of several diseases, such as cancer, atherosclerosis and diabetes mellitus type II [196,197] or even AD (see *Section 1.3.1*: CDK5 activity). Thereby, we could hypothesize that phosphorylation mediated by TrkB-ICD fragment could have an important role on AD pathophysiology. However, it is important to consider another group of enzymes: protein tyrosine phosphatases, since they have a direct role over proteins phosphorylated by kinases. Indeed, protein phosphatases are responsible for dephosphorylate proteins by removing the phosphate groups (Figure 7.10). Thus, these enzymes help to regulate cellular signalling, avoiding a sustained phosphorylation that would be constitutively triggering biological effects. Accordingly, it is described that dysregulations on protein phosphatases are also involved in pathogenesis of several diseases, such as AD, cardiovascular disease and

autoimmune disorders [198]. Concerning AD, it is known that disruption of Ca^{2+} homeostasis, one hallmark of AD, promotes dysregulations of Ca^{2+}-dependent phosphatases [198,199]. Therefore, this phosphatase dysregulation may indirectly lead to an increase of kinase activity and subsequent increased levels of phosphorylated proteins, such as tau protein [86]. Given the spontaneous kinase activity of TrkB-ICD fragment, we can hypothesize that the TrkB-FL cleavage by calpains and the consequent formation of TrkB-ICD fragment could contribute to dysregulate the kinase/phosphatase balance.
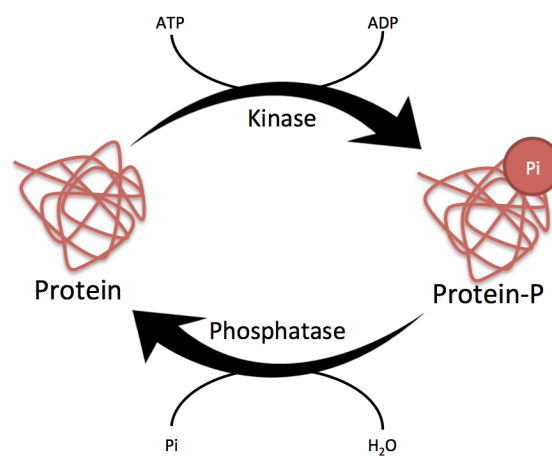
Figure 7.10 – Opposite roles of kinases and phosphatases. Kinase is an enzyme that uses ATP to add a phosphate group to a target substrate, whereas phosphatases hydrolyse the phosphate group, releasing a free phosphate ion. Abbreviations: ADP, adenosine diphosphate; ATP, adenosine triphosphate; H_2O, water; Pi, phosphate group; Protein-P, phosphorylated protein.

Although the existing evidence that the expression of TrkB-ICD induces a robust proteic phosphorylation, it is not clear whether it does so by directly phosphorylating proteins, or by an indirect mechanism. Consequently, overall, one could speculated that the phosphorylation mediated by TrkB-ICD fragment could be:

1) a direct mechanism – TrkB-ICD *per se* inducing the phosphorylation of all proteins (Figure 7.11A); or

2) an indirect mechanism – TrkB-ICD inducing the phosphorylation of an intermediate protein (other kinase, for instance) triggering cascade of other proteic phosphorylations (Figure 7.11B).
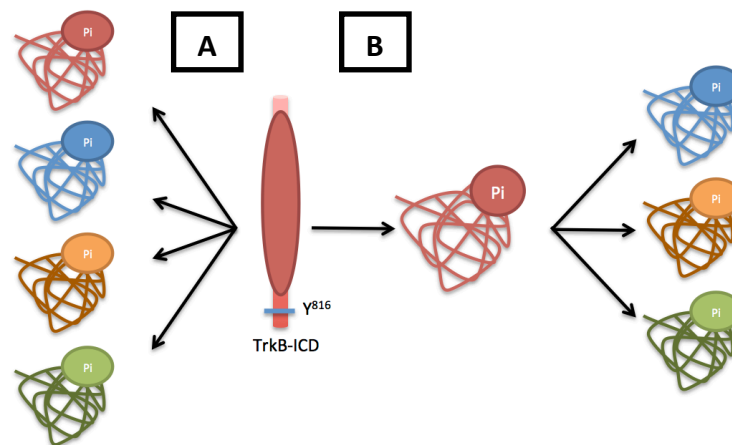
Figure 7.11 – Schematic representation of hypothetic phosphorylation mechanisms induced by TrkB-ICD fragment: (A) direct or (B) indirect phosphorylations. (A) TrkB-ICD *per se* directly induces the phosphorylation of a wide range of proteins. (B) TrkB-ICD induces the phosphorylation of an intermediate protein (such as other kinase) that, in turn, triggers the phosphorylation of several proteins. Abbreviations: Pi, phosphate group.

Given that TrkB-ICD has the kinase domain of TrkB-FL receptor, one could hypothesize on whether TrkB-ICD could spontaneously and directly activate the canonical pathways triggered by TrkB-FL (PLCγ, PI3K/AKT and MAPK pathways). However, preliminary data (not shown) do not point into that possibility, suggesting that TrkB-ICD fragment does not promote a robust activation of the signalling pathways mentioned above. So, further research is imperative to answer to this hypothesis and to unveil if TrkB-ICD is responsible for the phosphorylation of other substrates than TrkB-FL receptor. Moreover, in the future, there are several experimental approaches that could be performed to characterize and elucidate this complex signalling pathway induced by TrkB-ICD and phosphorylation dynamics, such as radioactive phosphorylation assays conjugated with radioactive phosphatase assays (which studies the dynamics of a radioactive phosphate group), immunoprecipitation assays, phosphoproteomics combined with mass spectrometry-based proteomics or even evaluation of genetic interactions between phosphorylated proteins and its targets.

7 Impact of TrkB-ICD fragment over cells phosphorylation pattern

Canonical pathways of TrkB-FL signalling require dimerization of TrkB-FL receptors to trigger its biological effects. Whether TrkB-ICD requires dimerization to trigger an effect is still unknown. Therefore, to clarify the exact mechanism of phosphorylation mediated by TrkB-ICD fragment, Bioluminescence Resonance Energy Transfer (BRET) assay or cross linking assays, will be performed in the future. These approaches will shed light about the possibility of TrkB-ICD isoforms be able to form homodimers.

Curiously, several works in 80's and 90's indicate that, on general, kinase activity is stimulated by autophosphorylation mechanisms [200–202]. Actually, in 1997, a study characterized the intracellular domain of TrkB-FL receptor (prepared by an insect cell expression system) and suggested that there is a sequential *Cis/Trans* autophosphorylation in TrkB-FL receptor. Interestingly, the authors studied a similar protein to TrkB-ICD fragment, only differing in the length of the protein in 66 aa. In that work, the authors observed that their protein was phosphorylated on tyrosine residues without any stimuli, in a mechanism requiring a divalent metal ion (Mn^{2+}) and with a biphasic progression: first a slow nonlinear phase, corresponding to an intramolecular activation (*cis*) and then a fast linear phase that corresponds to an intermolecular activation (*trans*) [203]. Later, the same authors used a modified yeast two-hybrid system that evaluates tyrosine phosphorylation-dependent protein-protein interactions in TrkB-mediated signalling and observed that Nck2 adaptor protein (regulator of cytoskeletal reorganization) interacts directly with the kinase domain of TrkB-FL receptor [204,205]. In this way, as future work, it would be important to evaluate if Nck2 adaptor protein is one of the proteins phosphorylated by TrkB-ICD fragment and if it could lead to possible downstream signalling proteins activation.

In parallel, our data also demonstrate that phosphorylation mediated by TrkB-ICD fragment is probably positively modulated by the PKA pathway. The results show that PKA and PKC inhibitors reduced the phosphorylation induced by TrkB-ICD. However, these inhibitors might not be specific and therefore might not directly inhibit TrkB-ICD kinase activity. It is reported that PKC pathway inhibitor (staurosporin) is an analogue compound of K252a [193,194] and also selectively inhibits the Trk tyrosine kinase activity by a direct mechanism [195]. Subsequently,

84

staurosporin could directly inhibit tyrosine kinase activity of TrkB-ICD. Similarly, H-89 compound (PKA inhibitor) is able, besides PKA inhibition, to inhibit eight kinases simultaneously [206]. However, at the concentration used (25 µM), H-89 compound selectively inhibits PKA substrate phosphorylation and related cellular functions [207]. In this way, in the present work, it is unlikely that H-89 could directly inhibit TrkB-ICD kinase, therefore, we hypothesized that PKA pathway could act as a positive modulator of the phosphorylation induced by TrkB-ICD fragment. The mechanisms underlying the H-89 effect are not known yet, however one could hypothesized that: A) TrkB-ICD could activate several substrates, including PKA, which in turn could phosphorylate other downstream proteins; B) TrkB-ICD phosphorylation could activate PKA pathway that, in turn, could phosphorylate its own targets; C) a certain protein (protein X) responsible for the inhibition of PKA could be the target of TrkB-ICD fragment triggering therefore the PKA downstream signalling (Figure 7.12).
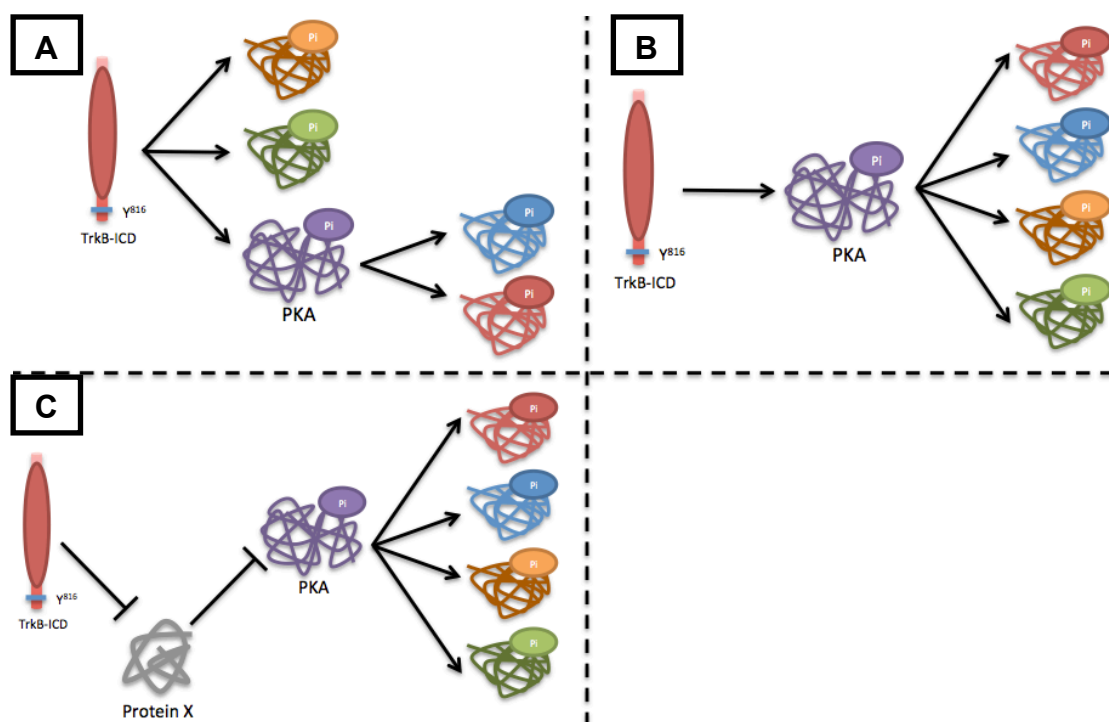
Figure 7.12 – Schematic representation of putative modulatory mechanisms involving PKA in phosphorylation induced by TrkB-ICD fragment. A) TrkB-ICD fragment could induce phosphorylation of several substrates, including PKA that, in turn, could phosphorylate its targets; B) TrkB-ICD phosphorylation could induce PKA phosphorylation that, in turn, could phosphorylate its targets or C) a particular protein (X, for instance) is responsible for the inhibition of PKA could be the target of TrkB-ICD fragment triggering therefore the PKA downstream signalling. Abbreviations: Pi, phosphate group; PKA, Protein Kinase A.

7 Impact of TrkB-ICD fragment over cells phosphorylation pattern

Concerning PKA pathway, it has been shown that its downstream signalling effects are dependent on the cell type and are involved in the regulation of mitochondrial dynamics, glycogen, sugar and lipid metabolism, as well as apoptosis, cell growth arrest and cell motility block [208–210]. Recently, it was also described that PKA plays, predominantly, a neuroprotective role, against several neurodegenerative diseases (such as AD and PD) [210].

Interestingly, our results also indicate that some inhibitors could affect TrkB-ICD levels, probably affecting its synthesis or degradation, which consequently have impact on phosphorylation induced by this fragment. For instance, it is known that protein synthesis requires Ras/Erk signalling [211] and so, when this signalling pathways are inhibited, protein synthesis might be affected. On the other hand, these inhibitors could also affect directly the phosphorylation levels, such is described to Src inhibitor used (PP2), once it is already described that its transient exposure could favour activation of Src kinase activity rather than its inhibition [212], which could probably explain the increased phosphorylation pattern seen with this inhibitor.

Finally, we observed that TrkB-ICD fragment induces phosphorylation mainly on fraction enriched in nuclear proteins, while phosphorylation of cytoplasmic and membrane proteins is almost absent. However, we should notice that fractionation protocol and immunofluorescence suggest different phosphorylation patterns. While immunofluorescence assays indicate that phosphorylation is present at nucleus and at neuronal processes, fractionation protocol suggests that phosphorylation is only present in fraction enriched on nuclear proteins. One hypothesis that could explain this difference concerns the methodology of fractionation protocol, since it only allows us to obtain enriched fractions and not pure fractions. Although markers used (GAPDH and Lamin B) stain correctly respective fractions, it is possible that other cells organelles, such as cytoskeleton, mitochondria or ribosome, for instance, could also be present on these fractions. So, for instance, if TrkB-ICD phosphorylates cytoskeleton proteins (as observed with immunofluorescence assays) and these proteins are not present in fraction enriched in cytoplasmic and membrane proteins,

we lost its expression, and therefore we could not ensure that there are no phosphorylated proteins on cytosol. In this way, as future work, we will use other fractionation protocols in order to better distinguish cell organelles and complement the results described so far.

Considering all discussed above, our data could suggest some different hypotheses, including that: A) cytosolic TrkB-ICD induces the phosphorylation of several proteins that are then translocated to the nucleus; B) cytosolic TrkB-ICD induces the phosphorylation of several proteins that are translocated to the nucleus, where they induce the phosphorylation of other proteins; C) cytosolic TrkB-ICD induces the phosphorylation of several proteins, part of them do not move from the cytosol and the other part is translocated to the nucleus; or D) nuclear TrkB-ICD promotes the phosphorylation of other nuclear proteins that could be translocated to cytosol and phosphorylates other proteins (Figure 7.13). Moreover, it is also possible that TrkB-ICD fragment is dispersed all over the cell and phosphorylates proteins at nucleus and at cytosol simultaneously.
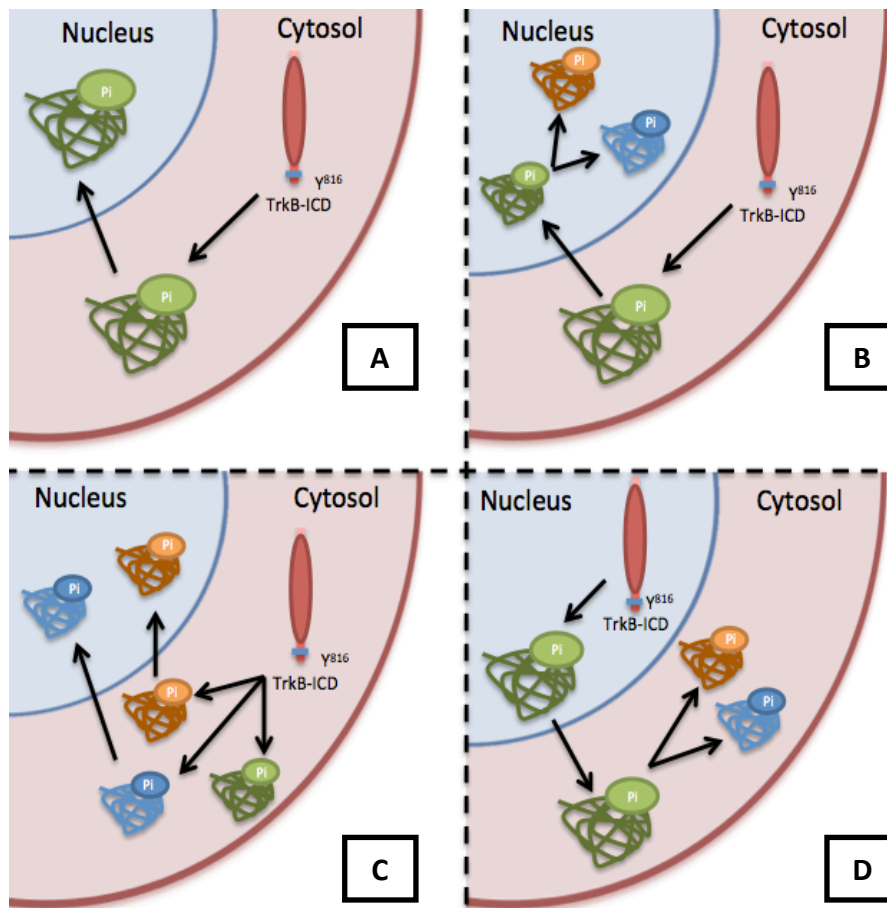
Figure 7.13 – Schematic representation of putative mechanisms of nuclear phosphorylation induced by TrkB-ICD fragment. A) cytosolic TrkB-ICD phosphorylates several proteins that are imported to the nucleus; B) cytosolic TrkB-ICD phosphorylates several proteins that are imported to the nucleus, where phosphorylates other proteins; C) cytosolic TrkB-ICD induces the phosphorylation of several proteins, being some of them translocated to the nucleus and other stays on the cytosol or D) nuclear TrkB-ICD phosphorylates other nuclear proteins, which could be translocated to cytosol and, in turn, phosphorylates other targets. Abbreviations: Pi, phosphate group.

Interestingly, we also demonstrated that nuclear translocation of TrkB-ICD requires its kinase activity dependent, since K252a incubation blocks TrkB-ICD nuclear translocation (Figure 7.9). It is important to mention that we obtained the same results using a subcellular fractionation protocol on HEK23T cells, showed in Appendix (*Section 10.2*), since it is a different type of cells than used on this work. Thus, our data suggest that phosphorylated TrkB-ICD could establish possible interactions with other proteins that facilitate its translocation. Furthermore, it is already described that NLS could be upregulated by phosphorylation, which facilitates nuclear translocation through distinct mechanisms, including the enhancement of binding affinity for importins, conformational changes that helps NLS recognition or anchorage of phosphorylated proteins with importin β7 or importin β2 [213]. However, it is possible that K252a can directly affect the nuclear translocation mechanism, which could consequently compromise TrkB-ICD translocation. In this way, as future work, we should perform other experiences to confirm that nuclear translocation of TrkB-ICD requires its kinase activity and to exclude the hypothesis of K252a as affecting nuclear import mechanisms.

8 Conclusions and Future Perspectives

This work demonstrates that TrkB-ICD fragment is a stable protein, that it has a significant tyrosine kinase activity and over time accumulates within the cell nucleus, suggesting that this fragment could have a biological role, which ultimately could be a key factor in AD pathophysiology.

The system constituted by BDNF and its FL receptor (TrkB-FL) is involved in one of the most important signalling pathways in the developing and adult mammalian brain implicated in neuronal differentiation, growth, survival and plasticity [4,23,36]. Therefore, the regulation of this system is crucial for the proper function of central nervous system and its dysregulation might lead to irreversible consequences, including a sustained neurodegeneration. So, the work here described could be an important startpoint for unveil the possible role of TrkB-ICD on this dysregulation. Moreover, it is also important to mention that there is yet any characterization of the transmembrane fragment generated after TrkB-FL cleavage by calpains (TrkB-T') and it might also be considered an important player in AD pathophysiology.

So, concerning TrkB-ICD, as future work, we will follow distinct roads in order to best characterize this fragment and to understand its role on AD pathophysiology. It is important to mention that possible effect of TrkB-ICD on cell viability was evaluated, however preliminary data do not allow us to build a conclusion these results are present on Appendix (*Section 10.1*). Thus, besides evaluation of TrkB-ICD effect on cell viability, at molecular level, we plan to: 1) evaluate the downstream effects of TrkB-ICD, evaluating its hypothetic effects on gene expression, 2) investigate the proteins directly phosphorylated by TrkB-ICD fragment, 3) analyze TrkB-ICD fragment dynamics after its formation and 4) unveil if TrkB-ICD fragment could contribute to the impairment of BDNF signalling. In addition, knowing that TrkB-ICD is increased in AD patients brain (Figure 1.13) which could ultimately be released into the cerebrospinal fluid (CSF), we will 5) study if TrkB-ICD levels in CFS could be correlated with AD progression and be considered as an AD biomarker.

Nevertheless, it is important to take into account that TrkB-ICD fragment might also be formed in other conditions where calpain activity is increased. Hence, possible results obtained about biological role of TrkB-ICD on AD context can be applied to other diseases, which might highlight TrkB-ICD importance.

It should be also highlighted that this work is one part of a bigger project that intends to describe dysregulations of neurotrophic actions and then, to identify new possibilities concerning the recovery of its functionality.

9 References

1.   Lewin, G. R. & Barde, Y.-A. Physiology of the Neurotrophins. *Annu. Rev. Neurosci.* **19,** 289–317 (1996).

2.   Reichardt, L. F. Neurotrophin-regulated signalling pathways. *Philos. Trans. R. Soc. Lond. B. Biol. Sci.* **361,** 1545–1564 (2006).

3.   Huang, E. J. & Reichardt, L. F. Neurotrophins: roles in neuronal development and function. *Annu. Rev. Neurosci.* **24,** 677–736 (2001).

4.   Arévalo, J. C. & Wu, S. H. Neurotrophin signaling: Many exciting surprises! *Cell. Mol. Life Sci.* **63,** 1523–1537 (2006).

5.   Götz, R. & Schartl, M. The conservation of neurotrophic factors during vertebrate evolution. *Comp. Biochem. Physiol. Pharmacol. Toxicol. Endocrinol.* **108,** 1–10 (1994).

6.   Levi-Montalcini, R. & Cohen, S. In vitro and in vivo effects of a nerve growth-stimulating agent isolated from snake venom. *Proc. Natl. Acad. Sci. U. S. A.* **42,** 695–9 (1956).

7.   Barde, Y., Edgar, D. & Thoenen, H. Neurotrophic Factor From Mammalian Brain. *EMBO J.* **I,** 549–553 (1982).

8.   Hohn, A., Leibrock, J., Bailey, K. & Barde, Y. A. Identification and characterization of a novel member of the nerve growth factor/brain-derived neurotrophic factor family. *Nature* **344,** 339–41 (1990).

9.   Lai, K. O., Fu, W. Y., Ip, F. C. & Ip, N. Y. Cloning and expression of a novel neurotrophin, NT-7, from carp. *Mol. Cell. Neurosci.* **11,** 64–76 (1998).

10.   Götz, R. *et al.* Neurotrophin-6 is a new member of the nerve growth factor family. *Nature* **372,** 266–9 (1994).

11.   Hallböök, F., Ibáñez, C. F. & Persson, H. Evolutionary studies of the nerve growth factor family reveal a novel member abundantly expressed in Xenopus ovary. *Neuron* **6,** 845–58 (1991).

9 References

12.   Maisonpierre, P. C. *et al.* Neurotrophin-3: a neurotrophic factor related to NGF and BDNF. *Science* **247,** 1446–51 (1990).

13.   Dechant, G. & Barde, Y. A. Signalling through the neurotrophin receptor p75NTR. *Curr. Opin. Neurobiol.* **7,** 413–8 (1997).

14.   Benito-Gutiérrez, E., Garcia-Fernàndez, J. & Comella, J. X. Origin and evolution of the Trk family of neurotrophic receptors. *Mol. Cell. Neurosci.* **31,** 179–92 (2006).

15.   Klein, R., Parada, L. F., Coulier, F. & Barbacid, M. trkB, a novel tyrosine protein kinase receptor expressed during mouse neural development. *EMBO J.* **8,** 3701–9 (1989).

16.   Lamballe, F., Klein, R. & Barbacid, M. trkC, a new member of the trk family of tyrosine protein kinases, is a receptor for neurotrophin-3. *Cell* **66,** 967–79 (1991).

17.   Martin-Zanca, D., Hughes, S. H. & Barbacid, M. A human oncogene formed by the fusion of truncated tropomyosin and protein tyrosine kinase sequences. *Nature* **319,** 743–8 (1989).

18.   Teng, K. K., Felice, S., Kim, T. & Hempstead, B. L. Understanding proneurotrophin actions: Recent advances and challenges. *Dev. Neurobiol.* **70,** 350–9 (2010).

19.   Leibrock, J. *et al.* Molecular cloning and expression of brain-derived neurotrophic factor. *Nature* **341,** 149–52 (1989).

20.   Hofer, M., Pagliusi, S. R., Hohn, A., Leibrock, J. & Barde, Y. A. Regional distribution of brain-derived neurotrophic factor mRNA in the adult mouse brain. *EMBO J.* **9,** 2459–64 (1990).

21.   Lessmann, V., Gottmann, K. & Malcangio, M. Neurotrophin secretion: Current facts and future prospects. *Prog. Neurobiol.* **69,** 341–374 (2003).

22.   Lee, R., Kermani, P., Teng, K. K. & Hempstead, B. L. Regulation of cell survival by secreted proneurotrophins. *Science* **294,** 1945–8 (2001).

23.   Chao, M. V. & Bothwell, M. Neurotrophins. *Neuron* **33,** 9–12 (2002).

24.   Binder, D. K. & Scharfman, H. E. Brain-derived neurotrophic factor. *Growth Factors*

22, 123–31 (2004).

25.   Mowla, S. J. *et al.* Differential sorting of nerve growth factor and brain-derived neurotrophic factor in hippocampal neurons. *J. Neurosci.* **19,** 2069–80 (1999).

26.   Pang, P. T. *et al.* Cleavage of proBDNF by tPA/plasmin is essential for long-term hippocampal plasticity. *Science* **306,** 487–91 (2004).

27.   Bibel, M., Hoppe, E. & Barde, Y. A. Biochemical and functional interactions between the neurotrophin receptors trk and p75NTR. *EMBO J.* **18,** 616–22 (1999).

28.   Middlemas, D. S., Meisenhelder, J. & Hunter, T. Identification of TrkB autophosphorylation sites and evidence that phospholipase C-??1 is a substrate of the TrkB receptor. *J. Biol. Chem.* **269,** 5458–5466 (1994).

29.   Klein, R., Conway, D., Parada, L. F. & Barbacid, M. The trkB tyrosine protein kinase gene codes for a second neurogenic receptor that lacks the catalytic kinase domain. *Cell* **61,** 647–56 (1990).

30.   Shelton, D. L. *et al.* Human trks: molecular cloning, tissue distribution, and expression of extracellular domain immunoadhesins. *J. Neurosci.* **15,** 477–91 (1995).

31.   Stoilov, P., Castren, E. & Stamm, S. Analysis of the human TrkB gene genomic organization reveals novel TrkB isoforms, unusual gene length, and splicing mechanism. *Biochem. Biophys. Res. Commun.* **290,** 1054–1065 (2002).

32.   Ansaloni, S. *et al.* TrkB Isoforms Differentially Affect AICD Production through Their Intracellular Functional Domains. *Int. J. Alzheimers. Dis.* **2011,** 729382 (2011).

33.   Eide, F. F. *et al.* Naturally occurring truncated trkB receptors have dominant inhibitory effects on brain-derived neurotrophic factor signaling. *J. Neurosci.* **16,** 3123–9 (1996).

34.   Biffo, S., Offenhäuser, N., Carter, B. D. & Barde, Y. A. Selective binding and internalisation by truncated receptors restrict the availability of BDNF during development. *Development* **121,** 2461–70 (1995).

35.   Segal, R. A. & Greenberg, M. E. Intracellular signaling pathways activated by neurotrophic factors. *Annu. Rev. Neurosci.* **19,** 463–89 (1996).

9 References

36.   Kaplan, D. R. & Stephens, R. M. Neurotrophin signal transduction by the Trk receptor. *J. Neurobiol.* **25,** 1404–17 (1994).

37.   Segal, R. A. Selectivity in neurotrophin signaling: theme and variations. *Annu. Rev. Neurosci.* **26,** 299–330 (2003).

38.   Stephens, R. M. *et al.* Trk receptors use redundant signal transduction pathways involving SHC and PLC-gamma 1 to mediate NGF responses. *Neuron* **12,** 691–705 (1994).

39.   Obermeier, A. *et al.* Neuronal differentiation signals are controlled by nerve growth factor receptor/Trk binding sites for SHC and PLC gamma. *EMBO J.* **13,** 1585–90 (1994).

40.   Chao, M. V. Neurotrophins and their receptors: a convergence point for many signalling pathways. *Nat. Rev. Neurosci.* **4,** 299–309 (2003).

41.   Minichiello, L. TrkB signalling pathways in LTP and learning. *Nat. Rev. Neurosci.* **10,** 850–860 (2009).

42.   Thomas, S. M., DeMarco, M., D'Arcangelo, G., Halegoua, S. & Brugge, J. S. Ras is essential for nerve growth factor- and phorbol ester-induced tyrosine phosphorylation of MAP kinases. *Cell* **68,** 1031–40 (1992).

43.   Xing, J., Kornhauser, J. M., Xia, Z., Thiele, E. A. & Greenberg, M. E. Nerve growth factor activates extracellular signal-regulated kinase and p38 mitogen-activated protein kinase pathways to stimulate CREB serine 133 phosphorylation. *Mol. Cell. Biol.* **18,** 1946–55 (1998).

44.   Chen, R. H., Abate, C. & Blenis, J. Phosphorylation of the c-Fos transrepression domain by mitogen-activated protein kinase and 90-kDa ribosomal S6 kinase. *Proc. Natl. Acad. Sci. U. S. A.* **90,** 10952–6 (1993).

45.   Atwal, J. K., Massie, B., Miller, F. D. & Kaplan, D. R. The TrkB-Shc site signals neuronal survival and local axon growth via MEK and P13-kinase. *Neuron* **27,** 265–77 (2000).

46.   Vetter, M. L., Martin-Zanca, D., Parada, L. F., Bishop, J. M. & Kaplan, D. R. Nerve growth factor rapidly stimulates tyrosine phosphorylation of phospholipase C-gamma 1 by a kinase activity associated with the product of the trk protooncogene. *Proc. Natl. Acad. Sci. U. S. A.* **88,** 5650–4 (1991).

47.   Ferrer, I. *et al.* BDNF and full-length and truncated TrkB expression in Alzheimer disease. Implications in therapeutic strategies. *J. Neuropathol. Exp. Neurol.* **58,** 729–39 (1999).

48.   Organization, W. H. D. I. WHO | Dementia: a public health priority. (2012). at <http://www.who.int/mental_health/publications/dementia_report_2012/en/>

49.   Przedborski, S., Vila, M. & Jackson-Lewis, V. Neurodegeneration: what is it and where are we? *J. Clin. Invest.* **111,** 3–10 (2003).

50.   Nieoullon, A. Neurodegenerative diseases and neuroprotection: current views and prospects. *J. Appl. Biomed.* **9,** 173–183 (2011).

51.   Winner, B., Kohl, Z. & Gage, F. H. Neurodegenerative disease and adult neurogenesis. *Eur. J. Neurosci.* **33,** 1139–51 (2011).

52.   Samii, A., Nutt, J. G. & Ransom, B. R. Parkinson's disease. *Lancet* **363,** 1783–1793 (2004).

53.   Selkoe, D. J. Alzheimer's disease: genes, proteins, and therapy. *Physiol. Rev.* **81,** 741–66 (2001).

54.   Caruso, C., Franceschi, C. & Licastro, F. Genetics of neurodegenerative disorders. *N. Engl. J. Med.* **349,** 193–4; author reply 193–4 (2003).

55.   Heemels, M.-T. Neurodegeneration. *Nature* **443,** 767–767 (2006).

56.   A, W. & M, P. *World Alzheimer Report 2010: The Global Economic Impact of Dementia. Alzheimer's Disease International*. (2010).

57.   von Strauss, E., Viitanen, M., De Ronchi, D., Winblad, B. & Fratiglioni, L. Aging and the occurrence of dementia: findings from a population-based cohort with a large sample of nonagenarians. *Arch. Neurol.* **56,** 587–92 (1999).

58.   Querfurth, H. W. & Laferla, F. M. Alzheimer's Disease. 329–344 (2010).

59.   Santana, I., Farinha, F., Freitas, S., Rodrigues, V. & Carvalho, Á. The Epidemiology of Dementia and Alzheimer Disease in Portugal: Estimations of Prevalence and

9 References

Treatment-Costs. *Acta Med. Port.* **28,** 182–188 (2015).

60.   Ferri, C. P. *et al.* Global prevalence of dementia: a Delphi consensus study. *Lancet* **366,** 2112–7 (2005).

61.   Ballard, C. *et al.* Alzheimer's disease. *Lancet* **377,** 1019–31 (2011).

62.   Bonaiuto, S. *et al.* Education and occupation as risk factors for dementia: a population-based case-control study. *Neuroepidemiology* **14,** 101–9 (1995).

63.   Zandi, P. P. *et al.* Reduced risk of Alzheimer disease in users of antioxidant vitamin supplements: the Cache County Study. *Arch. Neurol.* **61,** 82–8 (2004).

64.   Scarmeas, N., Stern, Y., Tang, M.-X., Mayeux, R. & Luchsinger, J. A. Mediterranean diet and risk for Alzheimer's disease. *Ann. Neurol.* **59,** 912–21 (2006).

65.   Castellani, R. J., Rolston, R. K. & Smith, M. A. Alzheimer disease. *Dis. Mon.* **56,** 484–546 (2010).

66.   Stelzmann, R. a., Schnitzlein, H. N. & Murtagh, F. R. An English translation of Alzheimer's 1907 paper, 'uber eine eigenartige erkankung der hirnrinde'. *Clin. Anat.* **8,** 429–431 (1995).

67.   Alois Alzheimer. Uber eine eigenartige Erkrankung der Hirnrinde. *Allg. Zeitschrift fur Psychiatr. und phychish- Gerichtl. Medizin* **64,** 146–148 (1907).

68.   Maurer, K., Volk, S. & Gerbaldo, H. Auguste D and Alzheimer's disease. *Lancet (London, England)* **349,** 1546–9 (1997).

69.   McDowell, I. Alzheimer's disease: insights from epidemiology. *Aging (Milano).* **13,** 143–162 (2001).

70.   Meek, P. D., McKeithan, K. & Schumock, G. T. Economic considerations in Alzheimer's disease. *Pharmacotherapy* **18,** 68–73; discussion 79–82

71.   Shah, R. The role of nutrition and diet in Alzheimer disease: a systematic review. *J. Am. Med. Dir. Assoc.* **14,** 398–402 (2013).

72.   Barnard, N. D. *et al.* Dietary and lifestyle guidelines for the prevention of Alzheimer's

disease. *Neurobiol. Aging* **35 Suppl 2,** S74–8 (2014).

73. Ahlskog, J. E., Geda, Y. E., Graff-Radford, N. R. & Petersen, R. C. Physical exercise as a preventive or disease-modifying treatment of dementia and brain aging. *Mayo Clin. Proc.* **86,** 876–84 (2011).

74. Cataldo, J. K., Prochaska, J. J. & Glantz, S. A. Cigarette smoking is a risk factor for Alzheimer's Disease: an analysis controlling for tobacco industry affiliation. *J. Alzheimers. Dis.* **19,** 465–80 (2010).

75. Gómez-Isla, T. *et al.* Profound loss of layer II entorhinal cortex neurons occurs in very mild Alzheimer's disease. *J. Neurosci.* **16,** 4491–4500 (1996).

76. Huang, Y. & Mucke, L. Alzheimer mechanisms and therapeutic strategies. *Cell* **148,** 1204–1222 (2012).

77. Chin, J. *et al.* Reelin depletion in the entorhinal cortex of human amyloid precursor protein transgenic mice and humans with Alzheimer's disease. *J. Neurosci.* **27,** 2727–33 (2007).

78. Pescosolido, N., Pascarella, A., Buomprisco, G. & Rusciano, D. Critical Review on the Relationship between Glaucoma and Alzheimer's Disease. *Adv. Ophthalmol. Vis. Syst.* **1,** (2014).

79. Tanzi, R. E. & Bertram, L. Twenty years of the Alzheimer's disease amyloid hypothesis: a genetic perspective. *Cell* **120,** 545–55 (2005).

80. Busciglio, J. *et al.* Altered metabolism of the amyloid beta precursor protein is associated with mitochondrial dysfunction in Down's syndrome. *Neuron* **33,** 677–88 (2002).

81. Levy-Lahad, E. *et al.* Candidate gene for the chromosome 1 familial Alzheimer's disease locus. *Science* **269,** 973–7 (1995).

82. Goate, A. *et al.* Segregation of a missense mutation in the amyloid precursor protein gene with familial Alzheimer's disease. *Nature* **349,** 704–6 (1991).

83. Chin, J. Selecting a mouse model of Alzheimer's disease. *Methods Mol. Biol.* **670,** 169–89 (2011).

9 References

84. Hashimoto, M., Rockenstein, E., Crews, L. & Masliah, E. Role of protein aggregation in mitochondrial dysfunction and neurodegeneration in Alzheimer's and Parkinson's diseases. *Neuromolecular Med.* **4,** 21–36 (2003).

85. Glenner, G. G. & Wong, C. W. Alzheimer's disease: initial report of the purification and characterization of a novel cerebrovascular amyloid protein. *Biochem. Biophys. Res. Commun.* **120,** 885–90 (1984).

86. Grundke-Iqbal, I. *et al.* Abnormal phosphorylation of the microtubule-associated protein tau (tau) in Alzheimer cytoskeletal pathology. *Proc. Natl. Acad. Sci. U. S. A.* **83,** 4913–7 (1986).

87. Haass, C. & Selkoe, D. J. Soluble protein oligomers in neurodegeneration: lessons from the Alzheimer's amyloid beta-peptide. *Nat. Rev. Mol. Cell Biol.* **8,** 101–12 (2007).

88. Kang, J. *et al.* The precursor of Alzheimer's disease amyloid A4 protein resembles a cell-surface receptor. *Nature* **325,** 733–6

89. Vassar, R. *et al.* Beta-secretase cleavage of Alzheimer's amyloid precursor protein by the transmembrane aspartic protease BACE. *Science* **286,** 735–41 (1999).

90. Hooper, N. M. Roles of proteolysis and lipid rafts in the processing of the amyloid precursor protein and prion protein. *Biochem. Soc. Trans.* **33,** 335–8 (2005).

91. Jarrett, J. T., Berger, E. P. & Lansbury, P. T. The C-terminus of the beta protein is critical in amyloidogenesis. *Ann. N. Y. Acad. Sci.* **695,** 144–8 (1993).

92. Devi, L. & Ohno, M. Mitochondrial dysfunction and accumulation of the β-secretase-cleaved C-terminal fragment of APP in Alzheimer's disease transgenic mice. *Neurobiol. Dis.* **45,** 417–24 (2012).

93. Kemppainen, S. *et al.* Impaired TrkB receptor signaling contributes to memory impairment in APP/PS1 mice. *Neurobiol. Aging* **33,** 1122.e23–1122.e39 (2012).

94. Arancibia, S. *et al.* Protective effect of BDNF against beta-amyloid induced neurotoxicity in vitro and in vivo in rats. *Neurobiol. Dis.* **31,** 316–26 (2008).

95. Hölscher, C. Possible causes of Alzheimer's disease: amyloid fragments, free radicals, and calcium homeostasis. *Neurobiol. Dis.* **5,** 129–41 (1998).

96.   Jerónimo-Santos, A. Brain-derived neurotrophic factor and adenosine signalling on amyloid-β peptide induced toxicity: impact on hippocampal function. (2014).

97.   Wang, H. Y. *et al.* beta-Amyloid(1-42) binds to alpha7 nicotinic acetylcholine receptor with high affinity. Implications for Alzheimer's disease pathology. *J. Biol. Chem.* **275,** 5626–32 (2000).

98.   Liu, S.-J., Gasperini, R., Foa, L. & Small, D. H. Amyloid-beta decreases cell-surface AMPA receptors by increasing intracellular calcium and phosphorylation of GluR2. *J. Alzheimers. Dis.* **21,** 655–66 (2010).

99.   Wu, J., Anwyl, R. & Rowan, M. J. beta-Amyloid selectively augments NMDA receptor-mediated synaptic transmission in rat hippocampus. *Neuroreport* **6,** 2409–13 (1995).

100.   Ferreiro, E., Oliveira, C. R. & Pereira, C. Involvement of endoplasmic reticulum Ca2+ release through ryanodine and inositol 1,4,5-triphosphate receptors in the neurotoxic effects induced by the amyloid-beta peptide. *J. Neurosci. Res.* **76,** 872–80 (2004).

101.   Arispe, N., Pollard, H. B. & Rojas, E. beta-Amyloid Ca(2+)-channel hypothesis for neuronal death in Alzheimer disease. *Mol. Cell. Biochem.* **140,** 119–25 (1994).

102.   Arispe, N., Pollard, H. B. & Rojas, E. Giant multilevel cation channels formed by Alzheimer disease amyloid beta-protein [A beta P-(1-40)] in bilayer membranes. *Proc. Natl. Acad. Sci. U. S. A.* **90,** 10573–7 (1993).

103.   Alberdi, E. *et al.* Amyloid beta oligomers induce Ca2+ dysregulation and neuronal death through activation of ionotropic glutamate receptors. *Cell Calcium* **47,** 264–72 (2010).

104.   Khachaturian, Z. S. Calcium hypothesis of Alzheimer's disease and brain aging. *Ann. N. Y. Acad. Sci.* **747,** 1–11 (1994).

105.   Berridge, M. J. Calcium hypothesis of Alzheimer's disease. *Pflugers Arch.* **459,** 441–9 (2010).

106.   Jerónimo-Santos, A. *et al.* Dysregulation of TrkB Receptors and BDNF Function by Amyloid-β Peptide is Mediated by Calpain. *Cereb. Cortex* (2014). doi:10.1093/cercor/bhu105

107.   Connor, B. *et al.* Brain-derived neurotrophic factor is reduced in Alzheimer's disease.

Brain Res. Mol. Brain Res. **49,** 71–81 (1997).

108. Narisawa-Saito, M., Wakabayashi, K., Tsuji, S., Takahashi, H. & Nawa, H. Regional specificity of alterations in NGF, BDNF and NT-3 levels in Alzheimer's disease. *Neuroreport* **7,** 2925–8 (1996).

109. Phillips, H. S. *et al.* BDNF mRNA is decreased in the hippocampus of individuals with Alzheimer's disease. *Neuron* **7,** 695–702 (1991).

110. Michalski, B. & Fahnestock, M. Pro-brain-derived neurotrophic factor is decreased in parietal cortex in Alzheimer's disease. *Brain Res. Mol. Brain Res.* **111,** 148–54 (2003).

111. Peng, S., Wuu, J., Mufson, E. J. & Fahnestock, M. Precursor form of brain-derived neurotrophic factor and mature brain-derived neurotrophic factor are decreased in the pre-clinical stages of Alzheimer's disease. *J. Neurochem.* **93,** 1412–21 (2005).

112. Ginsberg, S. D., Che, S., Wuu, J., Counts, S. E. & Mufson, E. J. Down regulation of trk but not p75NTR gene expression in single cholinergic basal forebrain neurons mark the progression of Alzheimer's disease. *J. Neurochem.* **97,** 475–87 (2006).

113. Rantamäki, T. *et al.* The impact of Bdnf gene deficiency to the memory impairment and brain pathology of APPswe/PS1dE9 mouse model of Alzheimer's disease. *PLoS One* **8,** e68722 (2013).

114. Nagahara, A. H. *et al.* Early BDNF treatment ameliorates cell loss in the entorhinal cortex of APP transgenic mice. *J. Neurosci.* **33,** 15596–602 (2013).

115. Devi, L. & Ohno, M. 7,8-dihydroxyflavone, a small-molecule TrkB agonist, reverses memory deficits and BACE1 elevation in a mouse model of Alzheimer's disease. *Neuropsychopharmacology* **37,** 434–44 (2012).

116. Croall, D. E. & DeMartino, G. N. Calcium-activated neutral protease (calpain) system: structure, function, and regulation. *Physiol. Rev.* **71,** 813–47 (1991).

117. Melloni, E. & Pontremoli, S. The calpains. *Trends Neurosci.* **12,** 438–44 (1989).

118. Adamec, E., Mohan, P., Vonsattel, J. P. & Nixon, R. a. Calpain activation in neurodegenerative diseases: Confocal immunofluorescence study with antibodies specifically recognizing the active form of calpain 2. *Acta Neuropathol.* **104,** 92–104 (2002).

119. Storr, S. J., Carragher, N. O., Frame, M. C., Parr, T. & Martin, S. G. The calpain system and cancer. *Nat. Rev. Cancer* **11,** 364–74 (2011).

120. Goll, D. E., Thompson, V. F., Li, H., Wei, W. & Cong, J. The calpain system. *Physiol. Rev.* **83,** 731–801 (2003).

121. Johnson, G. V, Jope, R. S. & Binder, L. I. Proteolysis of tau by calpain. *Biochem. Biophys. Res. Commun.* **163,** 1505–11 (1989).

122. Banik, N. L., Matzelle, D. C., Gantt-Wilford, G., Osborne, A. & Hogan, E. L. Increased calpain content and progressive degradation of neurofilament protein in spinal cord injury. *Brain Res.* **752,** 301–6 (1997).

123. Johnson, G. V, Litersky, J. M. & Jope, R. S. Degradation of microtubule-associated protein 2 and brain spectrin by calpain: a comparative study. *J. Neurochem.* **56,** 1630–8 (1991).

124. Potter, D. A. *et al.* Calpain regulates actin remodeling during cell spreading. *J. Cell Biol.* **141,** 647–62 (1998).

125. Fischer, I., Romano-Clarke, G. & Grynspan, F. Calpain-mediated proteolysis of microtubule associated proteins MAP1B and MAP2 in developing brain. *Neurochem. Res.* **16,** 891–8 (1991).

126. Ferreira, A. Calpain Dysregulation in Alzheimer's Disease. *ISRN Biochem.* **2012,** 1–12 (2012).

127. Shields, D. C. & Banik, N. L. Pathophysiological role of calpain in experimental demyelination. *J. Neurosci. Res.* **55,** 533–41 (1999).

128. Shields, D. C., Schaecher, K. E., Saido, T. C. & Banik, N. L. A putative mechanism of demyelination in multiple sclerosis by a proteolytic enzyme, calpain. *Proc. Natl. Acad. Sci. U. S. A.* **96,** 11486–91 (1999).

129. Iwamoto, N., Thangnipon, W., Crawford, C. & Emson, P. C. Localization of calpain immunoreactivity in senile plaques and in neurones undergoing neurofibrillary degeneration in Alzheimer's disease. *Brain Res.* **561,** 177–80 (1991).

130. Nixon, R. A. *et al.* Calcium-activated neutral proteinase (calpain) system in aging and Alzheimer's disease. *Ann. N. Y. Acad. Sci.* **747,** 77–91 (1994).

131. Tsuji, T., Shimohama, S., Kimura, J. & Shimizu, K. m-Calpain (calcium-activated neutral proteinase) in Alzheimer's disease brains. *Neurosci. Lett.* **248,** 109–12 (1998).

132. Liang, B., Duan, B.-Y., Zhou, X.-P., Gong, J.-X. & Luo, Z.-G. Calpain activation promotes BACE1 expression, amyloid precursor protein processing, and amyloid plaque formation in a transgenic mouse model of Alzheimer disease. *J. Biol. Chem.* **285,** 27737–44 (2010).

133. Grynspan, F., Griffin, W. R., Cataldo, A., Katayama, S. & Nixon, R. A. Active site-directed antibodies identify calpain II as an early-appearing and pervasive component of neurofibrillary pathology in Alzheimer's disease. *Brain Res.* **763,** 145–58 (1997).

134. Taniguchi, S. *et al.* Calpain-mediated degradation of p35 to p25 in postmortem human and rat brains. *FEBS Lett.* **489,** 46–50 (2001).

135. Saito, K., Elce, J. S., Hamos, J. E. & Nixon, R. a. Widespread activation of calcium-activated neutral proteinase (calpain) in the brain in Alzheimer disease: a potential molecular basis for neuronal degeneration. *Proc. Natl. Acad. Sci. U. S. A.* **90,** 2628–2632 (1993).

136. Rao, M. V *et al.* Marked calpastatin (CAST) depletion in Alzheimer's disease accelerates cytoskeleton disruption and neurodegeneration: neuroprotection by CAST overexpression. *J. Neurosci.* **28,** 12241–54 (2008).

137. Trinchese, F. *et al.* Inhibition of calpains improves memory and synaptic transmission in a mouse model of Alzheimer disease. *J. Clin. Invest.* **118,** 2796–807 (2008).

138. Bjorge, J. D., Jakymiw, A. & Fujita, D. J. Selected glimpses into the activation and function of Src kinase. *Oncogene* **19,** 5620–5635 (2000).

139. Encinas, M., Crowder, R. J., Milbrandt, J. & Johnson, E. M. Tyrosine 981, a novel ret autophosphorylation site, binds c-Src to mediate neuronal survival. *J. Biol. Chem.* **279,** 18262–9 (2004).

140. Encinas, M. *et al.* c-Src is required for glial cell line-derived neurotrophic factor (GDNF) family ligand-mediated neuronal survival via a phosphatidylinositol-3 kinase (PI-3K)-dependent pathway. *J. Neurosci.* **21,** 1464–72 (2001).

141. Hossain, M. I. *et al.* A truncated fragment of Src protein kinase generated by calpain-mediated cleavage is a mediator of neuronal death in excitotoxicity. *J. Biol. Chem.* **288,** 9696–9709 (2013).

142. Polakis, P. Wnt signaling and cancer. *Genes Dev.* **14,** 1837–51 (2000).

143. Logan, C. Y. & Nusse, R. The Wnt signaling pathway in development and disease. *Annu. Rev. Cell Dev. Biol.* **20,** 781–810 (2004).

144. Rios-Doria, J., Kuefer, R., Ethier, S. P. & Day, M. L. Cleavage of beta-catenin by calpain in prostate and mammary tumor cells. *Cancer Res.* **64,** 7237–40 (2004).

145. Abe, K. & Takeichi, M. NMDA-Receptor Activation Induces Calpain-Mediated β-Catenin Cleavages for Triggering Gene Expression. *Neuron* **53,** 387–397 (2007).

146. Gould, T. D. & Manji, H. K. The Wnt signaling pathway in bipolar disorder. *Neuroscientist* **8,** 497–511 (2002).

147. De Ferrari, G. V & Inestrosa, N. C. Wnt signaling function in Alzheimer's disease. *Brain Res. Brain Res. Rev.* **33,** 1–12 (2000).

148. Chen, J., Park, C. S. & Tang, S.-J. Activity-dependent synaptic Wnt release regulates hippocampal long term potentiation. *J. Biol. Chem.* **281,** 11910–6 (2006).

149. Patrick, G. N. *et al.* Conversion of p35 to p25 deregulates Cdk5 activity and promotes neurodegeneration. *Nature* **402,** 615–622 (1999).

150. Kusakawa, G. *et al.* Calpain-dependent proteolytic cleavage of the p35 cyclin-dependent kinase 5 activator to p25. *J. Biol. Chem.* **275,** 17166–72 (2000).

151. Nath, R. *et al.* Processing of cdk5 activator p35 to its truncated form (p25) by calpain in acutely injured neuronal cells. *Biochem. Biophys. Res. Commun.* **274,** 16–21 (2000).

152. Nguyen, M. D., Mushynski, W. E. & Julien, J.-P. Cycling at the interface between neurodevelopment and neurodegeneration. *Cell Death Differ.* **9,** 1294–306 (2002).

153. Tsai, L. H., Takahashi, T., Caviness, V. S. & Harlow, E. Activity and expression pattern of cyclin-dependent kinase 5 in the embryonic mouse nervous system. *Development*

119, 1029–40 (1993).

154. Nikolic, M., Dudek, H., Kwon, Y. T., Ramos, Y. F. & Tsai, L. H. The cdk5/p35 kinase is essential for neurite outgrowth during neuronal differentiation. *Genes Dev.* **10,** 816–25 (1996).

155. Rong, R. *et al.* PI3 kinase enhancer-Homer complex couples mGluRI to PI3 kinase, preventing neuronal apoptosis. *Nat. Neurosci.* **6,** 1153–61 (2003).

156. Zhu, P., DeCoster, M. A. & Bazan, N. G. Interplay among platelet-activating factor, oxidative stress, and group I metabotropic glutamate receptors modulates neuronal survival. *J. Neurosci. Res.* **77,** 525–31 (2004).

157. Xu, W. *et al.* Calpain-mediated mGluR1alpha truncation: a key step in excitotoxicity. *Neuron* **53,** 399–412 (2007).

158. Tauszig-Delamasure, S. *et al.* The TrkC receptor induces apoptosis when the dependence receptor notion meets the neurotrophin paradigm. *Proc. Natl. Acad. Sci. U. S. A.* **104,** 13361–13366 (2007).

159. Gomes, J. R. *et al.* Excitotoxicity Downregulates TrkB.FL Signaling and Upregulates the Neuroprotective Truncated TrkB Receptors in Cultured Hippocampal and Striatal Neurons. *J. Neurosci.* **32,** 4610–4622 (2012).

160. Al-Ashwal, R. H. Optimization of Lipofectamine 2000 reagent transfection method for delivering D1 domain of Coxsackievirus - Adenosine receptor into chinese hamster ovaries cell lines. (Universiti Teknologi Malaysia, 2009).

161. Voice, M. A. Investigation of the clathrin-dependent internalisation of cytotoxic T Lymphocyte antigen-4 and Analysis of the antigen-specific cytokine responses of CD4+ T-Lymphocytes. (University of Birmingham, 2011).

162. Belle, A., Tanay, A., Bitincka, L., Shamir, R. & O'Shea, E. K. Quantification of protein half-lives in the budding yeast proteome. *Proc. Natl. Acad. Sci.* **103,** 13004–13009 (2006).

163. Valadas, J. S. *et al.* Neuroprotection afforded by adenosine A2A receptor blockade is modulated by corticotrophin-releasing factor (CRF) in glutamate injured cortical neurons. *J. Neurochem.* **123,** 1030–1040 (2012).

164. Friend, D. S., Papahadjopoulos, D. & Debs, R. J. Endocytosis and intracellular processing accompanying transfection mediated by cationic liposomes. *Biochim. Biophys. Acta* **1278,** 41–50 (1996).

165. Dalby, B. *et al.* Advanced transfection with Lipofectamine 2000 reagent: Primary neurons, siRNA, and high-throughput applications. *Methods* **33,** 95–103 (2004).

166. Hunt, M. A., Currie, M. J., Robinson, B. A. & Dachs, G. U. Optimizing transfection of primary human umbilical vein endothelial cells using commercially available chemical transfection reagents. *J. Biomol. Tech.* **21,** 66–72 (2010).

167. Zabner, J., Fasbender, A. J., Moninger, T., Poellinger, K. A. & Welsh, M. J. Cellular and molecular barriers to gene transfer by a cationic lipid. *J. Biol. Chem.* **270,** 18997–9007 (1995).

168. Ohki, E. C., Tilkins, M. L., Ciccarone, V. C. & Price, P. J. Improving the transfection efficiency of post-mitotic neurons. *J. Neurosci. Methods* **112,** 95–99 (2001).

169. Ciccarone, V. *et al.* LIPOFECTAMINE 2000™ Reagent for rapid, efficient transfection of eukaryotic cells. *Focus (Madison).* **21 (2),** 54–5 (1999).

170. Fallini, C., Bassell, G. J. & Rossoll, W. High-efficiency transfection of cultured primary motor neurons to study protein localization, trafficking, and function. *Mol. Neurodegener.* **5,** 17 (2010).

171. Gomez-Nicola, D., Riecken, K., Fehse, B. & Perry, V. H. In-vivo RGB marking and multicolour single-cell tracking in the adult brain. *Sci. Rep.* **4,** 7520 (2014).

172. Schneider-Poetsch, T. *et al.* Inhibition of eukaryotic translation elongation by cycloheximide and lactimidomycin. *Nat. Chem. Biol.* **6,** 209–217 (2010).

173. Dastoor, Z. & Dreyer, J. L. Potential role of nuclear translocation of glyceraldehyde-3-phosphate dehydrogenase in apoptosis and oxidative stress. *J. Cell Sci.* **114,** 1643–53 (2001).

174. Colell, A., Green, D. R. & Ricci, J.-E. Novel roles for GAPDH in cell death and carcinogenesis. *Cell Death Differ.* **16,** 1573–81 (2009).

175. Alberts, B. *et al.* The Transport of Molecules between the Nucleus and the Cytosol. (2002). at <http://www.ncbi.nlm.nih.gov/books/NBK26932/>

9 References

176.   Silver, P. A. How proteins enter the nucleus. *Cell* **64,** 489–97 (1991).

177.   Macara, I. G. Transport into and out of the Nucleus. *Microbiol. Mol. Biol. Rev.* **65,** 570–594 (2001).

178.   Newmeyer, D. D. & Forbes, D. J. Nuclear import can be separated into distinct steps in vitro: nuclear pore binding and translocation. *Cell* **52,** 641–53 (1988).

179.   Conti, E., Uy, M., Leighton, L., Blobel, G. & Kuriyan, J. Crystallographic analysis of the recognition of a nuclear localization signal by the nuclear import factor karyopherin alpha. *Cell* **94,** 193–204 (1998).

180.   Lange, A. *et al.* Classical nuclear localization signals: definition, function, and interaction with importin alpha. *J. Biol. Chem.* **282,** 5101–5 (2007).

181.   Kosugi, S., Hasebe, M., Tomita, M. & Yanagawa, H. Systematic identification of cell cycle-dependent yeast nucleocytoplasmic shuttling proteins by prediction of composite motifs. *Proc. Natl. Acad. Sci.* **106,** 10171–10176 (2009).

182.   Haley, J. & Gullick, W. *EGFR Signaling Networks in Cancer Therapy*. (Springer, 2009). at <https://books.google.com/books?id=lUPbzFYc-TsC&pgis=1>

183.   Sandvig, K. & van Deurs, B. Entry of ricin and Shiga toxin into cells: molecular mechanisms and medical perspectives. *EMBO J.* **19,** 5943–50 (2000).

184.   Pelkmans, L., Kartenbeck, J. & Helenius, A. Caveolar endocytosis of simian virus 40 reveals a new two-step vesicular-transport pathway to the ER. *Nat. Cell Biol.* **3,** 473–83 (2001).

185.   Liao, H. J. & Carpenter, G. Regulated Intramembrane Cleavage of the EGF Receptor. *Traffic* **13,** 1106–1112 (2012).

186.   Liao, H.-J. & Carpenter, G. Role of the Sec61 translocon in EGF receptor trafficking to the nucleus and gene expression. *Mol. Biol. Cell* **18,** 1064–72 (2007).

187.   Chan, S. L. & Mattson, M. P. Caspase and calpain substrates: roles in synaptic plasticity and cell death. *J. Neurosci. Res.* **58,** 167–90 (1999).

188.   Lynch, G. & Baudry, M. Brain spectrin, calpain and long-term changes in synaptic efficacy. *Brain Res. Bull.* **18,** 809–15 (1987).

189.   Fortini, M. E. Signalling: γ-Secretase-mediated proteolysis in cell-surface-receptor signalling. *Nat. Rev. Mol. Cell Biol.* **3,** 673–684 (2002).

190.   Kimberly, W. T., Zheng, J. B., Guenette, S. Y. & Selkoe, D. J. The Intracellular Domain of the -Amyloid Precursor Protein Is Stabilized by Fe65 and Translocates to the Nucleus in a Notch-like Manner. *J. Biol. Chem.* **276,** 40288–40292 (2001).

191.   Cupers, P., Orlans, I., Craessaerts, K., Annaert, W. & De Strooper, B. The amyloid precursor protein (APP)-cytoplasmic fragment generated by gamma-secretase is rapidly degraded but distributes partially in a nuclear fraction of neurones in culture. *J. Neurochem.* **78,** 1168–78 (2001).

192.   Gafni, J. *et al.* Inhibition of calpain cleavage of Huntingtin reduces toxicity: Accumulation of calpain/caspase fragments in the nucleus. *J. Biol. Chem.* **279,** 20211–20220 (2004).

193.   Mizuno, K., Saido, T. C., Ohno, S., Tamaoki, T. & Suzuki, K. Staurosporine-related compounds, K252a and UCN-01, inhibit both cPKC and nPKC. *FEBS Lett.* **330,** 114–116 (1993).

194.   Zimmermann, A. & Keller, H. Effects of staurosporine, K 252a and other structurally related protein kinase inhibitors on shape and locomotion of Walker carcinosarcoma cells. *Br. J. Cancer* **66,** 1077–82 (1992).

195.   Ohmichi, M., Decker, S. J., Pang, L. & Saltiel, A. R. Inhibition of the cellular actions of nerve growth factor by staurosporine and K252A results from the attenuation of the activity of the trk tyrosine kinase. *Biochemistry* **31,** 4034–9 (1992).

196.   Ostman, a & Böhmer, F. D. Regulation of receptor tyrosine kinase signaling by protein tyrosine phosphatases. *Trends Cell Biol.* **11,** 258–266 (2001).

197.   Hunter, T. Protein kinases and phosphatases: the yin and yang of protein phosphorylation and signaling. *Cell* **80,** 225–36 (1995).

198.   Kuban-Jankowska, A., Gorska, M., Knap, N., Cappello, F. & Wozniak, M. Protein tyrosine phosphatases in pathological process. *Front. Biosci. (Landmark Ed.* **20,** 377–88 (2015).

199. Cohen, P. The Structure and Regulation of Protein Phosphatases. *Annu. Rev. Biochem.* **58,** 453–508 (1989).

200. Cobb, M. H., Sang, B. C., Gonzalez, R., Goldsmith, E. & Ellis, L. Autophosphorylation activates the soluble cytoplasmic domain of the insulin receptor in an intermolecular reaction. *J. Biol. Chem.* **264,** 18701–6 (1989).

201. Wei, L., Hubbard, S. R., Hendrickson, W. A. & Ellis, L. Expression, characterization, and crystallization of the catalytic core of the human insulin receptor protein-tyrosine kinase domain. *J. Biol. Chem.* **270,** 8122–30 (1995).

202. Hsu, C. Y., Hurwitz, D. R., Mervic, M. & Zilberstein, A. Autophosphorylation of the intracellular domain of the epidermal growth factor receptor results in different effects on its tyrosine kinase activity with various peptide substrates. Phosphorylation of peptides representing Tyr(P) sites of phospholipase C-. *J. Biol. Chem.* **266,** 603–8 (1991).

203. Iwasaki, Y., Nishiyama, H., Suzuki, K. & Koizumi, S. Sequential cis/trans autophosphorylation in TrkB tyrosine kinase. *Biochemistry* **36,** 2694–2700 (1997).

204. Yamada, M. *et al.* Analysis of tyrosine phosphorylation-dependent protein-protein interactions in TrkB-mediated intracellular signaling using modified yeast two-hybrid system. *J. Biochem.* **130,** 157–65 (2001).

205. Suzuki, S. *et al.* Brain-derived neurotrophic factor promotes interaction of the Nck2 adaptor protein with the TrkB tyrosine kinase receptor. *Biochem. Biophys. Res. Commun.* **294,** 1087–1092 (2002).

206. Lochner, A. & Moolman, J. A. The Many Faces of H89: A Review. *Cardiovasc. Drug Rev.* **24,** 261–274 (2006).

207. Chijiwa, T. *et al.* Inhibition of forskolin-induced neurite outgrowth and protein phosphorylation by a newly synthesized selective inhibitor of cyclic AMP-dependent protein kinase, N-[2-(p-bromocinnamylamino)ethyl]-5-isoquinolinesulfonamide (H-89), of PC12D pheochromocytoma . *J. Biol. Chem.* **265,** 5267–72 (1990).

208. Wilson, W. A. *et al.* Regulation of glycogen metabolism in yeast and bacteria. *FEMS Microbiol. Rev.* **34,** 952–85 (2010).

209. Caretta, A. & Mucignat-Caretta, C. Protein kinase a in cancer. *Cancers (Basel).* **3,** 913–26 (2011).

210. Dagda, R. K. & Das Banerjee, T. Role of protein kinase A in regulating mitochondrial function and neuronal development: implications to neurodegenerative diseases. *Rev. Neurosci.* **26,** 359–70 (2015).

211. Wang, L. Ras/Erk Signaling Is Essential for Activation of Protein Synthesis by Gq Protein-Coupled Receptor Agonists in Adult Cardiomyocytes. *Circ. Res.* **91,** 821–829 (2002).

212. Wu, S. S., Yamauchi, K. & Rozengurt, E. Bombesin and angiotensin II rapidly stimulate Src phosphorylation at Tyr-418 in fibroblasts and intestinal epithelial cells through a PP2-insensitive pathway. *Cell. Signal.* **17,** 93–102 (2005).

213. Nardozzi, J. D., Lott, K. & Cingolani, G. Phosphorylation meets nuclear import: a review. *Cell Commun. Signal.* **8,** 32 (2010).

214. Jerónimo-Santos, A. *et al.* Brain-derived neurotrophic factor mediates neuroprotection against A β -induced toxicity through a mechanism independent on adenosine 2A receptor activation. *Growth Factors* **33,** 298–308 (2015).

9 References

10 Appendix

10.1 Preliminary data about TrkB-ICD fragment toxicity

As discussed on *Section 4.4*, transfection process using Lipofectamine reagent has some challenges concerning the evaluation of cell death. To obtain transfection efficiency of about 15%, besides to be low, cells under cellular death process tend to detach from the growth surface dish. This might led to an underestimation of cell death that could indeed be attributed to the TrkB-ICD fragment. Moreover, TrkB-ICD fragment could have long-term effects that were not evaluated in the present study.

Nevertheless, the degree of cell viability and cell death were evaluated by several experimental procedures and techniques. Unfortunately, the obtained preliminary data do not allow us to build a conclusion. Actually, opposite data was obtained, as shown in the following table (Table 11.1).

Table 10.1 – Approaches performed to study TrkB-ICD toxicity.

		Evaluation of:	Toxicity (TrkB-ICD vs. CTR)
1	MTT	Cell viability	Toxic
2	Nuclear GAPDH	Cell death (apoptosis)	Non-Toxic
3	αII-spectrin breakdown	Extension of neuronal degeneration	Non-toxic
4	Cell detachment	Dead cells in suspension	Toxic

1) MTT assay

→ Methods: Viability of 7 DIV primary neuronal cultures cells was evaluated by the metabolism of 3-(4,5-dimethylthiazol-2-yl)- 2,5-diphenyl tetrazolium (MTT) bromide (Sigma, St. Louis, USA). Cells were transfected or treated with $A\beta_{25-35}$ (25 µM) (Bachem, Bubendorf, Switzerland) for 24 hours and MTT was added to the original culture medium and incubated for 3 hours. After incubation, the converted die was solubilized with dimethyl sulfoxide (DMSO, Merck, Kenilworth, USA). Absorbance of converted die was measured at 570 nm with background subtraction at 650 nm.

→ Results: data shown in Figure 10.1 showed that cell viability significantly decreased in 7 DIV primary neuronal cultures incubated with Lipofectamine reagent when compared to control (100.0% vs. 91.94±0.34; n=6; p<0.001, Student's *t*-Test), which suggest again that transfection process *per se* has toxic effects. Moreover, we observed that transfection with the empty vector decreases cell viability compared with Lipofectamine incubation, but this difference is not significant. Interestingly, results from MTT assays also suggest that TrkB-ICD fragment could have toxic consequences, once it significantly decreased cell viability, when compared to Lipofectamine incubation (68.76% vs. 91.94; n=6; p<0.005; ANOVA followed by Bonferroni *post-test*) and also with transfection with an empty vector (68.76% vs. 81.50; n=6; p<0.05; ANOVA followed by Bonferroni *post-test*). However, this decrease is not enough to reach cell death observed with $A\beta_{25-35}$ (25 µM) incubation, suggesting that TrkB-ICD could only explain part of all neurotoxic effects of $A\beta$ peptide. It is important to mention that data concerning viable neurons treated with $A\beta_{25-35}$ (25 µM) is similar to previous data obtained by our group and other descriptions in literature [94,214].
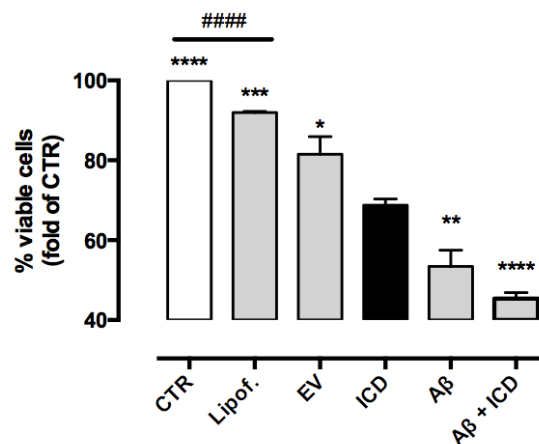

Figure 10.1 – TrkB-ICD fragment decreases cell viability on 7 DIV primary neuronal cultures. Percentage of viable neurons, capable of performing the MTT metabolism. Data is normalized for viable cells of CTR condition. Data represented are mean ± SEM of *n* independent experiments (n=6; *p<0.05; **p<0.01; ***p<0.005; ****p<0.001; compared to "ICD"; ANOVA followed by Bonferroni *post-test*) (####p<0.001; compared to "CTR"; Student's *t*-Test). Abbreviations: Aβ, amyloid-beta peptide; CTR, non-transfected cells; EV, empty vector; ICD, TrkB-ICD; Lipof., Lipofectamine.

2) Nuclear GAPDH

→ Methods: experimental procedure is mentioned on *Section 3.5* and the Figure 10.2 is a part of Figure 6.4 shown above.

→ Results: As previously referred on Discussion of nuclear translocation of TrkB-ICD fragment (*Section 6.4*), we detected a special isoform of GAPDH protein with lower molecular weight on nuclear fraction of primary neuronal cultures analysed (Figure 10.2). However, neurons expressing TrkB-ICD have similar levels of nuclear GAPDH isoform, when compared to transfection using an empty vector. Curiously, it is already demonstrated that nuclear GAPDH could have proapoptotic function or protective function [173,174] and, once its levels are similar in both conditions, data suggest that expression of TrkB-ICD for 24 hours do not affect cell viability.
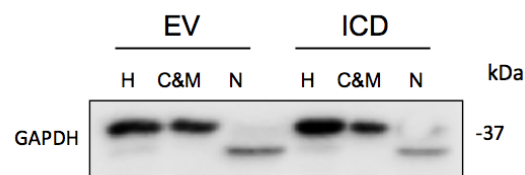

Figure 10.2 – TrkB-ICD fragment does not affect levels of nuclear GAPDH isoform. Western-blot image of homogenate, cytosolic and membrane and nuclear fractions of 7 DIV primary neuronal cultures transfected for 24 hours with an empty vector and with pcDNA-TrkB-ICD plasmid, showing the levels of GAPDH (complete image shown in *Section 6.3*). Abbreviations: C&M, fraction enriched in cytoplasmic and membrane; EV, empty vector; H, Homogenate; ICD, TrkB-ICD; N, fraction enriched in nuclear proteins.

3) αII-spectrin breakdown

→ Methods: αII-spectrin is a cytoskeletal protein that is cleaved by caspase-3 and calpain, allowing the measurement of neuronal degeneration extension. This cleavage is a signal of cell death and leads to two different proteins (αII-spectrin breakdown products, SBDP's): one with ~150 kDa that is a fragment formed by calpain cleavage and another with ~120 kDa, formed through a mechanism mediated by caspases. H4 cells were transfected or treated with Lipofectamine for 24 hours.

→ Results: As shown in Figure 10.3, TrkB-ICD-V5 does not induce αII-spectrin breakdown, as well as the remaining conditions, even with Lipofectamine incubation. Thus, despite missing a positive control in this test, these preliminary data suggest that cell viability is not affected in H4 cells studied at this time point.
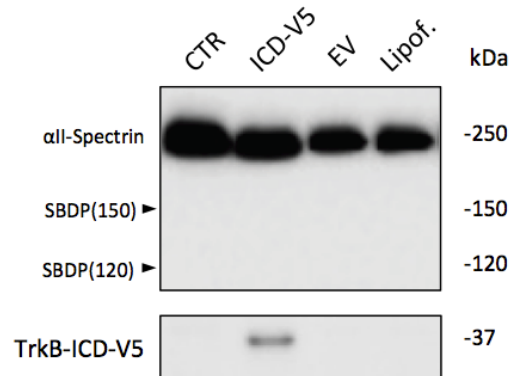

Figure 10.3 – TrkB-ICD-V5 does not promote αII-spectrin breakdown. Western-blot image representing αII-spectrin breakdown of H4 cells transfected with pcDNA-EV or pcDNA-TrkB-ICD-V5 and incubated with Lipofectamine for 24 hours. Abbreviations: CTR, non-transfected cells; EV, empty vector; ICD-V5, TrkB-ICD-V5; Lipof., Lipofectamine.

4) Cell detachment relative evaluation

→ Results: considering that dead cells tend to detach from the growth's surface more easily than viable cells, we performed a qualitative evaluation about the amount of cells present in supernatant of different conditions. After collection of supernatant, it was centrifuged at 200g for 10 minutes to obtain a pellet that could indicate the number of dead cells in suspension. Thus, we observed that pellet of cells transfected with pcDNA-TrkB-ICD is visibly bigger than cells transfected with the empty vector. In other words, this qualitative evaluation could suggest that TrkB-ICD fragment could have toxic effects and that might be involved on cell death induction, contributing to cell detachment and consequent formation of more pellet after centrifugation of suspension medium.

Overall, we not have enough observations about TrkB-ICD toxicity, being imperative to perform more robust assays or to explore possible long-term effects of TrkB-ICD fragment with other approaches.

10.2 Relationship between phosphorylation pattern and TrkB-ICD nuclear translocation using HEK293T cells

As discussed on *Section 7.7*, in order to evaluate if nuclear translocation of TrkB-ICD fragment was dependent on its kinase activity, we also used Human embryonic kidney (HEK) 293T cells (ATCC, Manassas, USA), since we could not performed the subcellular fractionation protocol on primary neuronal cultures so far. Concerning HEK 293T cells, it is important to mention that, similarly to H4 cells, these cells were also cultured in Opti-MEM, containing 10% of FBS, 100 units/mL penicillin, 100 μg/mL streptomycin and 2 mM L-glutamine at 37°C under a humidified 5% CO_2 atmosphere. Moreover, the main characteristics of transfection process and TrkB-ICD expression were similar to other cell types studied.

Thus, data presented in Figure 10.4 indicate that, the incubation of HEK293T cells with the K252a compound (5 μM) reduces drastically the TrkB-ICD levels on nuclear fraction and promotes an accumulation of TrkB-ICD on fraction enriched in cytoplasmic and membrane proteins, when compared to non-treated transfected cells ("ICD"). In other words, this result is in accordance with immunofluorescence assays using primary cortical neurons (Figure 7.9) and, taken together, both data provide evidence that TrkB-ICD requires kinase activity to be translocated to nucleus.
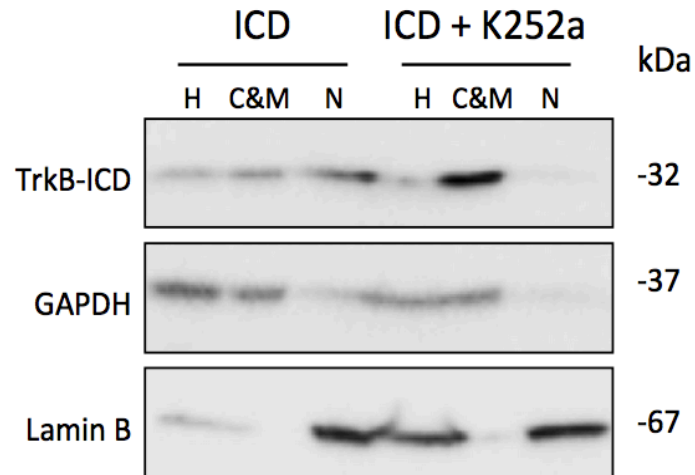
Figure 10.4 – K252a (5 µM) treatment effects on TrkB-ICD levels on different fractions of HEK293T cells transfected with pcDNA-TrkB-ICD. Western-blot image of homogenate (H), cytosolic and membrane (C&M) and nuclear (N) fractions of HEK293T cells transfected for 24 hours with pcDNA-TrkB-ICD plasmid (ICD), incubated or not with K252a (K) compound (5 µM), showing TrkB-ICD (probed with anti-Trk C-terminal tail antibody (C-14)), GAPDH (cytosolic protein) and Lamin B (nuclear protein) levels. Abbreviations: C&M, fraction enriched in cytoplasmic and membrane; EV, empty vector; H, Homogenate; ICD, TrkB-ICD; ICD+K252a, TrkB-ICD + K252a treatment; N, fraction enriched in nuclear proteins.